Aus dem

Department für Neurochirurgie und Neurotechnologie

Universitätsklinik für Neurochirurgie Tübingen

Immunohistochemical Markers in Aggressive Pituitary Adenomas

Inauguraldissertation
zur Erlangung des Doktorgrades
der Medizin

der Medizinischen Fakultät
der Eberhard Karls Universität
zu Tübingen

vorgelegt von

Hladik, Mirko

2023

Dekan: Professor Dr. B. Pichler

1. Berichterstatter: Professor Dr. med. J. Honegger
2. Berichterstatter: Professor Dr. med. R. Beschorner

Tag der Disputation: 03.05.2023

Meinen Eltern

Table of Contents

List of Figures

List of Tables

Abbreviations

ACTH	adrenocorticotroph hormone
ADH	anti-diuretic hormone
APA	atypical pituitary adenoma
ASCA	acidophil stem cell adenoma
aSU	alpha subunit
BC	bromocriptine
BM-40	basement membrane 40 protein
CAB	cabergoline
cAMP	cyclic adenosine monophosphate
CAM5.2	cytokeratin antibody
CART analysis	classification and regression tree analysis
CI	confidence interval
CBTRUS	Central Brain Tumor Registry of the United States
CC1	tris-based buffer and preserving agent
CC2	citrate buffer and preserving agent
CK20	cytokeratin 20
CNFA	clinically nonfunctioning adenoma
CS	cavernous sinus
CSI	cavernous sinus invasion
CSF	cerebrospinal fluid
CT	computer tomography
DA	dopamine agonist
DAB	3,3'-diaminobenzidine
DICER1	gene on chromosome 14q32.13
DGCA	densely granulated corticotroph adenoma
DGLA	densely granulated lactotroph adenoma
DGSA	densely granulated somatotroph adenoma
DNA	desoxyribonucleic acid
DWI	diffusion weighted imaging
EBRT	external beam radiotherapy
ECM	extracellular matrix
EDTA	ethylenediaminetetraacetic acid
EGF	epidermal growth factor
ER-alpha	estrogen receptor
EZH2	enhancer of zeste homologue 2
FGF	fibroblast growth factor
FGFR	fibroblast growth factor receptor
FOV	field of view
FPA	functioning pituitary adenoma
FSH	follicle stimulating hormone
FSRT	fractionated stereotactic radiotherapy
GATA2	GATA binding protein 2
GH	growth hormone
GnRH	gonadotropin releasing hormone
GNAS	guanine nucleotide binding protein, alpha stimulating
GPR101	G-protein-coupled-receptor 101

Gy	Gray
HCC	hepatocellular carcinoma
HE-section	hematoxylin and eosin section
H3K27me3	histone methylation of the core histone H3
H3K36me3	histone methylation of the core histone H3
HMGA	high mobility group A (protein or gene)
HNPCC	hereditary nonpolyposis colorectal cancer
HRP	horseradish peroxidase
ICA	internal carotid artery
IHC	immunohistochemistry
IRS	immunoreactive score
Ki-67 and MIB-1	Kiel antigen 67 or molecular immunology borstel 1
LAR	long-acting release
LCS	liquid color slip
LH	luteinizing hormone
LI	labeling index
LMWCK	low molecular weight cytokeratin
MEN	multiple endocrine neoplasia
Mixed SLA	mixed somatolactotroph adenoma
MGMT	O^6-methyl-guanine-DNA-methyltransferase
MSA	mammosomatotroph adenoma
MSH6	mismatch repair protein 6
MMP	matrix metalloproteinase
MRI	magnetic resonance imaging
mRNA	messenger ribonucleic acid
MVA	multivariate analysis
NFPA	nonfunctioning pituitary adenoma
NCA	null cell adenoma
OR	operating room
PA	pituitary adenoma
PAS	periodic acid-Schiff
PcG	Polycomb genes
PRL	prolactin
PIT-1	pituitary-specific positive transcription factor 1
PTTG	pituitary tumor transforming gene
p53	protein 53 (kilodalton)
RT	radiotherapy
SCA	silent corticotroph adenoma
SF-1	steroidogenic factor 1
SGA	silent gonadotroph adenoma
SGCA	sparsely granulated corticotroph adenoma
SGGA	sparsely granulated gonadotroph adenoma
SGLA	sparsely granulated lactotroph adenoma
SGSA	sparsely granulated somatotroph adenoma
SIADH	syndrome of inadequately elevated ADH secretion
siRNA	small interfering ribonucleic acid
SIPAP	suprasellar infrasellar parasellar anterior posterior
SPARC	secreted protein acidic and rich in cysteine

SR	slow release
SRS	stereotactic radiosurgery
SSA	somatostatin analogues
SSE	suprasellar extension
SSTR	somatostatin receptor
TMA	tissue microarray
TGF-β II	transforming growth factor beta two
TGF-β RI/II	transforming growth factor receptor type I/II
TMZ	temozolomide
TPIT	t-box transcription factor
TSH	thyroid stimulating hormone
TSH-oma	thyroid stimulating hormone-producing adenoma
USP8	Ubiquitin carboxyl-terminal hydrolase 8
VEGF	vascular endothelial growth factor
WHO	World Health Organization

1. Introduction

1.1. Epidemiology

Pituitary adenomas make up 10-15% of all primary brain tumors (Faglia et al., 1991). In the United States, 415,411 brain and other central nervous system tumors were recorded between 2013 and 2017 by the Central Brain Tumor Registry (CBTRUS) (Ostrom et al., 2020). 70.3% of all tumors were considered non-malignant and 29.7% malignant. By histological diagnosis, with a share of 16.9%, pituitary adenomas ranked second in frequency behind meningiomas (38.3%) and ahead of glioblastomas (14.5%). Prevalences of 75-115 cases per 100,000 and incidences of 4-5.8 cases per 100,000 annually are reported in the literature (Fernandez et al., 2010; Gruppetta et al., 2013; Agustsson et al., 2015; Raappana et al., 2010). Pituitary carcinomas present a malignant subgroup that is very rare. Of over 70,000 pituitary tumors in the United States, only 142 (0.2%) were considered malignant (Ostrom et al., 2020). Although any age group can be affected, the average pituitary adenoma patient is around 40 years of age according to several European epidemiological studies (Agustsson et al., 2015; Daly et al., 2006; Raappana et al., 2010). The male to female ratio is 1:1.2 and on average, women present with an adenoma at a younger age than men (Ostrom et al., 2020; Agustsson et al., 2015). Pituitary adenomas show variable clinical behavior, while most lesions are benign. However, what clinically relevant lesions have in common is that they, although benign, cause an increase of morbidity and mortality in their patients if they are left untreated (Tomlinson et al., 2001).

1.2. Etiology

Pituitary adenomas are benign tumors originating from adenohypophyseal cells of the pituitary gland, located in the sella turcica of the skull base and bounded by the cavernous sinus bilaterally. Etiology of pituitary adenomas is sporadic or hereditary. The plurality of the tumors occurs sporadically. Overall, the underlying mechanisms are poorly

understood, but two subtype-specific somatic mutations have been discovered. Firstly, mutation of the deubiquitinase gene ubiquitin carboxyl-terminal hydroxylase 8 (*USP8)* can cause corticotroph adenomas (Reincke et al., 2015). The mutation impairs downregulation of the epidermal growth factor (EGF) receptor, enabling EGF to constantly promote cell proliferation. Secondly, gain-of-function mutations of the guanine nucleotide binding protein, alpha stimulating (*GNAS*) gene can be found in 29-40% of somatotroph adenomas (Freda et al., 2007; Bi et al., 2017). *GNAS* encodes the alpha-subunit of a stimulatory G-protein coupled receptor which activates the growth-promoting cyclic adenosine monophosphate (cAMP) pathway (Bi et al., 2017). Studies estimate only 5% of all pituitary adenomas to derive from familial syndromes (Caimari & Korbonits, 2016; Vandeva et al., 2010). Hereditary causes of pituitary adenomas are multiple endocrine neoplasia (MEN) type 1 and 4, Carney complex, McCune Albright syndrome, neurofibromatosis type 1, 3P association (paraganglioma, pheochromocytoma, pituitary adenoma), DICER 1 syndrome and familial isolated pituitary adenoma (Caimari & Korbonits, 2016). These rare genetic diseases typically manifest at an early age during childhood or young adolescence. Another recent discovery has been a mutation of the G-protein-coupled receptor GPR101 resulting in gigantism in pediatric patients (Trivellin et al., 2014).

1.3. Clinical Presentation and Diagnosis

Pituitary adenomas can be divided into functioning and non-functioning adenomas (Asa & Ezzat, 2009). Functioning adenomas become symptomatic due to their production of adenohypophyseal hormones. By producing an excessive amount of growth hormone (GH), prolactin (PRL), adrenocorticotroph hormone (ACTH), thyroid-stimulating hormone (TSH), luteinizing hormone (LH) or follicle stimulating hormone (FSH), the tumors can cause conditions with significant hormone oversecretion – illnesses like Cushing's disease or acromegaly for example (Asa & Ezzat, 2009). Such adenomas are usually detected due to symptoms related to the hormone excess. Non-functioning adenomas that do not cause an excessive hormone secretion usually manifest with symptoms of compression of surrounding structures and are typically larger at diagnosis

(Ezzat et al., 2004). Table 1.1. at the end of this chapter summarizes possible presenting symptoms of all adenoma subtypes. Apart from symptomatic pituitary adenomas, autopsy studies have revealed that there is a considerable amount of incidentalomas: pituitary adenomas, which have not been symptomatic during lifetime, could be found in up to 27 percent of cases in one series (Molitch, 1997). Another review of 7 autopsy studies reported an overall prevalence of 14.4% (Ezzat et al., 2004).

The diagnostic triad for evaluation of suspected pituitary adenoma consists of ophthalmologist consultation, endocrinological testing and a cranial magnetic resonance imaging (MRI). Due to the increasing availability of cranial imaging, there is a rising incidence of pituitary incidentalomas (Famini et al., 2011; Boguszewski & Musolino, 2019) and regular follow-up MRIs are necessary. The current German guideline for non-functioning adenomas recommends an MRI after three to six months postoperatively with further follow-ups after two, five and eight years if no residual tumor or annually for five years if a residual tumor was detected on the initial postoperative imaging (Deutschbein et al., 2020). Computer tomography (CT) is indicated in certain macroadenomas to visualize bone erosion, detect calcifications (Donovan & Nesbit, 1996) and if an MRI is contraindicated (Klingmüller et al., 2001). On MRI, pituitary adenomas are subdivided into microadenomas (<10mm in diameter) and macroadenomas (>10mm in diameter). Generally, most pituitary adenomas present hypointense on T1-weighted imaging, show variable intensities on T2-weighted imaging and enhance after contrast agent application (Johnsen et al., 1991). Some microadenomas, most notably corticotroph adenomas in Cushing patients, may be too small to be detected by MRI (Honegger et al., 2019). Nevertheless, dynamic MRI has high sensitivity and specificity values for the detection of such microadenomas of up to 96% and 84%, respectively (Friedman et al., 2007). Dynamic means that the image is taken within seconds after gadolinium injection. While dynamic MRI proved to be superior in sensitivity (Friedman et al., 2007; Sakamoto et al., 1991; Tabarin et al., 1998), specificity is reported to be lower compared to conventional MRI (Tabarin et al., 1998). Diffusion-weighted imaging (DWI) can provide information about the consistency of an adenoma (Chaudhary, 2011). Regardless of the technique, MRI is the most reliable diagnostic tool as of today.

Adenoma type	Prevalence (% of all)	Presenting symptoms
Prolactinoma	40-45	♀: oligomenorrhea, amenorrhea, galactorrhea ♂: impotence, loss of libido, mass effects
Somatotroph adenoma	20%	**Gigantism** (only pediatric patients): excessive linear growth, abnormal height **Acromegaly**: bony overgrowth, facial deformations, soft tissue swelling, comorbidities: diabetes mellitus, hypertension, sleep disorders
Corticotroph adenoma	10-12%	**Cushing's disease**: central obesity, supraclavicular and dorso-lateral fat pads, easy bruisability, striae, hypertension, osteoporosis, hyperglycemia, hirsutism, menstrual irregularity, mood changes
Gonadotroph adenoma	15%	**Mass effects:** visual field deficit, ocular muscle deficit, cephalgia, hypopituitarism If functioning (rare): ♀: ovarian hyperstimulation syndrome ♂: increase of libido and serum testosterone
Null cell adenoma	5-10%	**Mass effects:** visual field deficits, ocular muscle deficit, cephalgia, hypopituitarism
Thyrotroph adenoma	1-2%	Goiter, hyperthyroidism, hypopituitarism, headache, visual field deficit

Table 1.1.: Clinical characteristics of pituitary adenomas.
Adopted from (Arafah & Nasrallah, 2001)

1.4. Classification by Hormonal Subtypes

1.4.1. Immunohistochemistry – The WHO Classification

Adenomas of the pituitary gland are classified according to the World Health Organization (WHO) Classification of Tumors of Endocrine Organs (Lloyd et al., 2017). The underlying criteria for each subtype are specified in Table 1.2. and in Chapter 1.4.2 to 1.4.8. Therapy and prognosis highly depend on the result of the exact immunohistochemical examination of adenoma tissue. The updated WHO Classification of 2017 contains three novel approaches compared to previous versions: routine assessment of proliferative potential, abandonment of the diagnosis adenoma of atypical character and the new definition of the null cell adenoma (Mete & Lopes 2017). The null cell adenoma definition makes a reclassification of all hormonally negative tumors, based on transcription factors to define their lineage, necessary (Asa & Mete, 2018). The intention of the atypical adenoma (APA) diagnosis was to differentiate aggressive pituitary adenomas from adenomas with a benign clinical course. Its diagnostic criteria were an invasive growth pattern, a Kiel antigen 67 (Ki-67) labeling index (LI) >3%, an increased number of mitoses and excessive protein 53 kDA (p53) immunoreactivity (DeLellis, 2004; Miermeister et al., 2015; Al-Shraim & Asa, 2006). Lack of prognostic value and ambiguity of the definition led to its abandonment (Chesney et al., 2017). Several studies found no statistical association between APAs and higher incidence of recurrence (Miermeister et al., 2015; Chiloiro et al., 2015; Rutkowski et al., 2018). Today the research focus has therefore shifted to finding other more reliable criteria for aggressive behavior of pituitary adenomas.

Adenoma type	Immunophenotype	Transcription factors
Somatotroph adenoma		
• DGSA *	GH ± PRL ± aSU, LMWCK (perinuclear)	PIT-1
• SGSA	GH ± PRL ± aSU, LMWCK (dot-like)	PIT-1
• mammosomatotroph	GH ± PRL ± aSU	PIT-1, ER-alpha
• mixed somatotroph and lactotroph	GH ± PRL ± aSU	PIT-1, ER-alpha
Lactotroph adenoma		
• SGLA *	PRL	PIT-1, ER-alpha
• DGLA	PRL	PIT-1, ER-alpha
• Acidophilic stem cell (ASCA)	PRL, GH, LMWCK (fibrous bodies)	
Thyrotroph adenoma	TSH-beta, aSU	PIT-1, GATA2
Corticotroph adenoma		
• DGCA *	ACTH, LMWCK (diffuse)	TPIT
• SGCA	ACTH, LMWCK (diffuse)	TPIT
• Crooke cell	ACTH, LMWCK (ring-like)	TPIT
Gonadotroph adenoma		
• SGGA	FSH-beta, LH-beta, aSU (various)	SF1, GATA2, ER-alpha (variable)
Null cell adenoma	none	none
Plurihormonal adenoma		
• PIT-1 pos.	GH, PRL, TSH-beta, ± aSU	PIT-1
• unusual combinations	various combinations	variable

Table 1.2.: Morphofunctional classification of pituitary adenomas.
** = most common subtype, DGSA: densely granulated somatotroph adenoma, SGSA: sparsely granulated somatotroph adenoma, SGLA: sparsely granulated lactotroph adenoma, DGLA: densely granulated lactotroph adenoma, DGCA: densely granulated corticotroph adenoma, SGCA: sparsely granulated corticotroph adenoma, SGGA: sparsely granulated gonadotroph adenoma, PIT-1: pituitary-specific positive transcription factor 1, GH: growth hormone, PRL: prolactin, aSU: alpha subunit, LMWCK: low molecular weight cytokeratin, TSH: thyroid-stimulating hormone subunit beta, ACTH: adrenocorticotrophic hormone, FSH: follicle-stimulating hormone, LH: luteinizing hormone, ER: estrogen receptor, GATA2: GATA binding protein 2, TPIT: t-box transcription factor, SF1: steroidogenic factor 1, -beta: subunit beta, -alpha: subunit alpha*
Adopted from (Lloyd et al., 2017).

1.4.2. Lactotroph Adenomas

Lactotroph adenomas, also called prolactinomas, are tumors characterized by an expression of prolactin (PRL), estrogen receptor (ER-alpha) and the mutated transcription factor PIT-1 (Lloyd et al., 2017). Accounting for about 40%, they are the most frequently observed pituitary adenomas. While >70% of these tumors concern women in their childbearing age, macroprolactinomas and giant prolactinomas (>4cm) occur more often in men (Yatavelli et al., 2018; Iglesias et al., 2018). Prolactinomas become symptomatic either because of hyperprolactinemia and its associated symptoms or because of causing mass effects. Although papers suggest that a PRL value >200ng/ml is almost an evidence for a lactotroph adenoma (Klingmüller et al., 2001), there are many other possible causes of elevated PRL levels which have to be ruled out. The WHO classification divides prolactinomas in sparsely granulated lactotroph adenomas (SGLA) which are the most common subgroup, densely granulated lactotroph adenomas (DGLA) and acidophilic stem cell adenomas which are both more aggressive (Asa & Ezzat, 2009; Gomez-Hernandez et al., 2015; Mete & Asa, 2012, 2013; Lloyd et al., 2017). SGLA can be differentiated from DGLA as its cells have chromophobic cytoplasms and a typical perinuclear Golgi-type staining for PRL, while DGLA show a more diffuse pattern of PRL expression and are rather eosinophilic or acidophilic (Asa & Ezzat, 2009; Gomez-Hernandez et al., 2015; Mete & Asa, 2012, 2013; Lloyd et al., 2017). The acidophilic stem cell subtype can contain fibrous bodies and stromal fibrosis and its nuclei are pleomorphic (Asa & Ezzat, 2009; Brat et al., 2001; Gomez-Hernandez et al., 2015; Sweiss, Lee & Sherman, 2015; Lloyd et al., 2017). The first line treatment for prolactinomas are dopamine agonists as shown in detail in Chapter 1.5.3.

1.4.3. Somatotroph Adenomas

This type of pituitary adenoma is called somatotroph because of its histological over-expression of growth hormone (GH). Like in any other subtype, it can be inactive and therefore clinically silent or active, causing either gigantism in pediatric patients who still

have open epiphyses or acromegaly in adults. Somatotroph adenomas rank second in frequency of functioning adenomas behind prolactinomas (Fernandez et al., 2010).

Clinically silent somatotroph adenomas are rare entities that accounted for 2% of all pituitary adenomas in large surgical series (Langlois et al., 2017; Chinezu et al., 2017) and need close follow-up given their known increased likelihood of recurrence as well as more frequent need of supplementary radiation therapy in comparison to other clinically nonfunctioning adenomas (CNFA) (Langlois et al., 2018, 2017; Chinezu et al., 2017).

There are four types of GH-secreting adenomas: densely granulated somatotroph adenomas (DGSA), sparsely granulated somatotroph adenomas (SGSA), mammosomatotroph adenomas and mixed lactotroph and somatotroph adenomas (Lloyd et al., 2017). In Lloyd et al.'s latest WHO classification of 2017, these previously mentioned adenomas are categorized by their immunophenotype, namely GH, alpha subunit (aSU), PRL and low molecular weight cytokeratin (LMWCK) and PIT-1. In the eosinophilic DGSA cells, LMWCK can be typically found perinuclear (Gomez-Hernandez et al., 2015; Mete & Asa, 2012, 2013; Obari et al., 2008). In contrast to that, the mostly chromophobic SGSA cells with pleomorphic nuclei only show fibrous bodies of LMWCK and do not express aSU (Bando et al., 1992; Kontogeorgos et al., 1993; Gomez-Hernandez et al., 2015; Mete & Asa, 2012; Obari et al., 2008; Lloyd et al., 2017). This differentiation between DGSA and SGSA based on their LMWCK expression pattern is clinically important. SGSA are more often invasively growing and DGSA respond better to somatostatin analogues (Bhayana et al., 2005; Gomez-Hernandez et al., 2015; Mete & Asa, 2012, 2013; Fougner et al., 2012; Heck et al., 2012; Potorac et al., 2015; Lloyd et al., 2017). Studies revealed that biochemical remission of somatotroph adenomas with surgery alone can be reached in around 60-73% of cases, additional postsurgical medical therapy (see Chapter 1.5.3.) was demonstrated to further increase the remission rate to up to 87% (Taghvaei et al., 2018; Dehghani et al., 2021; Cardinal et al., 2020).

1.4.4. Gonadotroph Adenomas

This hormonal subtype is usually clinically silent and only in rare cases a functioning pituitary adenoma (FPA), which explains why it is more often diagnosed as a macroadenoma causing mass effects (Snyder et al., 2018). In a study with 213 CNFA, 64% of them proved to be gonadotroph adenomas (Yamada et al., 2007), making them the most common phenotype of CNFA. Gonadotroph adenomas are typically immunoreactive for aSU, beta follicle stimulating hormone (beta-FSH) and beta luteinizing hormone (beta-LH) with variable intensity and develop from cells with steroidogenic-factor 1 (SF1) expressing nuclei (Ntali et al., 2014). Microscopically, the tumors consist of chromophobic cells showing no cellular or nuclear pleomorphism but pseudorosette formations, which are elongated cells aligning near blood vessels (Ntali et al., 2014; Lloyd et al., 2017). The etiology of gonadotroph adenomas remains mostly unidentified. Kottler et al. found out that no mutation of the gonadotropin releasing hormone (GnRH) receptor is causative and the current WHO classification by Lloyd and colleagues hints at epigenetic changes rather than somatic mutations explaining the pathogenesis of gonadotroph adenomas (Kottler et al., 1998; Lloyd et al., 2017). Treatment trials with the GnRH antagonist Nal-Glu GnRH have shown to be effective at decreasing levels of gonadotropin secreted by FPA but failed at reducing the size of gonadotroph adenomas (McGrath et al., 1993).

1.4.5. Corticotroph Adenomas

The famous neurosurgeon Harvey Cushing was the first one to link a state of hypercortisolism in the human body to the existence of a causative tumor in the anterior lobe of the pituitary gland, a corticotroph adenoma (Haas, 2002). In honor of his pioneering work, this state of hormonal derailment is known as Cushing's disease today. Besides Cushing's disease, functional corticotroph adenomas may also be linked to Nelson syndrome, a complication of bilateral adrenalectomy (Patel et al., 2015a). Like other hormonal subtypes, corticotroph adenomas can be subdivided according to their microscopical morphology. There are densely granulated (DGCA), sparsely granulated

(SGCA) and Crooke cell adenomas and what all of them have in common, is the characteristic immunopositivity for adrenocorticotroph hormone (ACTH), LMWCK and the transcription factor TPIT (Gomez-Hernandez et al., 2015; Mete & Asa, 2012, 2013; Lloyd et al., 2017). This subdivision is of special interest as it also has implications on the disposition to an invasive behavior. Crooke cell adenomas and silent corticotroph adenomas are thought to be invasive lesions more often than other types of corticotroph adenomas and other hormonally negative adenomas in general (Hague et al., 2000; Kim et al., 2019). Reviews of multiple studies show recurrence rates of silent corticotroph adenomas of up to 31% (Fountas et al., 2018). Crooke cell changes are an accumulation of cytokeratin filaments resulting from persistently elevated blood cortisol levels and this ultrastructural adaptation is not limited to tumoral cells but can be found in all corticotroph cells (Rotondo et al., 2012). Cytokeratin CK20 has been proven to be a sensitive marker of Crooke cells (Eschbacher & Coons, 2006) and interestingly, while Crooke cell adenomas often seem to be invasive and tend to recur more often, peritumoral absence of Crooke cell changes seems to be a factor associated with postsurgical recurrence (Hague et al., 2000). Many aspects about the pathophysiology of Crooke cell adenomas are still not understood. Another more intensively studied pathophysiological aspect is the *USP8* mutation as a cause of Cushing's disease (Reincke et al., 2015; Albani et al., 2018; Ma et al., 2015; Wanichi et al., 2019; Losa et al., 2019). The mutation is detectable in more than 50% of cases in some corticotroph adenoma cohorts (Ma et al., 2015) and has a higher prevalence in female patients (Wanichi et al., 2019; Losa et al., 2019; Ma et al., 2015). Regarding its clinical implication, there is evidence of an increased likelihood of surgical remission of *USP8*-mutated adenomas compared to the unmutated wildtype adenomas (Wanichi et al., 2019; Losa et al., 2019; Ma et al., 2015).

1.4.6. Thyrotroph Adenomas

Thyrotroph adenomas are rare entities and are reported to account for less than 1 to up to 2,8% of all pituitary adenomas (Beck-Peccoz et al., 2019; Mindermann & Wilson, 1993; Brucker-Davis et al., 1999; Samuels & Ridgway, 1995). Thyrotroph adenomas (TSH-omas) produce thyroid-stimulating hormone (TSH) and can be clinically active causing secondary hyperthyroidism or clinically silent. A requirement for the diagnosis of a

clinically functioning TSH-oma is a non-suppressed or elevated TSH level. It is crucial to successfully differentiate an adenoma as the source of hyperthyroidism from other possible causes as a therapeutic thyroid ablation can further stimulate growth of a thyrotroph adenoma (Beck-Peccoz et al., 1996). The notion that patients with a TSH-oma tend to lack typical physical traits of Graves disease such as exophthalmos, pretibial edema or acropachy might help the clinican with this differentiation (Buchfelder, 2002). Immunohistochemically, thyrotroph adenomas derive from PIT-1-lineage cells and, apart from TSH, often stain immunopositive for aSU (Lloyd et al., 2017). They show a chromophobic appearance and are usually arranged in cords with polymorphous large nuclei (Beck-Peccoz et al., 2019) and often have a characteristic fibrous or calcified "stone-like" consistency (Webster et al., 1994). TSH-omas are predominantly invasive lesions at diagnosis and, although TSH normalization rates of up to 80% can be achieved by surgery (Angelis & Cappabianca, 2014), in one study 31% of active and silent thyrotroph adenomas recurred (Kirkman et al., 2014).

1.4.7. Null Cell Adenomas

Having no specific immunohistochemical differentiation by hormones or transcription factors, null cell adenomas (NCAs) are a diagnosis of exclusion with the necessity to rule out pituitary paragangliomas or a metastatic neuroendocrine tumor in the diagnostic process (Mete & Asa, 2012; Lloyd et al., 2017). Together with silent gonadotroph adenomas (SGAs), these pituitary tumors are the largest fraction of hormonally negative adenomas. In a Greek center of almost 1.500 surgically removed adenomas 3.4% (51 adenomas respectively) were null cell adenomas (Kontogeorgos & Thodou, 2016). This rate is lower than the estimated 5-10% shown in Table 1.1 (Arafah & Nasrallah, 2001). One potential reason for this are similar histological aspects of NCAs and SGAs which complicate the correct diagnosis of NCAs. Just like SGAs, the chromophobic or weakly acidophilic NCA cells are negative in the periodic acid-Schiff (PAS) reaction and contain characteristic intracellular pseudorosette formations (Kontogeorgos & Thodou, 2016; Lloyd et al., 2017). Nevertheless, they are considered an own subtype independent from SGAs (Balogun et al., 2015). This overlap of characteristic features results in a significant

amount of potential misdiagnoses, especially in the past. Not until the publication of the latest WHO classification, clear diagnostic criteria were established, namely an absence of immunohistochemical staining for hormones as well as transcription factors (Lloyd et al., 2017). There is also a special type of NCA, the oncocytoma. In contrast to regular NCAs, oncocytomas contain many mitochondria and there is a slight male preponderance instead of the female excess of all NCA cases combined (Greenman & Melmed, 1996; Feng et al., 2014).

1.4.8. Plurihormonal Adenomas

As the name implies, plurihormonal adenomas are all adenoma types that express or secrete more than one adenohypophyseal hormone. It has been assumed that this adenoma subtype accounts for 10 to as much as 31% of all pituitary adenoma types (Scheithauer et al., 1986; Ho et al., 2001), however the latest WHO Classification of 2017 excludes the common combinations GH/PRL and FSH/LH from the diagnosis and conceives of 0,9% of all adenomas being plurihormonal (Erickson et al., 2009; Lloyd et al., 2017). A peculiarity is the age distribution of plurihormonal adenomas. The tumors occur more often in childhood and adolescence than in adulthood (Scheithauer et al., 1986) and especially in these young patients the adenoma can be directly linked to the causality of MEN type 1 syndrome (Horvath et al., 1988; Erickson et al., 2009). Owing to its aggressive behavior, silent subtype 3 adenomas occupy a special position within plurihormonal adenomas. Originally this entity was counted to variants of corticotroph adenomas. Today, however, it is known that silent subtype 3 adenomas derive from PAS-negative, monomorphous cells with PIT-1-positive nuclei and, since a significant proportion of these tumors show hormonal excess, the term “silent subtype 3” is reviewed as inapt (Mete et al., 2016). Between 30 and 60% of all plurihormonal PIT-1-positive adenomas showed invasive growth on imaging and more than half showed a progressive residual tumor in one series (Mete et al., 2016; Erickson et al., 2009).

1.5. Treatment

1.5.1. Surgery

Surgical resection is the first-line therapy for most pituitary adenoma subtypes. However, for prolactinomas the preferred treatment is medical due to the good response rate to dopamine agonists (see Chapter 1.5.3). Microsurgical resection is indicated whenever there is clinically significant hormonal aberration, mass effect by a pituitary adenoma or significant tumor growth. The standard procedure is an endonasal, transsphenoidal approach which can be used for both the microscopic as well as the endoscopic operation technique. For both techniques, reviews and meta-analyses show similar outcomes (Rotenberg et al., 2010; Goudakos et al., 2011) and no significant differences in the incidence rates of complications (Gao et al., 2014; Goudakos et al., 2011) . Some macroadenomas with extensive suprasellar extension might require a craniotomy and a transcranial approach. In rare cases, there is even the need for a combination of the transsphenoidal and the transcranial approach as a two-staged resection (Kuga et al., 2019).

Transsphenoidal surgery of a pituitary adenoma is relatively successful and safe. Even in cases of giant macroadenomas, resections of >90% of the tumor volume were achieved in two third of the patients in a series of 54 patients on endoscopic resection (Koutourousiou et al., 2012). It is also possible to remove most tumors with suprasellar extension. In a series of 105 of such adenomas complete removal was achieved in 83% (Honegger et al., 2007). Nevertheless, 10-25% of macroscopically completely resected tumors show recurrence (Arafah & Nasrallah, 2001; Brochier et al., 2010) and authors of a review study with a focus on resection rates of surgery speculate that biomarker studies of invasive pituitary adenomas are likely to be a more promising approach to predict likelihood of tumor recurrence (Dhandapani et al., 2016). Unsurprisingly, residual tumors after incomplete resection have higher rates of recurrence (Brochier et al., 2010; Lelotte et al., 2018). Regarding the functional outcome, it is seen that visual function improves more often than hormonal deficiencies (Karamouzis et al., 2018; Chang et al., 2010). Rates of visual function normalization or improvement range from a reported 69% in first-time operated adenoma patients to an even higher rate of 95% in an analysis of

recurrent adenoma cases with repeated surgery (Young Jr. et al., 1996; Chang et al., 2010). Generally, repeated surgery in recurrent adenomas has a lower gross total resection rate (44% vs. 75%) than initial surgery (Toyota et al., 2019), but it is still more effective at reducing tumor volume than achieving remission of hormonal hypersecretion (Benveniste et al., 2005). Interestingly, high rates of residual tumor do not automatically lead to tumor mass progression according to two studies. While residual tumors were present in 35% (Chang et al., 2010) and 75% (Benveniste et al., 2005) of cases on imaging after the second operation in these series, tumor mass progression was only seen in 8% and 15% of the cases, respectively. Mortality rates for pituitary surgery are very low. Rates of 0.2% and 0.9% are reported in the literature (Wilson, 1984; Ciric et al., 1997). Data from 958 neurosurgeons revealed anterior pituitary insufficiency and diabetes insipidus as the two most common complications (Ciric et al., 1997). Diabetes insipidus and its counterpart syndrome of inadequately elevated ADH levels (SIADH) are both usually transient complications and while diabetes insipidus typically has a direct onset 24-48 hours postoperatively, the onset of SIADH is delayed within 4-7 days postoperatively (Alzhrani et al., 2018; Schreckinger et al., 2013). Another notable complication is cerebrospinal fluid fistula which requires a lumbar drainage or, in some cases, surgical revision (Zhang et al., 2017).

1.5.2. Radiotherapy

The use of radiation therapy is an additional treatment option for pituitary adenomas. It can be considered if there is progression of residual tumor, hormonal hypersecretion after surgery or if the adenoma is refractory to medical treatment (Ajithkumar & Brada, 2016). There are two different procedures: external beam radiotherapy (EBRT) and stereotactic radiosurgery (SRS). The latter has the advantage of a higher precision by mapping the target with three-dimensional coordinates and thereby allowing for a reduction of radiation dose to healthy tissue (Plowman, 1999). That might explain why SRS has significantly less visual complications than the conventional EBRT (Sebastian et al., 2016). Fractioned stereotactic radiotherapy (FSRT) is a subform of SRS. It is

recommended over the conventional SRS for tumor sizes above 2,5cm and involvement of the optic apparatus (Minniti et al., 2016).

Recommended dose ranges for SRS are 14-18 Gy for nonfunctioning adenomas or 20-25 Gy for functioning adenomas and for FSRT 45-54 Gy at 1.8 Gy per fraction (Loeffler & Shih, 2011).

Radiotherapy (RT) is effective at preventing tumor growth. Studies indicate that FSRT and SRS can control tumor size in 85-95% for up to 10 years (Minniti et al., 2016; Ajithkumar & Brada, 2016). Similar to surgical results, RT is more effective at achieving tumor size control (rates of 96-100%) than biochemical control of hormonal hypersecretion (rates of 42-93.6%) as shown by multiple long-term outcome studies (Sasaki et al., 2000; Colin et al., 2005; Rim et al., 2011; Scheick et al., 2016; Sebastian et al., 2016). Reported prognostic factors associated with a worse outcome in the literature are functional status of an adenoma, male gender and CS extension (Rim et al., 2011; Colin et al., 2005; Brada et al., 1993). Apart from its therapeutic value, RT has potential side effects. Hypopituitarism is the most common side effect and a recent multicenter study revealed that it develops in almost one fourth (248 of 1,023 patients) of cases (Cordeiro et al., 2019). Growth hormone is the hormone most sensitive to irradiation (Toogood, 2004). Besides potential endocrine consequences, visual deterioration is another possible side effect (Gilliot et al., 2007).

1.5.3. Pharmacotherapy

Dopamine Agonists

Dopamine agonists (DA) are the first line treatment for symptomatic lactotroph adenomas. The hypothalamic hormone dopamine functions as the inhibitor of prolactin secretion. Its synthetical agonists are also able to bind the dopamine receptors on lactotroph cells. There are three substances in use: cabergoline (CAB), bromocriptine (BC) and quinagolide (Colao & Savastano, 2011).

CAB is preferred over BC due to a higher frequency of normalizing prolactin levels and decrease in tumor size (Yatavelli et al., 2018), a lower prevalence of therapy resistance

(20-30% for BC vs. 10% for CAB) (Maiter, 2019) and due to less adverse effects (Nunes et al., 2011). CAB also seems to be advantageous when compared with quinagolide, according to a study that found a higher rate of tumor shrinkage, a better tolerance and a better cost:effectiveness ratio of CAB (Sarno et al., 2000).

Therapy resistance has three dimensions and can be defined as failure to achieve normalization of prolactin levels, failure to achieve tumor size decrease by at least 50% and failure to restore fertility (Melmed et al., 2011). In a study of 122 patients, a CAB dosage of 0.5-1.5mg weekly was effective in the majority of patients with lactotroph macroadenomas, however about 20% of patients were resistant and needed higher doses (Delgrange et al., 2009). According to Delgrange et al., male gender and CS invasion were predictive factors for these cases of resistance.

Resistance needs to be distinguished from intolerance, a consequence of side effects. Known side effects of DA include neurological symptoms (cephalgia, vertigo, apathy, agitation), gastrointestinal complications (nausea, emesis, abdominal pain) and cardiovascular symptoms (syncope, cardiac fibrous and serous inflammation) (Karow & Lang-Roth, 2020).

There are clinical guidelines for patients in special situations like pregnancy. The predominant scientific opinion is that DA treatment has no harmful effect on the fetus in early pregnancy (Molitch, 2006; Bronstein, 2005). Nevertheless, DA therapy should be discontinued during pregnancy whenever possible and only be continued if an adenoma is invasive or abuts the optic chiasm (Melmed et al., 2011). There is more evidence of the safety of BC as it has larger published experience in pregnancy (Melmed et al., 2011).

Somatostatin Analogues

Somatostatin analogues (SSA) are agonists of the hypothalamic hormone somatostatin which inhibits secretion of growth hormone by binding somatostatin receptors (SSTR). Interestingly, SSTR are also expressed on thyrotroph adenomas (SSTR2) and corticotroph adenomas (SSTR5 and SSTR2) besides the obvious expression on somatotroph adenomas (SSTR5 and 2, less frequent SSTR1 and 3), which explains why they are potentially effective at treating all three types of adenomas (Raverot et al., 2018). Substances in use are lanreotide, octreotide and pasireotid. The latter is the only centrally

efficacious pharmaceutical officially approved for treatment of Cushing's disease (Raverot et al., 2018). The main use of SSA is the treatment of acromegaly. However, besides SSA, the GH receptor antagonist pegvisomant can help normalize levels of IGF-1 (Giustina et al., 2017). IGF-1 is a polypeptide structurally similar to the peptide hormone insulin with serum levels correlating with GH levels (Rinderknecht & Humbel, 1976; Laron, 2001). It mediates the metabolic effects of GH.

SSA used in the clinical practice differ in their duration of action and efficiacy. Octreotide is also available as a short-acting variant, which is administered subcutaneously. Generally, long-acting release (LAR) and slow release (SR) depot forms are more widely used. Therapy efficacy of SSA is measured either by decrease in tumor size or by decrease of serum levels of GH and IGF-1. In a meta-analysis of 37 studies, 382 of 920 somatotroph adenoma patients (42%) treated with octreotide SR, octreotide LAR or lanreotide SR showed reduction in tumor size (Bevan, 2005). Another meta-analysis with data from 1,792 patients showed that primary SSA treatment is more likely to induce tumor response than adjunctive SSA treatment after surgery or radiotherapy and that increase of tumor size during SSA therapy is rare as it was reported to occur in under 2% (Freda et al. 2005). Concerning the biochemical response, octreotide LAR has proved to be more effective than lanreotide SR in normalizing IGF-1 and suppressing GH levels (Freda et al., 2005). In a study of 358 medically naive patients, pasireotide appeared to be even more efficacious than octreotide in achieving biochemical control, especially of IGF-1 levels (Colao et al., 2014). Like any other pharmaceutical, SSA have potential side effects. The most common adverse effects are diarrhea, cholelithiasis, headache and hyperglycemia (Colao et al., 2014).

Chemotherapy (Temozolomide)

While most studies on temozolomide (TMZ) have been conducted with data from malignant melanoma, glioblastoma and other glioma patients, a small number of studies has been conducted that focused on the use of TMZ for the treatment of pituitary adenomas. According to current guidelines TMZ is the preferred first line therapy for aggressive pituitary adenomas and pituitary carcinomas (Raverot et al., 2018). TMZ is an alkylating agent, which works by damaging a tumor's DNA and leading its corresponding

cell to apoptosis through a methylation of the O^6 position of the base guanine (Hirohata et al., 2013). A common TMZ administration is 150-200mg/m^2/day for 5 consecutive days given in monthly cycles with an advisable evaluation of response to therapy after 3 of such cycles (Raverot et al., 2018). Owing to the lack of prospective studies with large pituitary adenoma patient cohorts, information on efficacy of TMZ chemotherapy is lacking. In one study, the effect of TMZ was not dependent on tumor subtype and almost half of the patients (10 of 21, 48%) responded to therapy (Bengtsson et al., 2015).

More data is available on the question why some patients remain treatment refractory. There are at least two factors which have been detected to influence TMZ response. Firstly, the expression of O^6-methyl-guanine-DNA-methyltransferase (MGMT) is known to influence treatment outcome in glioblastomas (Hegi et al., 2009). The DNA repair protein can counteract the action of TMZ as it transfers the alkyl group from the O^6 guanine position to a sulfur group of cysteine (Hegi et al., 2009). Fittingly, significantly lower MGMT expression was also detected in TMZ responders compared to nonresponders in a series of 16 aggressive PA and 8 pituitary carcinomas (Bengtsson et al., 2015). Secondly, loss of the DNA mismatch repair protein MSH6, a gene primarily known for its association with Hereditary Non-Polyposis Colorectal Cancer (HNPCC or Lynch syndrome), can be causative for an increase of tumor growth (Hirohata et al., 2013). This effect has been observed in glioblastomas (Cahill et al., 2007) as well as aggressive pituitary adenomas (Hirohata et al., 2013). Another impact factor on therapy efficacy are limitations caused by advisory effects which might cause a patient to reduce or discontinue treatment. Thrombocytopenia, extreme fatigue urinary tract infection, elevated liver enzymes, hearing loss as well as nausea and vomiting are known side effects of TMZ (Bengtsson et al., 2015; Hirohata et al., 2013).

1.6. Invasiveness and its Prognostic Impact

Invasion is defined as infiltration of adjacent structures by an adenoma. If infiltration of the dura mater is included in this definition, its prevalence can reach up to 61 or 63% of all tumors in the literature (Jaffrain-Rea et al., 2002; Watts et al., 2017; Lelotte et al., 2018).

Radiologic criteria to detect invasive adenomas have limitations of reliability and predictive value and there is also controversy about the association of certain biomarkers with invasiveness given inconclusive findings so far (see next chapter). Meaningful results have come from clinical scores which take into account radiological as well as histological criteria: in 3 studies prediction of recurrence or progression was possible by a score which includes both tumor cell proliferation (two of the three criteria: Ki-67 > 3%, p53 positive, mitoses n>2/10 400x magnification fields) as well as invasiveness criteria (histological or MRI signs of cavernous sinus (CS) or sphenoid invasion) (Trouillas et al., 2013; Lelotte et al., 2018; Raverot et al., 2018).

A common misconception is the synonymous use of the terms aggressiveness and invasiveness for pituitary adenomas. Like therapy resistance, early recurrence and rapid tumor growth, invasiveness is just one aspect of an aggressive pituitary adenoma, an entity that differs from benign pituitary adenomas, which in fact can also show invasive behavior, and malignant pituitary carcinomas (Chatzellis et al., 2015).

The following high-risk adenomas have been identified for a clinically aggressive behavior: sparsely granulated somatotroph adenomas, densely granulated lactotroph adenomas, acidophil stem cell adenomas, thyrotroph adenomas, Crooke's cell adenomas, sparsely granulated corticotroph adenomas, plurihormonal PIT-1 positive adenomas (previously silent subtype 3 adenomas) and null cell adenomas (Asa, 1998; Asa & Ezzat, 2009; Mete & Asa, 2012; Mete & Lopes, 2017; Lopes, 2017). However, what has not been defined so far, are histological markers which may help predict aggressive tumor behavior (Thapar et al., 1996a; Wierinckx et al., 2007; Chesney et al., 2017).

The prognosis of pituitary adenomas depends on responsiveness to treatment and the tendency to show recurrence after treatment. An independent risk factor for postsurgical recurrence that was identified by different researchers is a young patient age (Lelotte et al., 2018; Kim et al., 2016; Watts et al., 2017). In an Australian study age under 41 years at diagnosis posed a 2.8-fold risk increase for tumor regrowth (Watts et al., 2017). Lelotte et al. found a recurrence risk reduction of 5.6% for every year older, however their series only featured nonfunctioning pituitary adenomas (NFPAs). In a Korean study of 136 adenomas, the mean age at diagnosis of recurrent cases was 43 compared to 50 years of recurrent cases (Kim et al., 2016). Besides that, suprasellar extension has been found to

be a prognostically relevant factor. Pituitary adenomas with suprasellar extension (SSE) have an increased risk of residual or recurrence of almost 40% (Mohr et al., 1990). Especially in adenomas with an SSE of irregular shape or multilobulated configuration, complete removal is less likely (Honegger et al., 2007).

Due to worse surgical accessibility and increased difficulty of resection, an association of invasive adenomas with an increased likelihood of a postoperative residual tumor was found in several studies. However, the findings vary regarding the question whether a higher frequency of residual tumors automatically also led to an increased rate of recurrence. In a previously mentioned study of 120 NFPAs, a residual tumor after surgery was frequently more often observed in invasive lesions (82% compared to 31% of noninvasive tumors) and invasion also led to a significantly increased rate of recurrence (40% compared to 29% of noninvasive tumors) (Lelotte et al., 2018). Another study with a similar cohort composition of 142 NFPAs found cavernous sinus invasion (CSI) to be an independent factor with a negative influence on recurrence risk (Brochier et al., 2010). The presence of a postoperative residual only was a significant risk factor for recurrence if CSI was not considered in the multivariate analysis, which prompted Brochier et al. to conclude that CSI and postoperative residuals are two closely associated factors. A consistent result was presented in a Korean series of 275 NFPAs, as CSI was associated with a worse extent of resection and a lower median progression-free survival (Hwang et al., 2016). A contrary finding was made in a study that featured 354 adenomas of all subtypes and found a residual tumor significantly more frequently in cases with microscopic dural invasion (Meij et al., 2002). Nevertheless, the latter was not significantly associated with an increased recurrence rate. A large meta-analysis with data from 143 studies overall found microscopic or macroscopic evidence of invasion unrelated to recurrence (Roelfsema et al., 2012). However, only recurrence after clinical cure, defined as lack of a remnant on postoperative imaging in case of NFPAs or endocrine remission in FPAs, was considered. This means that all studies that also defined regrowth of a residual as recurrence were excluded. Another Korean series of 167 PAs did not detect invasion to be a significant predictor of recurrence (Kim et al., 2019). The authors suggested it might depend on the location of invasion or invasion might only be of predictive value in combination with other adenoma features. In their retrospective analysis of 343 adenomas, Chiloiro et al. indeed found CSI to be a significant factor for

recurrence potential, while cases with other forms of invasion were not statistically significant regarding tumor recurrence (Chiloiro et al., 2015).
In the end, the existing prognostic studies that addressed the role of invasion had cohort sizes of at most 350 adenomas, some only featured NFPAs and their definition of invasion was non-uniform. So far, an approach for a more uniform identification of PA invasion are radiographic classifications.

1.6.1. Radiological Criteria of Invasiveness

A particularly striking effect of unfavorable prognostic influence is attributed to CSI as described in Chapter 1.6. Multiple other studies also detected CSI to be the strongest risk factor for incomplete surgical resection (Dhandapani et al., 2016; Frank & Pasquini, 2006; Woodworth et al., 2014; Bao et al., 2016; Taniguchi et al., 2015). Established with encephalograms in 1976, the Hardy classification was the first radiographic classification of pituitary adenomas. It was modified with regard to operative findings and found to be of prognostic relevance a decade later (Wilson, 1984). The Hardy classification consists of grade 0 through IV for the degree of sellar wall invasion and types 0 through D for the degree of suprasellar extension (Hardy & Vezina, 1976; Mooney et al., 2017a). Lack of interrater reliability for intermediate grades (II, III, A, B) was described as a drawback in one study (Mooney et al., 2017a). Other classifications such as SIPAP (Edal et al., 1997) reach higher interobserver agreements of 79% (Meyer et al., 2011), but lack data that link certain grades to invasive tumor behavior.
Currently, the most frequently applied classification for CSI is the Knosp scale. It uses the internal carotid artery (ICA) as a reference point and values the adenoma's growth at the border to and beyond the ICA with the aid of three imaginary lines (Knosp et al., 1993). The general scientific consensus is that higher Knosp grades are correlated with an increased likelihood of CSI and a decreased rate of gross total resection and of endocrinological remission (Micko et al., 2015; Dhandapani et al., 2016). In their review of 40 studies, Dhandapani et al. pointed out that Knosp grades ≥3 can indeed reliably indicate CSI with a high specificity of 90% overall. On the other hand, it was also demonstrated that Knosp grades ≥3 only have a low sensitivity which may explain why

the association of these grades with CSI lacks statistical significance (Cottier et al., 2000; Vieira et al., 2006). Another disadvantage is that adenomas with a Knosp grade 3 show a highly inhomogeneous distribution of CSI. On direct observation in one endoscopic surgical study, CSI in Knosp grade 3 adenomas was present significantly more often in adenomas with extension into the inferior CS compartment (70.6%) compared to extension into the superior compartment (26.5%) in one study (Micko et al., 2015). The authors of the study therefore recommended a subdivision of grade 3 in subgroups 3A and 3B as illustrated in Figure 1.1. Besides that, similar to the findings for the Hardy classification, the intermediate grades 2 and 3 of the Knosp scale were shown to have low interrater reliability (Mooney et al., 2017b).

All in all, predictive value of the Knosp scale for CSI detection is limited and so far, only non-visualization of two or more venous compartments or of the inferior venous compartment and ICA encasement of ≥30% have been singled out as radiographic criteria that are significantly associated with CSI (Vieira et al., 2006).

Generally radiographic assessment of pituitary adenomas tends to overestimate the true prevalence of CSI. While it is radiographically reported in 30-63% (Messerer et al., 2011; Hofstetter et al., 2012; Dhandapani et al., 2016), it is directly observed in surgery in only 9-30% (Dehdashti & Gentili, 2007; Woodworth et al., 2014) of cases in studies (Dhandapani et al., 2016). Unfortunately, to date, the research focus has been on radiological criteria for CSI only, while sufficient amount of data regardings invasion of other anatomical structures is still missing.

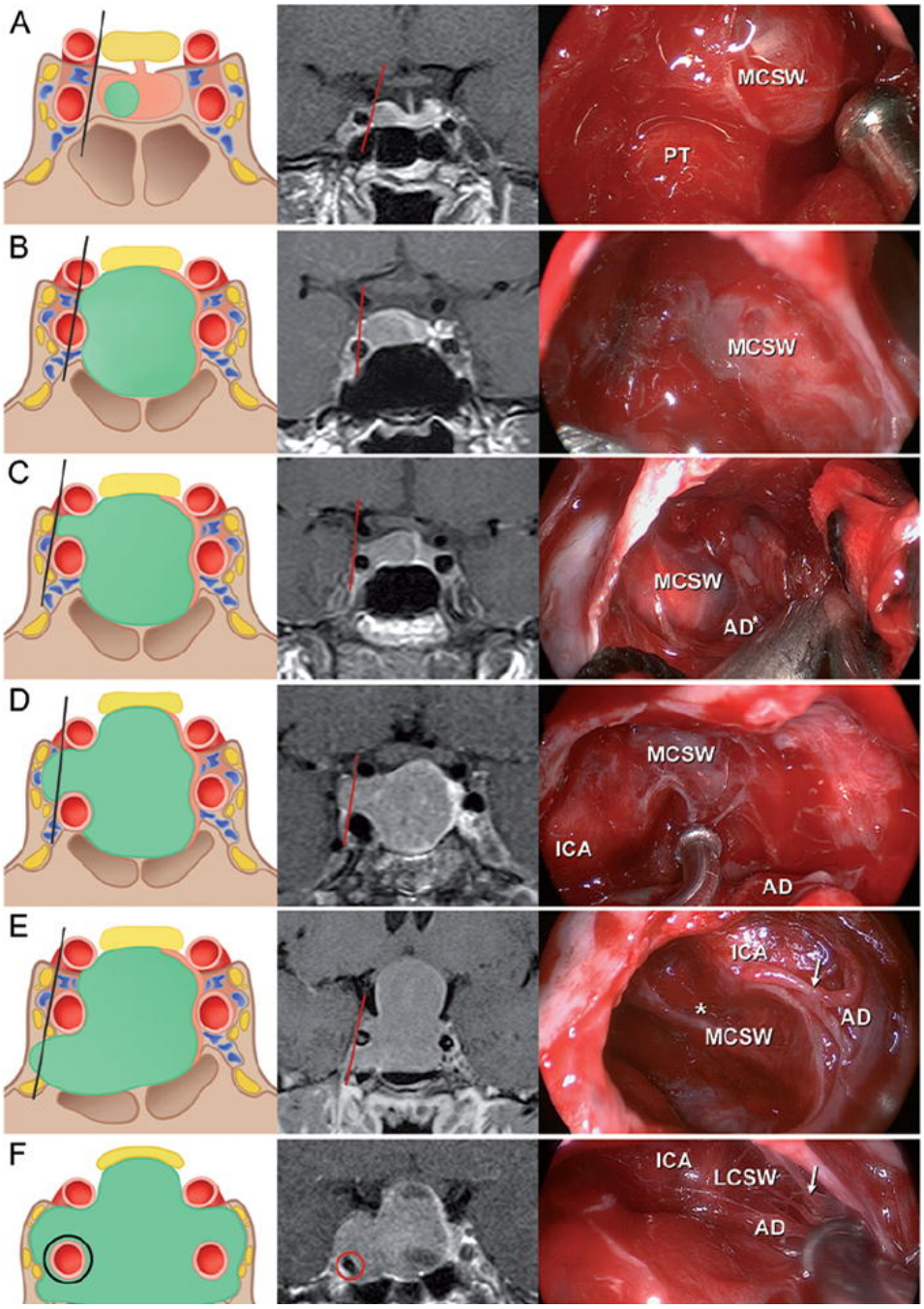

Figure 1.1.: The Knosp scale of CS invasion with the adapted subdivision of grade 3.

Graphic schemes *(left),* coronal MR images *(center),* endoscopic view *(right)*
A: Grade 0: The adenoma does not invade the CS.
B: Grade 1: The medial tangent of the intracavernous and supracavernous ICA is passed, but the extension does not go beyond the intercarotid line.
C: Grade 2: The tumor extends beyond the intercarotid line, but does not pass the lateral tangent of the intracavernous and supracavernous ICA.
D: Grade 3A: Extension lateral from the lateral tangent into the superior CS compartment.
E: Grade 3B: Extension lateral from the lateral tangent into the inferior CS compartment.
F: Grade 4: Total encasement of the ICA.
AD = adenoma; *LCSW* = lateral CS wall; *MCSW* = medial CS wall; *PT* = pituitary gland; *asterisk*: invaded medial CS wall; *arrows*: trabeculae.
Adopted from: Micko et al., 2015 with permission from Engelbert Knosp.

1.6.2. Discussed Markers of Invasiveness

MMP and PTTG

Matrix metalloproteinases (MMP) are proteolytic enzymes that can induce tumor invasion owing to their ability to degrade the extracellular matrix (Amar et al., 1994). Among a total of 23 MMP subtypes, MMP-2 and -9 can especially degrade collagen type IV (Murphy & Nagase, 2008). This physiologic function and the fact that collagen type IV is an essential component of the dura mater led to first suggestions of a possible correlation between the expression of these metalloproteinases and CSI (Kawamoto et al., 1996). There is interaction between both enzymes as MMP-2 can stimulate MMP-9 by prodomain cleavage (Chakraborti et al., 2003; Toth et al., 2003). Several studies have detected an association of expression of MMP-2 and -9 with invasiveness. Especially significantly higher MMP-9 expression has been described in invasive adenomas (Gong et al., 2008; Gültekin et al., 2015; Hussaini et al., 2007; Liu et al., 2005; Wang & Liu, 2004). A relatively new meta-analysis comprising the results of 24 studies confirms these findings (Liu et al., 2016) and further adds data that links higher MMP-9 expression to tumor recurrence (Gong et al., 2008; Turner et al., 2000), an important feature of aggressiveness. However, Liu et. al also demonstrate lack of data regarding the influence of adenoma size and functional status as possible confounding factors on MMP expression.

Interestingly, there is a relation between MMPs and the Pituitary tumor transforming gene (PTTG). PTTG appears to initiate the enzymatic effect of MMPs as the proto-oncogene was found to induce MMP expression on mRNA and protein level in vitro (Malik & Kakar, 2006) and in human gliomas (Yan et al., 2015). PTTG is identical to the human securin gene and not only controls sister chromatid separation during metaphase (Zou et al., 1999) but also regulates many other cellular functions such as DNA repair, gene regulation and cell transformation (McCabe et al., 2003; Zhang et al., 1999; Pei, 2001; Romero et al., 2001). In transgenic mice, tumors developed at the PTTG injection site within only 3 three weeks (Pei & Melmed, 1997), suggesting a causal relationship. Besides induction of MMPs, this promoting effect of PTTG on tumor development and

progression is suspected to be caused by stimulation of fibroblast growth factor 2 (FGF-2) mediated vascular endothelial growth factor (VEGF) expression leading to increased tumor angiogenesis (McCabe et al., 2002). This hypothesis is supported by a meta-analysis of 15 studies with a total of 752 pituitary adenomas that demonstrated both microvessel density and PTTG expression to be higher in invasive adenomas compared to noninvasive adenomas (Li et al., 2014). In a series comprising of 45 pituitary adenomas, PTTG was found to be significantly correlated with Ki-67 and a PTTG/Ki-67 score of >2.9% reliably predicted aggressive behavior (Filippella et al., 2006). Another study showed increased PTTG expression levels in invasive-aggressive adenomas compared to noninvasive ones, however without statistical significance and featuring only functional PRL-producing adenomas (Wierinckx et al., 2007).

p53

Widely known as “guardian of the genome” (Lane, 1992), p53 plays a central role in cell proliferation. The tumor suppressor protein can induce apoptosis in damaged cells. Mutations of the encoding *TP53* gene can lead to malfunctions of the p53 protein and the resulting loss of cell cycle control can support malignant degeneration of a cell (Kanapathipillai, 2018; Luo et al., 2017)

A study in 1996 linked immunopositivity of mutated p53 to aggressive behavior of pituitary adenomas, the proportion of p53 expression in noninvasive adenomas, invasive adenomas and pituitary carcinomas being 0, 15.2 and 100% respectively (Thapar et al., 1996b). This conclusion conforms with the findings of a study on prolactinomas where p53 was statistically different in 5 aggressive-invasive entities compared to tumor variants with a benign clinical course (Wierinckx et al., 2007). Other studies have had conflicting results. One study only found p53 levels to be elevated in premetastatic or metastatic pituitary tumors, but not in invasive adenomas compared to noninvasive forms (Scheithauer et al., 2006). Canadian scientists demonstrated that recurrent adenomas do not have a significantly different p53 LI than nonrecurrent adenomas (Hentschel et al., 2003). The reason for these conflicting results could be due to the fact that standardized methods for the quantification of p53 values are lacking (Chesney et al., 2017).

Ki-67

Ki-67 is a nuclear antigen detectable with the molecular immunology borstel 1 (MIB-1) antibody and is present in all dividing cells as a marker of cell proliferation. This means it can be detected in all stages of the cell cycle except the G0 phase (Paek et al., 2005). As early as in 1989, there were first indications that adenomas with dural infiltration have higher proliferation activity measurable with a higher Ki-67 value than noninvasive adenomas (Knosp et al., 1989). These findings let to numerous studies focusing on Ki-67 in pituitary adenomas in the following years with partially variable results and controversy regarding the implications of a high Ki-67 value. In a series of 159 samples in Brazil, Ki-67 appeared to be significantly higher in invasive adenomas than in macroadenomas without invasion and the authors were able to additionally exclude age-related and gender differences as confounding factors (Pizarro et al., 2004). Other studies, however, reported that Ki-67 only correlates with growth velocity which itself is independent from invasive behavior (Honegger et al., 2003) or that there is no correlation at all between Ki-67 values and invasive behavior and recurrence rates, at least not in thyrotroph adenomas (Angelis & Cappabianca, 2014). In 1996, Thapar et al. proposed a cutoff LI of 3% for Ki-67 to differentiate invasive from non-invasive adenomas with a 97% specificity and 73% sensitivity (Thapar et al., 1996a). The sensitivity was then criticized as too low and therefore not useful for all types of pituitary adenomas as each one needs individual threshold values (Righi et al., 2012). As a matter of fact, owing to an overlap of Ki-67 values between invasive and noninvasive adenomas which hinders differentiation of these two groups (Pizarro et al., 2004), the proposed Ki-67 LI thresholds range from 1.5 to 4% in the literature (Miermeister et al., 2015; Chiloiro et al., 2015; Chesney et al., 2017). In their guidelines for the management of aggressive pituitary adenomas (Raverot et al., 2018), the European Society of Endocrinology sums up the current state of scientific knowledge. It states that Ki-67 appears to be the most frequent positive marker for aggressive behavior in pituitary adenomas. Nevertheless, the variable research results indicate that it is not sufficient as a sole marker for invasive behavior (Raverot et al., 2018).

H3K27me3 and H3K36me3

Trimethylation of lysine 27 on histone H3 (H3K27me3) and of lysine 36 on histone H3 (H3K36me3) are epigenetic modifications, changes within the chromatin organizing structures without changing the DNA sequence itself (Nichol et al., 2016). Depending on the degree of methylation, these modifications can lead to repression or activation of gene transcription (Varier & Timmers, 2011). In pediatric pontine gliomas somatic missense mutations of histone 3 with lysine 27 to methionine change (H3K27M) lead to reduced H3K27 methylation (H3K27me) and have been shown to be predictive of short survival compared to wildtype for histone 3 (Khuong-Quang et al., 2012; Sturm et al., 2012). Similarly, a substantial amount of giant cell tumors of the bone and chondroblastoma harbor missense mutations of histone 3 with lysine 36 to methionine change (H3K36M), also resulting in reduced H3K36me (Behjati et al., 2013; Nichol et al., 2016). Contrary to that, a study on B cell lymphomas found mutations leading to elevated trimethylation of H3K27me (H3K27me3) to be causative for repression of genes required for differentiation, thereby promoting malignancy (Béguelin et al., 2013). Two complexes of the Polycomb (PcG) protein family, PRC1 and PRC2, and their core component enhancer of zeste homologue 2 (EZH2) catalyze di- and trimethylation of H3K27me (Nichol et al., 2016; Schuettengruber et al., 2011). So far, only two studies have examined histone methylation status and expression of its catalytic proteins in pituitary adenomas. High EZH2 expression had a positive correlation with the proliferation marker Ki-67 in a study on 163 pituitary adenomas and two pituitary carcinomas, but no statistically significant association with an invasive growth pattern (Schult et al., 2015). Despite that, another study of 103 pituitary adenomas of different subtypes demonstrated significantly elevated H3K27me levels in invasive compared to noninvasive pituitary adenomas (Xue et al., 2017).

SPARC/Osteonectin

The secreted protein acidic and rich in cysteine (SPARC), also known as osteonectin or basement-membrane protein 40 (BM-40), is a matricellular glycoprotein whose expression is limited to areas of extracellular matrix (ECM) turnover (Brekken & Sage,

2000). Besides the ability to bind ECM proteins and modulation of proliferation by regulation of growth factors such as VEGF or FGF, SPARC also affects MMPs (Brekken & Sage, 2000; Bradshaw & Sage, 2001; Gilles et al., 1998). Unsurprisingly, these functions of SPARC have been linked to prognostically unfavorable effects in tumor microenvironments (Chlenski & Cohn, 2010). There is considerable amount of evidence that SPARC has prognostic impacts and influences cellular invasion in multiple solid tumor entities (Drev et al., 2019; Zhang et al., 2020; Guweidhi et al., 2005; Rossi, Gnanamony & Gondi, 2016; Amaral et al., 2018) as well as brain tumors like medulloblastomas, meningiomas, craniopharyngiomas or gliomas (Shi et al., 2007; Schultz et al., 2002; Wirthschaft et al., 2019; Yang & Li, 2020; Rempel, Ge & Gutiérrez, 1999; Ebrahimi et al., 2013). Multiple in vivo studies significantly correlated SPARC expression with invasion of gliomas. The invasion of white matter structures by human glioblastoma cells injected into mice brains appeared to be dependent on the expression of SPARC in one trial (Wirthschaft et al., 2019). In another study, artificially decreasing SPARC expression in two glioma cell lines with the help of siRNA interference also lead to a decrease of cellular invasion (Shi et al., 2007). Results of studies on a potential role of SPARC on the invasive potential of meningiomas are inconclusive. In one series, SPARC expression was negative in 9 benign, noninvasive meningiomas but positive in 20 invasive, recurrent tumors (Rempel et al., 1999). However, in more recent findings, SPARC expression lacked a significant correlation with meningioma malignancy grade and was not able to distinguish invasive from noninvasive (Schittenhelm et al., 2006). Different from that, in an immunohistochemical evaluation of 43 craniopharyngiomas, high SPARC expression significantly correlated with increased rates of recurrence and brain infiltration (Ebrahimi et al., 2013). Studies on SPARC expression in pituitary adenomas are scarce and did not enclose large patient cohorts in the past. So far, one comparison of 25 noninvasive with 15 invasive adenomas according to the Hardy classification did not detect any relation of invasiveness with SPARC expression (Onoz et al., 2015).

1.7. Aim of This Project

Some pituitary adenomas show an aggressive behavior which worsens their clinical course. Previous studies have shown that the value of many immunohistochemical markers, which are thought to be associated with aggressive behavior, are still not clinically established. That means that there is still no systematic risk stratification by histopathological features of a pituitary adenoma's probability of recurrence or progression in the clinical routine so far.

By assessing the immunohistochemical profile of almost 1.000 pituitary adenoma specimen, our project aims at finding reliable information about the predictive value of a selection of possible markers for aggressiveness. In the long term, we hope that patients that have been operated on will be able to know their individual risk of relapse allowing them an enhanced aftercare. Besides, relevant markers may provide as a pharmacological target structure in the future.

2. Materials and Methods

2.1. Patient and Clinical Data Acquisition

This study included patients who presented to the Department of Neurosurgery of the University Hospital Tübingen for surgical treatment of a pituitary adenoma between 1st October 2004 and 6th April 2018. Considered were primary and recurrent cases that were surgically removed using a transsphenoidal or transcranial approach. All cases were pseudonymized and the associated clinical information was organized in a list. Tumor tissue and clinical data were used for this study in accordance with the Ethics Committee of the Faculty of Medicine Tübingen (Projekt-Nr. 263/2018BO2, 23th April 2018). Existence of signed patient consent forms for scientific use was verified for cases since 1st January 2009. With agreement of the Ethics Committee, we abstained from a retroactive request for consent for all cases that date further back. Signed consent was absent in 43 cases. The neuropathological reports as well as clinical records and radiographic images were reviewed and the following data were collected: patient date of birth and age at diagnosis, patient gender, histopathological diagnosis and immunohistochemical markers of adenoma differentiation (aSU, FSH, LH, PRL, ACTH, GH, TSH, MIB-1, p53), date of surgery, operating surgeon, primary or recurrent treatment, intraoperative aspects of invasive growth, presenting symptoms, transsphenoidal or transcranial approach, extent of resection (by intraoperative assessment and radiologically with postoperative MRI), adenoma consistency, complications and their management (surgical material for closure or hemostasis, drainages, revision surgery). Apart from the intraoperative aspects of invasive growth, a supplementary radiological evaluation of invasiveness was conducted (Dr. med. Isabella Nasi-Khordisti, Department of Neurosurgery, University Hospital Tübingen). For this purpose, MR images were rated using the Knosp scale to grade invasion of the cavernous sinus (grades A-F) as well as dichotomized scales for invasion of the paranasal sinuses and suprasellar growth (0 = no invasion of paranasal sinuses/no suprasellar growth, 1 = invasion of paranasal sinuses/suprasellar growth). Postoperative follow-up data was collected to detect recurrences and determine recurrence-free survival times. Exclusion criteria of cases were incomplete clinical data, unavailable tissue samples and insufficient

viable tissue amount. The process of case selection is depicted in detail in a consort diagram in the next chapter (Figure 3.1.). In total, 927 cases were included for immunohistochemical analysis in this study.

2.2. Tumor Specimen Selection

In collaboration with the Department of Neuropathology of the University Medical Center Tübingen, paraffin-embedded tumor samples were obtained from the department's tissue bank and suitability for tissue microarray (TMA) processing and immunohistochemistry was assessed. All specimens were derived from therapeutic surgical primary or recurrent tumor resections. Only cases with the doubtless diagnosis of a pituitary adenoma were included in this study. The diagnoses were made histopathologically according to the criteria of the WHO Classification of Tumors of Endocrine Organs (Lloyd et al., 2017; DeLellis, 2004). Special attention was put on assuring that a sufficient amount of viable tumor tissue was present in the tissue sample in order to allow for the evaluation of representative tumor tissue via TMA processing. Therefore, the hematoxylin and eosin section (HE-sections) of each case were sent to Prof. Dr. med. Jens Schittenhelm and microscopically evaluated in detail. Samples were only considered eligible if they depicted the diagnostic histopathological criteria of the tumor and if these areas were large enough in size for sample cylinder extraction. Paraffin-embedded tissue samples with little tumor tissue or which mainly consisted of necrosis or blood were excluded from further work-up. The most suitable areas for sample cylinder extraction were marked on HE-sections. By projecting this marked area on an HE-section onto the paraffin-embedded tissue an exact location for tissue extraction during tissue microarray processing became identifiable (see Figure 2.1.).

2.3. Tissue Microarray Processing

Tissue microarray is a well-established and widely used method in oncologic pathology that allows for an optimized comparative analysis of high numbers of tumor samples. Small stains of several paraffin-embedded tumor samples are merged onto one paraffin block and can, after subsequent processing, be conveniently evaluated and compared on one microscopic slide. The main advantage of the method is that a large number of samples can be analyzed in a fast and cost-effective manner with very good comparability of identically stained tissue samples of the same size.

2.3.1. Layout of a Tissue Microarray Recipient Block

Each recipient block was labeled and numbered on its side for distinct identification and held up to 57 slots with a diameter of 1 mm. Pituitary adenoma tissue was vertically placed into 9 columns, each column held 6 slots. The majority of samples contained enough tissue for two slots. A tenth column held 3 slots for controls. Metastases of a breast carcinoma and of a renal clear cell carcinoma served as neoplastic controls and cerebral tissue of the temporal lobe derived from epilepsy surgery was used as a non-neoplastic control (see Figure 2.2.).

2.3.2. TMA Manufacture

The TMA procedure consists of two steps which are repeatedly done in the same manner. First is the creation of a slot with a 1mm-bore biopsy puncher on the recipient block at a defined array coordinate. Following that, a representative region of a sample on the donor block is punched out with a second 1mm-bore biopsy puncher and placed into its designated slot. The representative region on a donor block is localized by reviewing the areas of interest previously marked on a corresponding HE slide (see Figure 2.1.). Special attention was put on keeping equal and sufficient distances between neighboring slots to prevent the paraffine of the recipient block from cracking. To achieve an even surface for

ideal microtomy, samples were accurately adjusted for an exact fit into their slots. During TMA processing large overlaps were carefully removed with a scalpel. In addition to that, when all slots of a block had been entirely filled, the block was incubated at 40°C for 2 minutes. This served to soften the paraffin and increase the purchase of all samples in the recipient block's paraffin. A flat metal object was then mildly and uniformly pushed onto the surface of the block which ultimately established a level surface of the samples and their respective recipient block. To increase representativity of our 1mm biopsy cores for whole sections and counteract the effect of tumor tissue heterogeneity, two tissue samples per case were obtained whenever possible. In case of uncertainty of tissue quality within a whole section, three samples per case were attained. By the end of the TMA procedure, of the 927 pituitary adenoma cases which were declared suitable for this study, 2,013 tissue samples were obtained and fitted onto 38 tissue microarray blocks.

Table 2.1.: Materials used for TMA procedure and microtomy.

Material	**Provider**
Paraffin	SAV LP[1]
Paraffin Embedding Machine	Thermo Fisher Scientific[2]
Tissue Microarrayer	Beecher Instruments[3]
1.00mm Biopsy Punch	Estigen[4]
Microtome	Thermo Fisher Scientific
Microtome blades	pfm medical[5]
Incubator	Memmert[6]

[1] SAV LP GmbH, Flintsbach am Inn, Germany
[2] Thermo Fisher Scientific Inc., Waltham, MA, USA
[3] Beecher Instruments Inc., Sun Prairie, WI, USA
[4] Estigen OÜ, Tartu, Estland
[5] pfm medical ag, Köln Germany
[6] Memmert GmbH + Co.KG, Schwabach, Germany

Figure 2.1.: Example of marked HE section and corresponding stained Paraffin block.

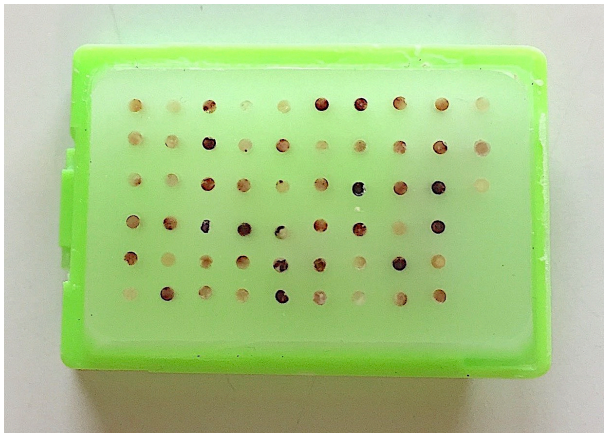

Figure 2.2.: Finished TMA block right before microtomy.

2.4. Microtomy

Finalized TMA blocks were further processed with a microtome. In advance of placement into the microtome, a TMA block was put facedown on a -20°C cooling plate. By this means, the wax turned harder which stabilizes tissue samples within a block and enabled thinner cutting. The congealed block was then fixed with an object clamp to the microtome and positioned in a way that the entire surface of the block evenly met the cutting edge of the microtome blade. Trimming of blocks at a thickness of 10µm was performed until first sample cylinders were obtained. After adjusting the cutting thickness to 3µm, the actual paraffin sections for immunohistochemical staining were cut. To fully expand, these sections were placed on a distilled water surface at a temperature of 50°C for 20-30 seconds. Finally, the sections were put on glass slides with forceps and dried for 24 hours at room temperature in an upright position. Debris on the microtome blades was frequently removed with brushes and the distilled water skimmed to avoid degradation of section quality. A total of 20 unstained paraffin sections were cut out of

one TMA block. HE staining was done with the first sample section of each TMA block to assess the quality and tumor content of the sample.

2.5. HE Staining

HE staining consists of two separate dyeing steps. After microtomy, each section of the paraffin-embedded tumor samples was deparaffinized by incubating at 59°C followed by three cycles of bathing in xylene for 10 minutes each. Sections were subsequently hydrated in 100% alcohol twice for 5 minutes and in a serial dilution of 96% and 70% alcohol 5 minutes each. Hydration was completed with distilled water which leached alcohol out for 3 minutes. Sections were now prepared for the first dye with Mayer's hemalum and were therefore bathed in it for 90 seconds. Hemalum is a combination of aluminum ions and oxidized hematoxylin, and as a basic agent stains basophilic structures like nuclei. Excessive non-adhering hemalum was rinsed off three times with distilled water. After placing the sections in tap water for 10 minutes, nuclei showed their characteristic blue color. For the second dyeing step with eosin, sections were then bathed in 0.1% erythrosine solution for 90 seconds. Eosin is an acidic synthetical dye which stains the mostly eosinophilic cytoplasm in different shades of pink color. Sections were dehydrated in a serial of alcohols again, this time in an ascending order (70% and 96% 5 minutes each and 100% twice for 5 minutes.). For the purpose of losing water solubility, sections were placed in xylene for 10 minutes. In a final step, stained sections were placed on microscope slides, mounted with HICO-MIC and fixated with cover glasses.

Table 2.2.: Materials used for HE staining.

Material	Provider
0.1% Erythrosine	Merck[1]
Mayers hemalaum	Merck
HICO-MIC mounting agent	HICO Medical systems[2]
Xylene	AppliChem[3]
Isopropyl alcohol	Alkoholvertrieb Süd[4]
SuperFrost Adhesive Glas Slides	R. Langenbrinck[5]
Incubator	Memmert[6]

2.6. Immunohistochemistry

Indirect immunohistochemistry (IHC) was used to detect and comparatively analyze the antibodies MIB1, H3K27me3, H3K36me3 and osteonectin (also known as secreted protein acidic and rich in cysteine or SPARC) in this study. Figure 2.3. illustrates the concept of indirect IHC. A primary antibody is targeted at the respective antigen of interest and binds to it with its antigen-binding fragment (Fab) region. Accordingly chosen to the origin of the primary antibody (mouse, rabbit, etc.), a secondary antibody binds to the constant fragment (Fc) region of the primary antibody. Originally, secondary antibodies contained biotin molecules whose high affinity for avidin-bound enzymes linked them to avidin horseradish peroxidase (HRP) complexes. For this study, a newer technique was utilized. HRP was bound to a polymer instead of avidin which is advantageous as it enabled significant signal amplification. The addition of H_2O_2, the substrate of peroxidase, and 3,3'-diaminobenzidine (DAB) to the tissue sample leads to the oxidation and precipitation of DAB. When oxidized, DAB precipitates and causes a characteristic brown discoloration of the tissue.

[1] Merck KGaA, Darmstadt, Germany
[2] HICO Medical Systems – Hirtz & Co.KG, Köln, Germany
[3] AppliChem GmbH, Darmstadt, Germany
[4] Alkoholvertrieb Süd GmbH, Nagold, Germany
[5] R. Langenbrinck GmbH, Emmendingen, Germany
[6] Memmert GmbH & Co.KG, Schwabach, Germany

This reaction results in a highly reliable chromogenic detection of antigens as it is restricted to areas where primary and secondary antibody have successfully bound to the antigen of interest.

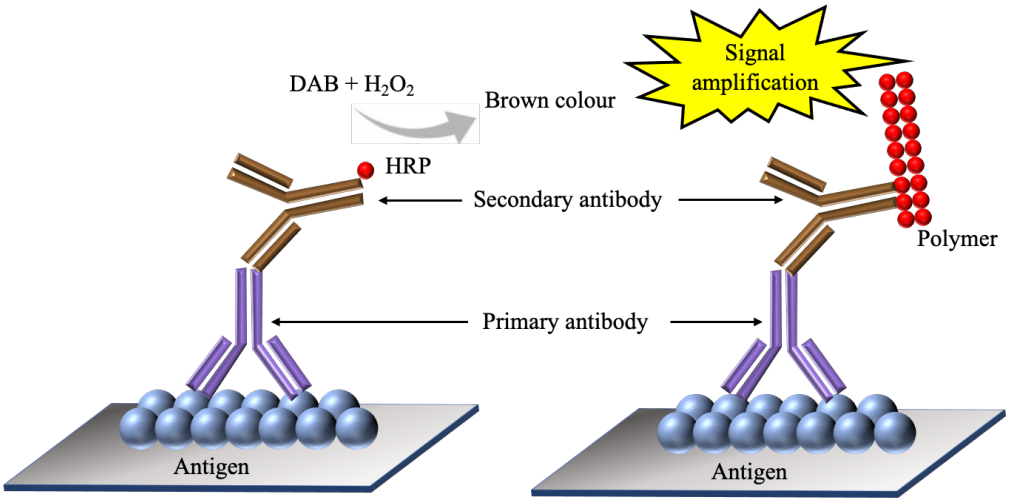

Figure 2.3.: Illustration of indirect immunohistochemistry and signal amplification by HRP polymers.
DAB: diaminobenzidine, HRP: horseradish peroxidase
Adapted from: Kim et al., 2016

The immunohistochemical staining process of the tissue samples included in this study was fully automated using Roche's Benchmark XT device for the purpose of increased reproducibility compared to manual processing. With full automation of the entire process, exact dosages of reactive agents and durations of reactions or incubation were predetermined. The following passage is designed to provide a better understanding of each working step of the IHC machine during the process. Exactly as prior to the HE staining, the first step is the deparaffinization and hydration of the samples. The dried sections derived from microtomy were placed on heating pads to melt the paraffin and subsequently bathed in xylene as well as 100% alcohol and dilutions of 90%, 70% and 50% in consecutive order. Rinsing with distilled water finished off the deparaffinization process. Next, two cell conditioning solutions, a basic tris-buffer-based CC1 and a slightly acidic citrate-buffer-based CC2, the latter only for the osteonectin antibody, served as antigen retrieval agents and were applied at an approximate temperature of 95°C for 10-20 mins. This heat-induced protein denaturation by loss of covalent bonds caused by formalin fixation led to an increase of antibody binding capacity.

Following the antigen retrieval, endogenous peroxidase activity was blocked with the help of 3% hydrogen peroxide. This step was crucial in preventing false positive results as exogenous peroxidase was later used to detect the antigen of interest.

Another potential source of false positive results was eliminated by adding sera to the sample as this prevents non-specific antibody binding. A diluted tris-based reaction buffer solution constantly maintained humidity within the IHC machine reaction chamber to avoid drying and damage of tissue and was also used to wash the samples in-between each step. An air vortex mixer and liquid color slip, a protective layer placed on top of a sample to cover the reactive agents, ensured homogenous distribution of all applied agents during the process.

During the central step of the procedure, the samples were incubated with the respective primary antibodies for a predetermined duration at the ideal temperature, precisely following the laboratory protocol (MIB-1 20 mins at 42°C, H3K27me3 and H3K36me3 antibodies 32 mins at room temperature, Osteonectin 32 mins at room temperature). Subsequently, diluted secondary antibodies matching the origin of the primary antibodies (mouse, rabbit etc.) were applied to bind to the primary antibodies. Treatment with an HRP polymer complex was followed by the development process, for which DAB was added to the samples. The developing process was stopped with a thorough wash with distilled water. Hematoxylin was used to counterstain the nuclei as a means of contrast enhancement between immunohistochemically detected antigens and other cellular structures. Dehydration of the samples was achieved by a repeat of the steps of the deparaffinization process in a reverse order. Samples were washed with distilled water and bathed in 50%, 70%, 90% and 100% alcohol as well as xylene, consecutively. The stained slides were mounted with HICO-MIC mounting agent and finally fully processed to undergo thorough microscopic evaluation.

Table 2.3.: Materials used for immunohistochemistry.

Material	**Provider**
Benchmark XT	Ventana Medical Systems[1]
OptiView DAB IHC Detection Kit • Citric acid monohydrate • CC1: tris-based buffer and preserving agent • CC2: citrate buffer and ProClin3000 preserving agent • Horse raddish peroxidase (HRP) • Hydrogen peroxide • H_2O_2 • DAB • Ethylenediaminetetraacetic acid (EDTA) • Liquid Color Slip (LCS)	Ventana Medical Systems
Antibody diluent	Zytomed Systems[2]
Hematoxyline	Thermo Fisher Scientific[3]
Xylene	AppliChem[4]
Isopropyl alcohol	Alkoholvertrieb Süd GmbH[5]
TOMO ICH Adhesive Glas Slides	Matsunami[6]
HICO-MIC mounting agent	HICO Medical systems[7]
Incubator	Memmert[8]

[1] Ventana Medical Systems Inc., Oro Valley, AZ, USA
[2] Zytomed Systems GmbH, Berlin, Germany
[3] Thermo Fisher Scientific, Waltham, MA, USA
[4] AppliChem GmbH, Darmstadt, Germany
[5] Alkoholvertrieb Süd GmbH, Nagold, Germany
[6] Matsunami Glass USA Inc., Bellingham, WA, USA
[7] HICO Medical Systems – Hirtz & Co.KG, Köln, Germany
[8] Memmert GmbH & Co.KG, Schwabach, Germany

Table 2.4.: Antibodies used for immunohistochemistry.

	Provider	Isotype	Dilution
Primary			
MIB1	Dako[1]	mouse	1:200
H3K27me3	Cell Signaling[2]	rabbit	1:200
H3K36me3	abcam[3]	rabbit	1:4000
Osteonectin	Haematologic Technologies[4]	mouse	1:4000
Secondary			
Anti-mouse	Ventana Medical		<50µg/ml
Anti-rabbit	Systems[5]		<50µg/ml
	Ventana Medical Systems		

2.7. Reassessment of Pituitary Adenoma Tissue Samples according to the Updated WHO Classification of 2017

Simultaneous to the immunohistochemical analysis of potential markers of aggressive adenoma behavior, our research group investigated the immunohistochemical expression of the antibodies for the transcription factors PIT-1, ER and of the LMWCK antibody CAM5.2 for all cases of our cohort. The assessment of these antibodies combined with the information on hormonal expression of tissue samples was sufficient for an exact subtype identification by a simplified scheme (see Figure 2.4.). This classification algorithm was developed by Prof. Dr. med. Jens Schittenhelm (Department of Neuropathology, University Hospital Tübingen), orienting itself and, though abbreviated, fully in accordance with the updated diagnostic criteria of the latest WHO Classification of Tumors of Endocrine Organs of 2017 (see Table 1.2.). Data gained by this means was used to examine potential correlations of specific subtypes with invasiveness or unfavorable prognosis. In 47 cases, poor staining quality or lack of data on hormonal expression hindered subtype identification. As a result, of the 927 adenoma samples

[1] Dako Deutschland GmbH, Hamburg, Germany
[2] Cell Signaling Technology Europe B.V., Frankfurt am Main, Germany
[3] Abcam, Cambridge, United Kingdom
[4] Haematologic Technologies, LLC, Essex Junction, VT, USA
[5] Ventana Medical Systems Inc., Oro Valley, AZ, USA

eligible for immunohistochemical analysis, a categorization into the exact subtype was possible in 880 adenomas.

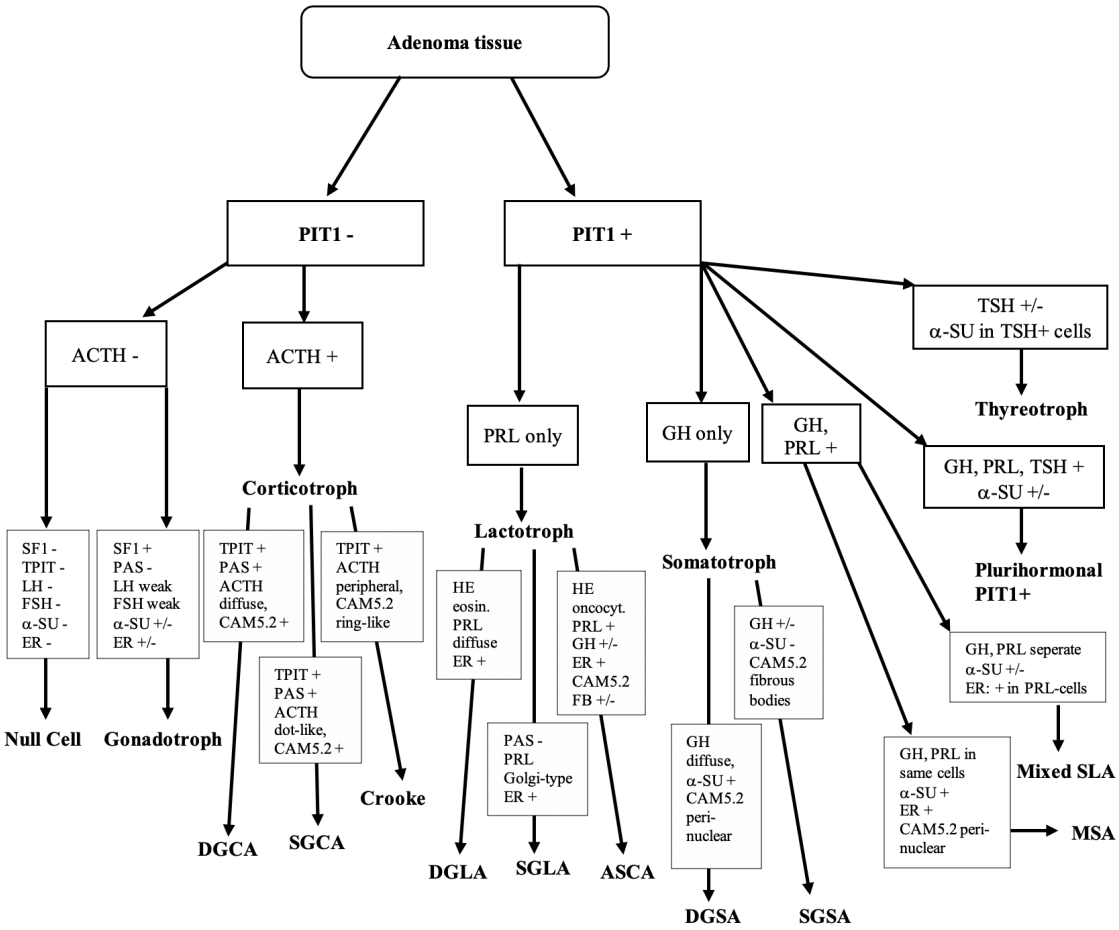

Figure 2.4.: Scheme of subtype classification according to WHO criteria of 2017.
PAS: periodic acid Schiff, FB: fibrous bodies
Adopted from: Prof. Dr. med. Jens Schittenhelm, Department of Neuropathology, University Hospital Tübingen

2.8. Microscopic Evaluation

HE and immunohistochemical stains were evaluated by light microscopy under 20-, 100-, 200- and 400-fold magnification. The Olympus C-35AD-4 camera attached to the Olympus Vanox AHBT3 light microscope was used to take microscopic images. Operation of the camera and processing of digital images was done with the IMS ImageClient software by Imagic Bildverarbeitung AG. Tumor samples were not

considered if less than one fifth of a cylinder's diameter contained properly stained viable tumor tissue. Potential reasons for exclusion were large areas of necrosis or hemorrhage within a sample, incomplete adhesion of a sample leading to tissue loss during microtomy and lack of tumor tissue cylinder in the slot at a particular sectioning level.

2.9. Quantification of Expression Levels

Tumor samples showed variable expression rates of the antigens of interest. Therefore, quantification of expression levels for each tumor marker that was considered in this study (MIB-1, H3K27me3, H3K36me3, osteonectin) was required for accurate statistical analysis. The expression pattern of MIB-1, H3K27me3 and H3K36me3 is nuclear and accounts for immunohistochemical staining which results in nuclear coloring.

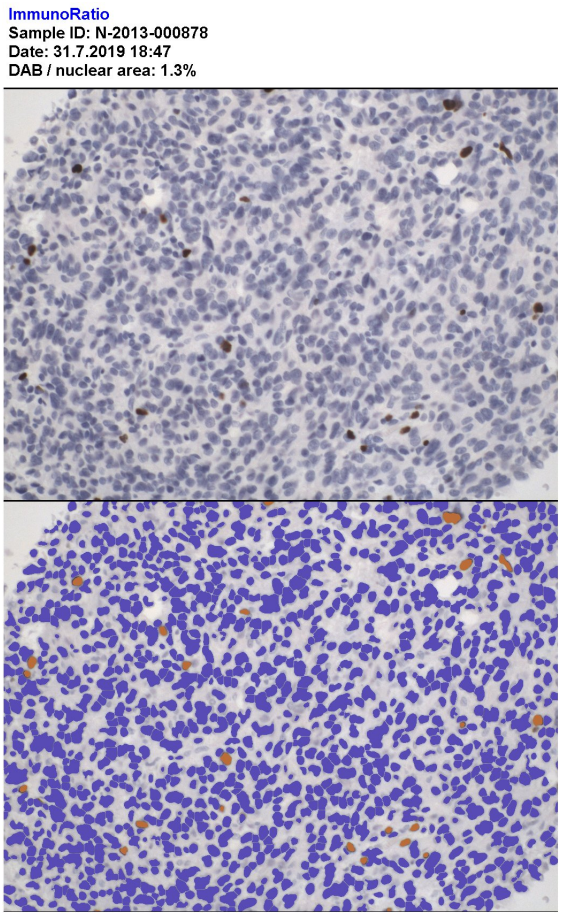

Determination of MIB-1 expression levels was done using digital images and the ImageJ software (see Figure 2.5.). Representative regions within a sample were located and photographed. The percentage of immunopositive nuclei was calculated with the help of the software.

Figure 2.5.: Quantification of MIB-1 immunopositivity.

Brown staining of nuclei resembles positivity for MIB-1. Color detection sensitivity by the software was adapted case-by-case to avoid false-positive results.

For the quantification of H3K27me3, in an initial microscopic overview of the respective sample, a representative region was chosen. Nuclei of endothelial cells within a sample which typically stain positive served as controls. A visual estimate of the percent range of positive nuclei of the tumor cells was then converted into a numeric score (Score 0 = 0 - <5% positive, 1 = 5 - <25%, 2 = 25 - <50%, 3 = 50 - <75%, 4 = ≥75%). Multiple stains of one case with different scores were summarized by mathematically correct rounding up. Figure 2.6. shows examples of quantifications of H3K27me3 expression using the described score. H3K36me3 was quantified accordingly (see Figure 2.7.).

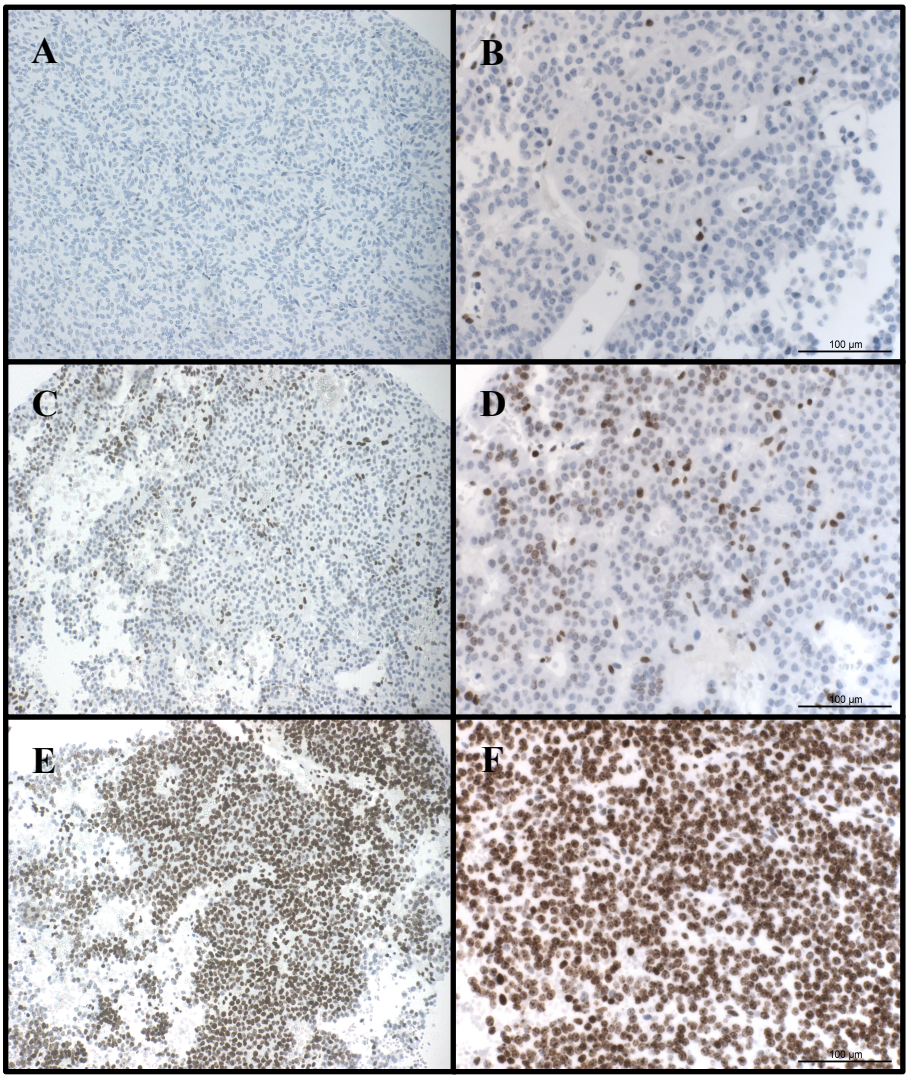

Figure 2.6.: Quantification of H3K27me3 immunopositivity.
Brown staining of nuclei resembles positivity for H3K27me3.
First row (A and B): Score 0 (0 - <5% of nuclei positive)
Second row (C and D): Score 2 (25 - <50% of nuclei positive)
Third row (E and F): Score 4 (≥75% of nuclei positive).
100-fold magnification on the left side, 200-fold magnification on the right side.

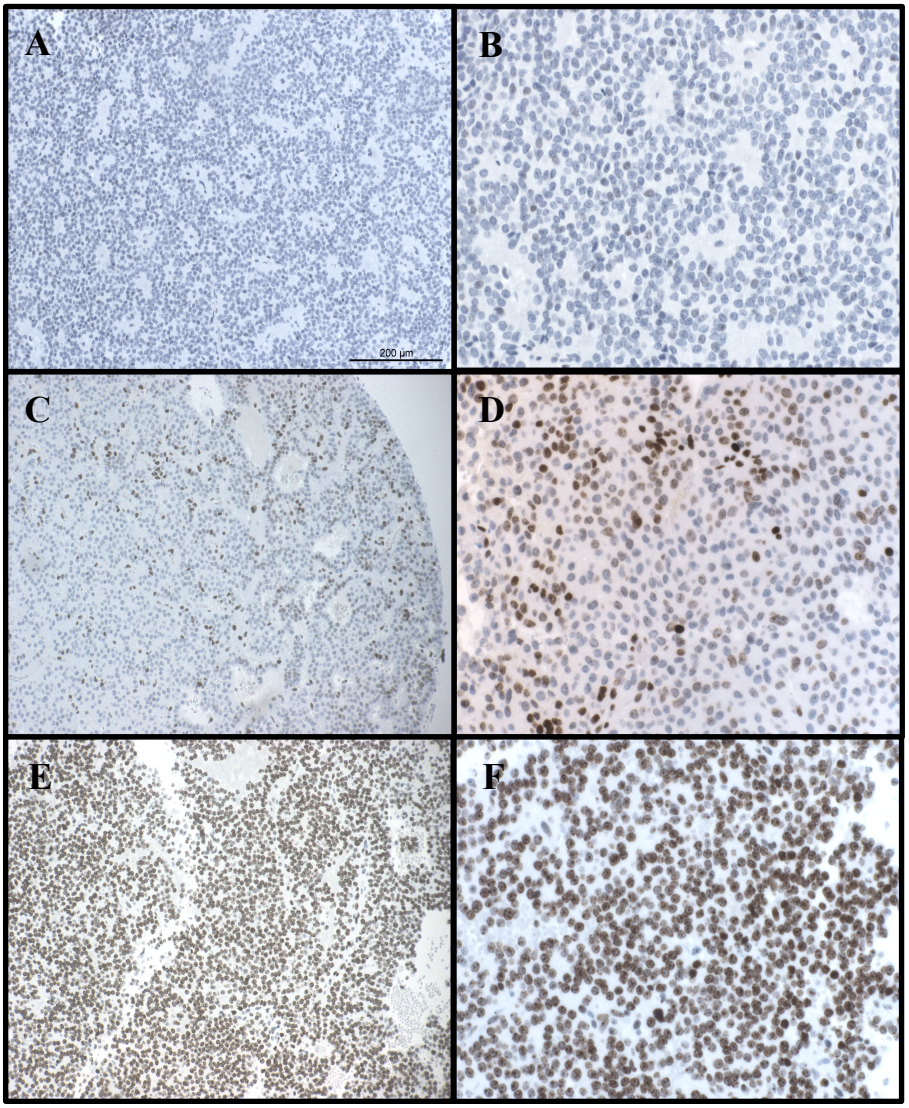

Figure 2.7.: Quantification of H3K36me3 immunopositivity.
Brown staining of nuclei resembles positivity for H3K36me3.
First row (A and B): Score 0 (0- <5% of nuclei positive)
Second row (C and D): Score 2 (25- <50% of nuclei positive)
Third row (E and F): Score 4 (≥75% of nuclei positive).
100-fold magnification on the left side, 200-fold magnification on the right side.

The assessment of osteonectin was more challenging due to its perinuclear staining pattern. An adapted version of an immunoreactive score (IRS) that was previously used in other immunohistochemical assessments (Boltze et al., 2009; Remmele et al., 1986; Ebrahimi et al., 2013) was applied to quantify the degree of osteonectin expression (see Figure 2.8.).

Composed of the product of a staining intensity score (1 = weak, 2 = medium, 3 = strong) and a percentage of positivity score (0 = 0 - <5% positive, 1 = 5 - <25%, 2 = 25 - <50%, 3 = 50 - <75%, 4 = ≥75%), the IRS was supplemented with information of the distribution pattern of osteonectin within a sample (see Figure 2.9.)

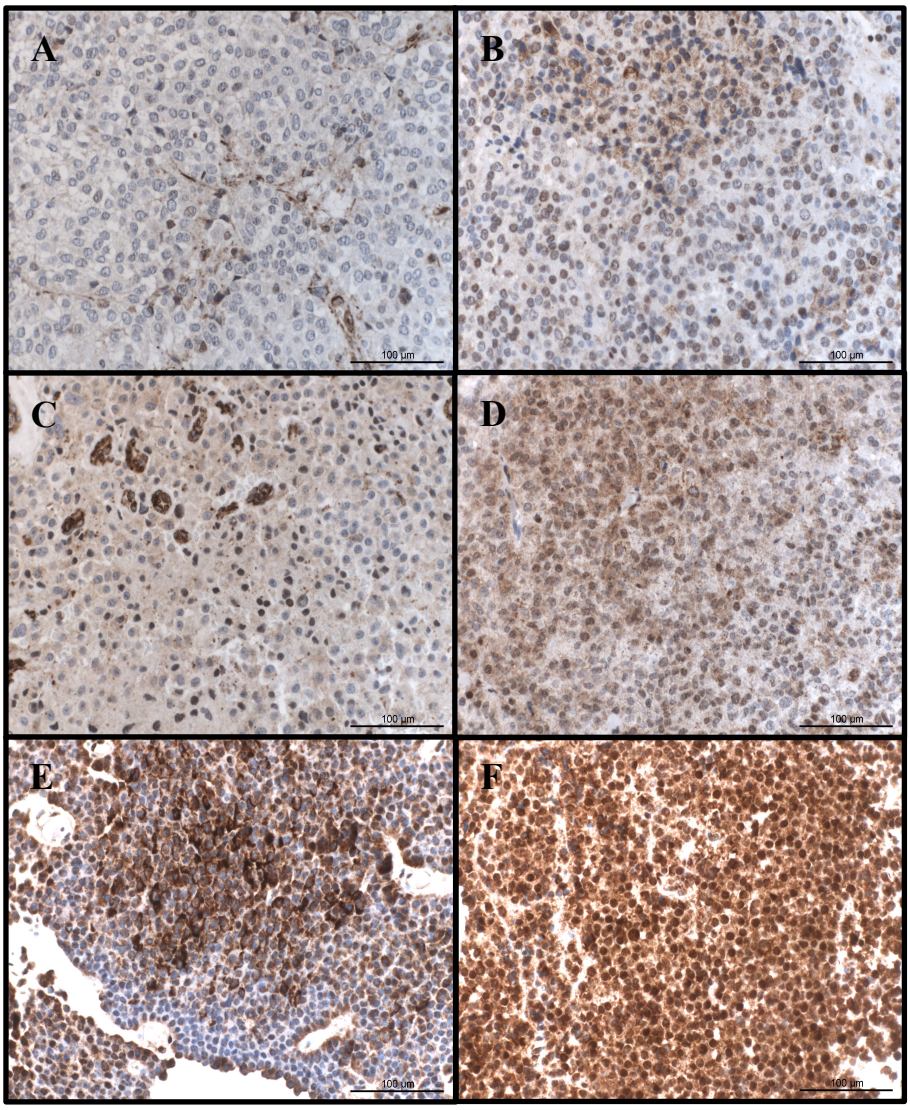

Figure 2.8.: Quantification of Osteonectin by using the IRS.
Brown perinuclear staining resembles positivity for osteonectin. 200-fold magnification.
A: IRS 0 (score 1 for intensity, score 0 for percentage of positivity). Only endothelial cells stain positive in this sample, this was a frequent false-positive finding.
B: IRS 1 (1 for intensity, 1 for percentage of positivity).
C: IRS 3 (1 for intensity, 3 for percentage of positivity). Besides the perinuclear expression of osteonectin, note the much stronger positivity of endothelial cells in this sample.
D: IRS 6 (2 for intensity, 3 for percentage of positivity).
E: IRS 9 (3 for intensity, 3 for percentage of positivity).
F: IRS 12 (3 for intensity, 4 for percentage of positivity).
In samples strongly positive for osteonectin (existent in D and F), cross reactions of the antibody with nuclear proteins can lead to accidental false-positive nuclear staining.

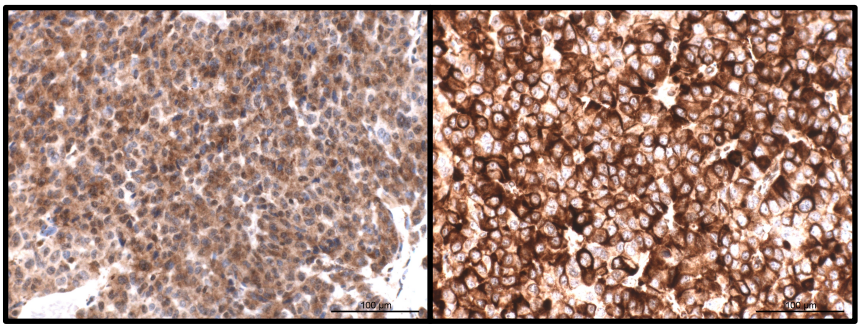

Figure 2.9.: Distribution pattern of Osteonectin.
Left: Membranous expression pattern.
Right: Cytoplasmatic expression pattern.
200-fold magnification.

2.10. Statistical Analysis

Assembly and organization of raw data and clinical information was done with Microsoft Excel Version 16.43. Statistical analysis was performed with JMP 15.0.0. The Gehan's Wilcoxon test was applied to assess statistical significance of Kaplan-Meyer curves. In the univariate analysis of gender and adenoma subtypes, as well as with the help of specific cutoffs for age at diagnosis and the immunohistochemical markers, data was dichotomized in nominal and ordinal variables and evaluated with the Pearson Chi^2 test. The independent two sample t-test was used to determine the impact of the clinical factor age at diagnosis. To define cutoffs for dichotomization for the variable age and the immunohistochemical markers, classification and regression tree (CART) analyses were conducted. For multivariate analysis, cox regression analysis and linear regression analysis was performed. The significance level was set at alpha <0.05.

Table 2.5.: Computer software used in this study.

Software	**Provider**
Microsoft Office 365	Microsoft[1]
IMS ImageClient	Imagic[2]
ImageJ	Wayne Rasband
JMP 15.0.0	SAS Institute GmbH[3]

[1] Microsoft Corporation, Redmond, WA, USA
[2] Imagic Bildverarbeitung AG, Glattbrugg, Switzerland
[3] SAS Institute GmbH, Heidelberg, Germany

3. Results

3.1. Characterization of Patient Cohort

The aim of this dissertation is to evaluate tumor markers and to detect potential correlations with clinical and prognostic parameters with a special emphasis on the aspect of tumor invasiveness. For this means, 1,220 cases of pituitary adenomas were studied by retrieval of their paraffin-embedded tumor sample and collection of clinical data from patients' files.

In total, 927 cases underwent further processing by TMA and immunohistochemistry. The initial cohort selection process is illustrated in Figure 3.1.

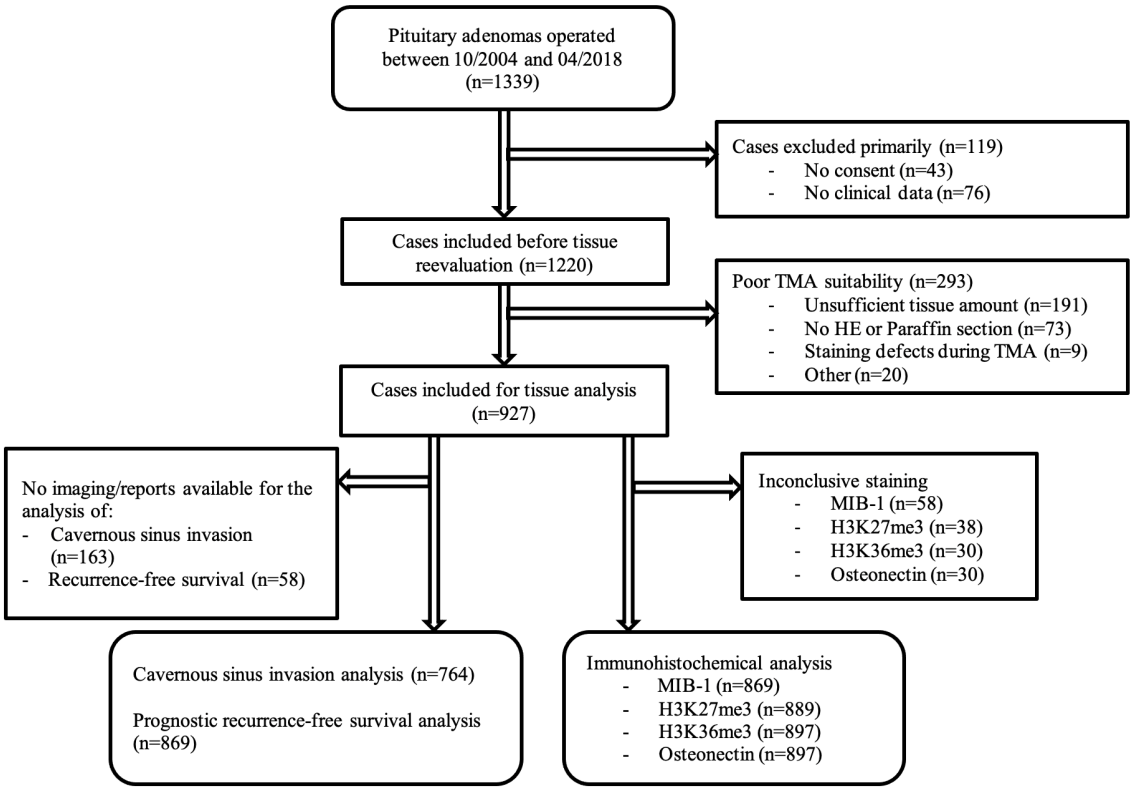

Figure 3.1.: Consort diagram showing excluded and included cases.

All patients of our cohort received surgical treatment. The vast majority of 1,181 cases was operated using a transsphenoidal approach (96.80%). Only for 37 pituitary adenomas solely a transcranial approach was chosen (3.03%) and for 2 tumors both surgical pathways were combined. By intraoperative assessment, complete macroscopic resection was achieved in 948 cases (79.53%), while in 244 cases (20.47%) only subtotal removal was feasible. Patients' files lacked clinical data regarding the extent of resection in 28 cases. Postoperative MRI was available for 1150 patients and detected residual tumor in 311 cases (27.04%).

The majority of patients were symptomatic at the time of diagnosis, either due to symptoms related to compression of surrounding anatomic structures or endocrinological abnormalities (see Table 3.1.). The most common main presenting symptom, that was encountered in 258 patients (21.15%), was visual field deficit. More than one third of patients suffered from endocrinological symptoms including the two syndromes acromegaly (225 patients, 18.44%) and Cushing disorder (147 patients, 12.05%). Less common symptoms were cephalgia, fatigue, vertigo or nausea and vegetative irregularities. There were 190 patients (15.57%) among the cohort who received cranial imaging for other reasons and in whom a pituitary adenoma was diagnosed as incidental finding.

Table 3.1.: Leading symptoms sustained by patients at the time of diagnosis.

Symptom or syndrome	**Number of cases (%)**
Visual field defects	258 (21.15%)
Acromegaly	225 (18.44%)
Cushing disorder	147 (12.05%)
Incidentaloma (= asymptomatic, diagnosis by chance)	190 (15.57%)
Cephalgia	102 (8.36%)
Sex hormone dysfunction (galactorrhea, amenorrhea, changes in potency and libido)	91 (7.46%)
Fatigue	41 (3.36%)
Vertigo, nausea	40 (3.28%)
Vegetative (fever, weight, hunger/thirst)	34 (2.89%)
Other	92 (7.54%)

Patients of our cohort had a mean age of 51.98 years at the time of diagnosis. While the youngest patient was 9 and the oldest 86 years old, approximately three fourth of patients were older than 40 years of age at the time of diagnosis (921 of 1,220 patients, 75.49%). Figure 3.2. provides a detailed overview of our cohorts' age distribution.

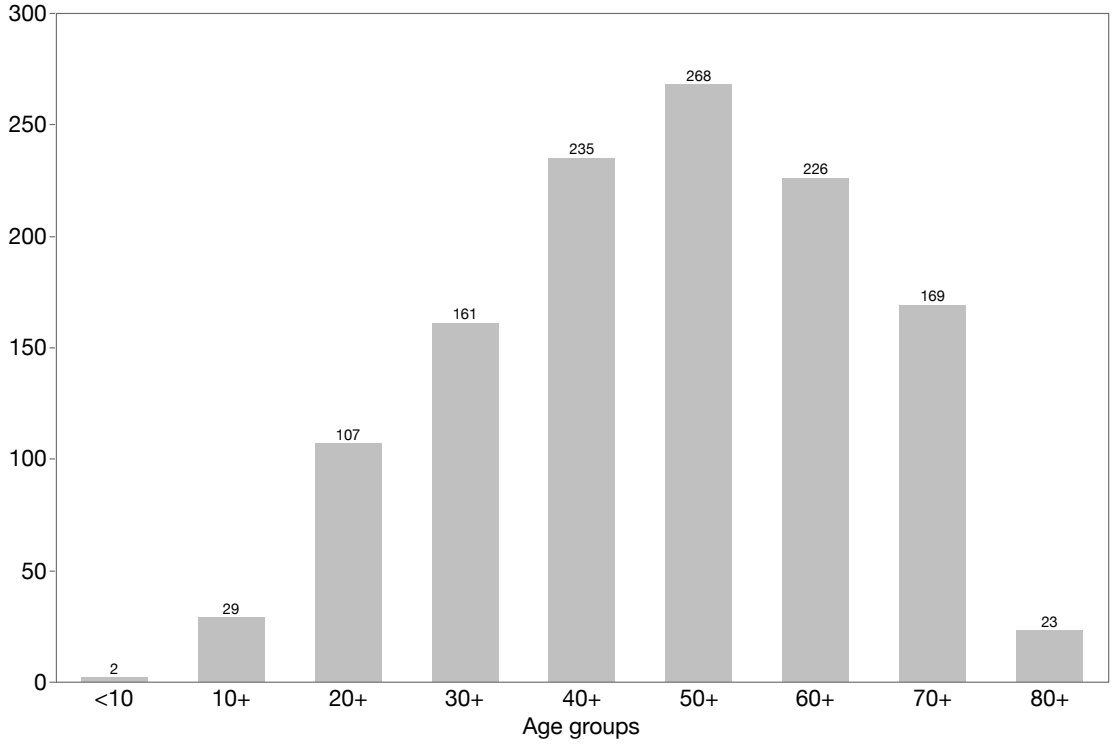

Figure 3.2.: Distribution of age at the time of diagnosis.

Our cohort comprised of 571 male and 649 female patients, resulting in a male-to-female incidence ratio of 0.87. With a mean age of 54.41 compared to 49.85 years of women, men were significantly older at the time of diagnosis (p=0.0001). As far as the surgical result is concerned, there was no significant difference between both genders regarding the rate of gross total resection (81.10% of female as opposed to 77.74% of male patients, p=0.1509).

The assembled data on hormonal expression of each adenoma, as well as immunohistochemical staining of the transcription factors PIT-1, ER and the cytokeratin antibody CAM5.2 allowed for an exact categorization of the cases of our cohort into adenoma subtypes. Figure 3.3. provides an overview of the adenoma types and Table 3.2. more detailed information on the different subtypes. In total, 880 of the 927 adenoma

cases eligible for tissue analysis could be categorized. In our surgical series, gonadotroph adenomas formed the largest fraction, amounting for 400 cases (45.45%). One fifth of adenomas were categorized into the three different types of somatotroph adenomas (189 cases, 21.48%). 89 lactotroph and 101 corticotroph adenomas each accounted for about one tenth of cases (10.11% and 11.47% respectively). Thyreotroph (9 cases, 1.02%), densely granulated lactotroph (DGLA, 9 cases, 1.02%) and Crooke cell adenomas (2 cases, 0.23%) made up the rarest subtypes.

Apart from gonadotroph adenomas (male-to-female ratio of 1.48), thyreotroph adenomas (2.0), DGLA (1.25) and DGSA (1.25), all other subtypes occurred more frequently in women than in men. By mean age at diagnosis, most subtypes were diagnosed during the fifth or sixth decade of life. The only exception was the occurrence of lactotroph adenomas at an average age of 41 years (SGLA mean age of 36, DGLA of 45, ASCA of 42 years). The rate of complete resection according to intraoperative estimation and postoperative MRI exceeded the 75% margin in all cases but DGLA, an entity which was completely resected in 55.56% of cases. Crooke cell adenomas and MSA had total macroscopic resection in 100% of cases, closely followed by a complete resection rate of 94.44% of the mixed SLA subtype.

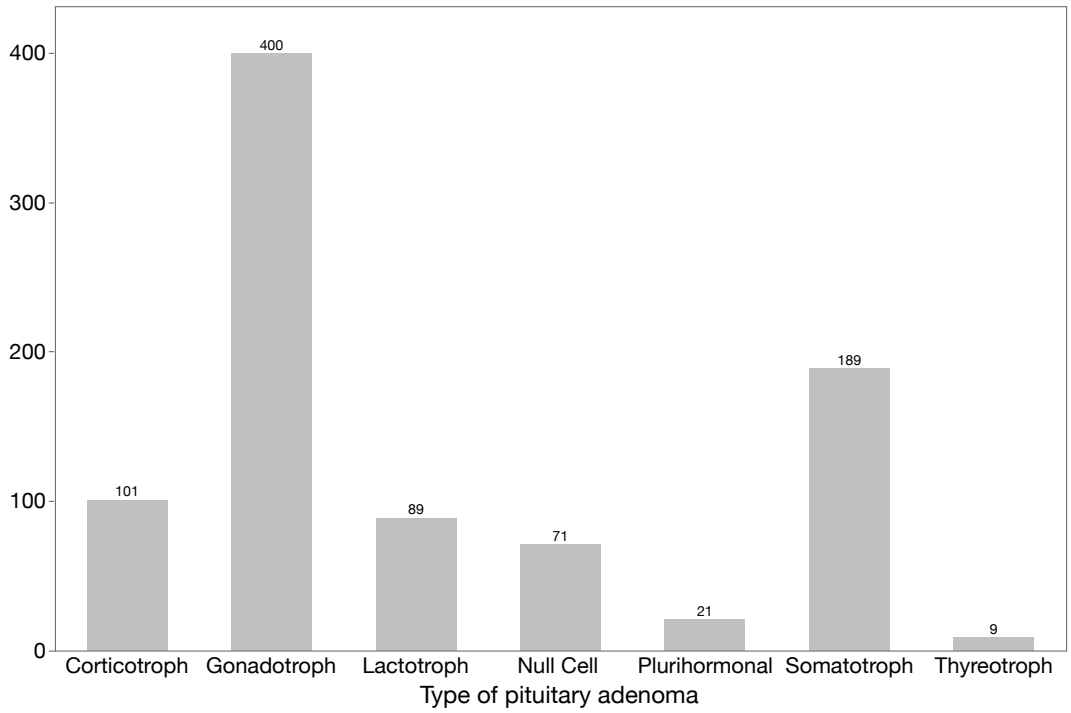

Figure 3.3.: Overview of pituitary adenoma types.

Table 3.2.: Distribution and clinical characteristics of adenoma subtypes.

	N (%)	N by Sex		Mean	Extent of resection	
		m	f	Age	% CR	% STR
Corticotroph	**101 (11.48%)**	**28**	**73**	**52**		
- SGCA	30 (3.41%)	8	22	54	79.31	20.69
- DGCA	69 (7.84%)	20	49	48	76.12	23.88
- Crooke	2 (0.23%)	0	2	54	100	0
Gonadotroph	**400 (45.46%)**	**239**	**161**	**60**	**78.46**	**21.54**
Lactotroph	**89 (10.11%)**	**32**	**57**	**41**		
- SGLA	64 (7.27%)	21	43	36	82.81	17.19
- DGLA	9 (1.02%)	5	4	45	55.56	44.44
- ASCA	16 (1.82%)	6	10	42	75.00	25.00
Null Cell	**71 (8.07%)**	**34**	**37**	**56**	**76.06**	**23.94**
Plurihormonal	**21 (2.39%)**	**8**	**13**	**50**	**85.71**	**14.29**
Somatotroph	**189 (21.48%)**	**89**	**100**	**49**		
- SGSA	75 (8.52%)	31	44	46	78.38	21.62
- DGSA	79 (8.98%)	44	35	49	83.33	16.67
- MSA	16 (1.82%)	7	9	50	100	0
- Mixed SLA	19 (2.16%)	7	12	50	94.44	5.56
Thyreotroph	**9 (1.02%)**	**6**	**3**	**56**	**100**	**0**

3.2. Assessment of Intraoperative Invasiveness

Among the total of 1,220 available surgical reports of pituitary adenomas, the presence of invasive growth was reported in 494 cases (40.49%) by the respective surgeon. Since only the 927 cases who underwent tissue analysis were taken into consideration for the following analyses, intraoperatively visible invasiveness was present in 395 cases (42.61%).

Differences of clinical parameters (age, gender, adenoma subtype) and associations with immunohistochemical markers (MIB-1, H3K27me3, H3K36me3 and osteonectin) of invasive tumors were assessed. For the numeric parameter of age as well as the immunohistochemical antibodies, classification and regression tree analyses (CART analyses) were run to mathematically identify suitable cutoff values (see Table 3.3.).

Table 3.3.: CART-proposed cutoffs for target variable invasiveness.

Parameter	CART-proposed cutoff
Age	71 years
MIB-1	0.6%
H3K27me3	1
H3K36me3	4
Osteonectin	No adequate cutoff

3.2.1. Age and Gender

Overall, patients with an invasive adenoma were slightly older in this study than patients with a noninvasive adenoma (mean age of noninvasive cases 52.41 years, mean age of invasive cases 54.44 years, p=0.0275, see Figure 3.4., Graph A). CART analysis revealed an age of 71 years at diagnosis as the optimal cutoff for this cohort. With statistical significance, patients older than 71 years at diagnosis had an invasive adenoma more frequently than patients in the younger group (p=0.0255). An invasive adenoma was present in 68 of 132 patients ≥71 years (51.25%) and in 327 of 795 patients <71 years (41.13%), a small but statistically significant difference (see Figure 3.4., Graph B).

There was no statistically significant difference of invasive growth according to gender (see Figure 3.4., Graph C). While 211 of the 462 male patients had an invasive adenoma (45.67%), an invasive adenoma existed in 184 of 465 female patients (39.57%, p=0.0604).

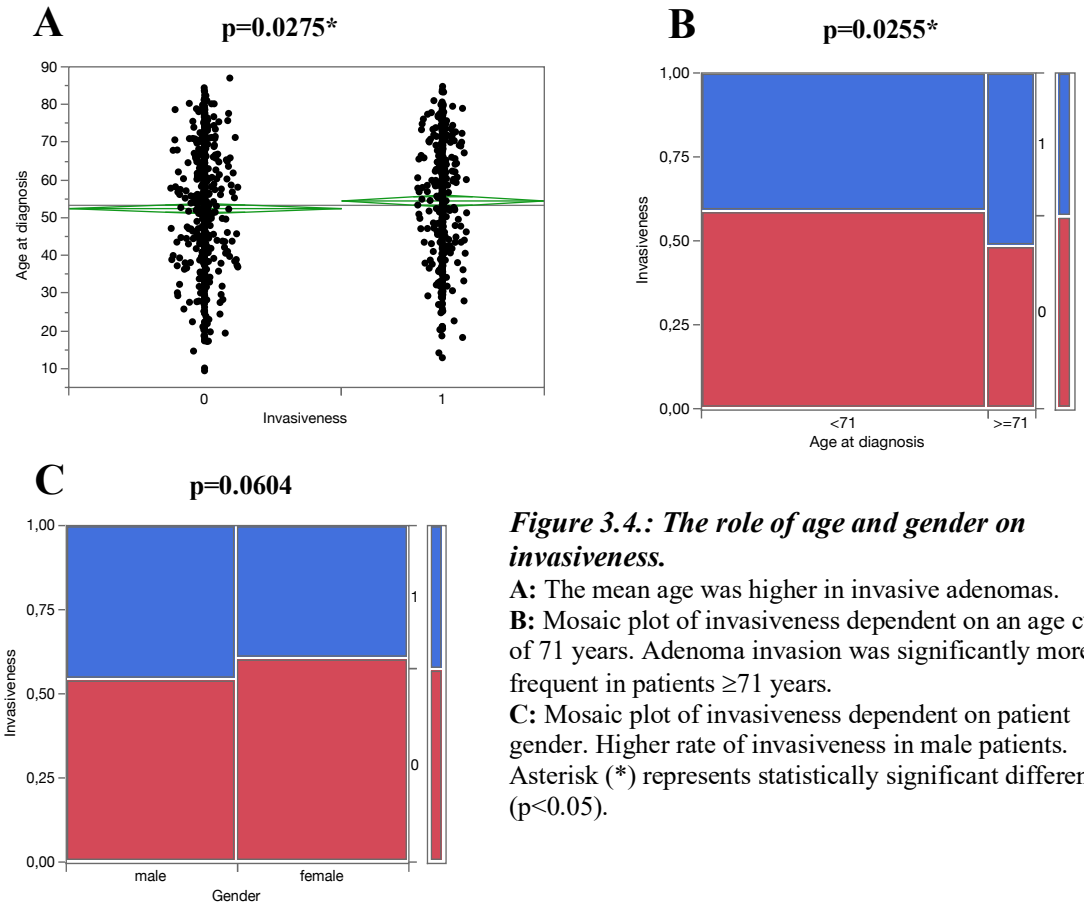

Figure 3.4.: The role of age and gender on invasiveness.
A: The mean age was higher in invasive adenomas.
B: Mosaic plot of invasiveness dependent on an age cutoff of 71 years. Adenoma invasion was significantly more frequent in patients ≥71 years.
C: Mosaic plot of invasiveness dependent on patient gender. Higher rate of invasiveness in male patients.
Asterisk (*) represents statistically significant differences ($p<0.05$).

3.2.2. Adenoma Subtype

The categorization of our cohort into adenoma subtypes is illustrated and described in chapters 2.7. and 3.1. in detailed fashion. Table 3.4. depicts the rate of invasiveness of each subtype in comparison to the rest of the cohort. Prevalence of invasiveness was variable and rates of invasive cases among the different subtypes ranged between 0% and 60%.

Subtypes that comprised of more invasive than noninvasive cases were SGCAs (18 invasive and 12 noninvasive), null cell adenomas (37 invasive and 34 noninvasive), DGLAs (5 invasive and 4 noninvasive) and SGSAs (38 invasive and 37 noninvasive). For the analysis of each subtype, our cohort was dichotomized multiple times in a respective subtype and the rest of cases. Neither SGCAs (p=0.0517) or null cell adenomas (0.0954) nor DGLAs (p=0.4342) or SGSAs (0.1462) were significantly associated with invasiveness when compared with the rest of the cohort. With p-values below 10%, SGCAs and null cell adenomas showed a tendency towards more invasive behavior.

Table 3.4.: Subtype-specific rate of invasiveness in comparison to rest of cohort.

Subtype	Invasiveness		p value
	Subtype N (%)	Rest of cohort N (%)	(Pearson test)
Corticotroph			
- SGCA	18 of 30 (60.00%)	358 of 850 (42.12%)	0.0517
- DGCA	26 of 69 (37.68%)	350 of 811 (43.16%)	0.3774
- Crooke	0 of 2 (0.00%)	376 of 878 (42.82%)	0.2214
Gonadotroph	165 of 400 (41.25%)	211 of 480 (43.96%)	0.4187
Lactotroph			
- SGLA	26 of 64 (40.63%)	350 of 816 (42.89%)	0.7240
- DGLA	5 of 9 (55.56%)	371 of 871 (42.59%)	0.4342
- ASCA	7 of 16 (43.75%)	369 of 864 (42.71%)	0.9335
Null Cell	37 of 71 (52.11%)	339 of 809 (41.90%)	0.0954
Plurihormonal	7 of 21 (33.3%)	369 of 859 (43.0%)	0.3784
Somatotroph			
- SGSA	38 of 75 (50.67%)	338 of 805 (41.99%)	0.1462
- DGSA	36 of 79 (45.57%)	340 of 801 (42.45%)	0.5924
- MSA	4 of 16 (25.00%)	372 of 864 (43.06%)	0.1480
- Mixed SLA	6 of 19 (31.58%)	370 of 861 (42.97%)	0.3207
Thyreotroph	1 of 9 (11.11%)	375 of 871 (43.05%)	0.0539

p-values: * <0.05; ** <0.01

3.2.3. MIB-1

While the average MIB-1 value was 0.81%, MIB-1 levels ranged from 0.00 to 15.5% in the study population. 75% of cases had a MIB-1 value of 0.95% or lower. All calculated scores combined did not have a significant correlation with invasiveness (see Figure 3.5., Graph A), the mean MIB-1 value was 0.85% in invasive adenomas as opposed to 0.77% in noninvasive adenomas (p=0.1375). A CART analysis was conducted and produced 0.6% as the most adequate cutoff for the analysis of invasiveness. Adenomas with a MIB-1 value ≥0.6% were significantly more likely to be invasive than those with a MIB-1 value below the cutoff (see Figure 3.5., Graph B). While in the group with a MIB-1 ≥0.6% 278 of 606 (45.87%) adenomas were invasive, in the group with a MIB-1 below the cutoff 100 of 263 (38.02%) adenomas were invasive (p=0.0320).

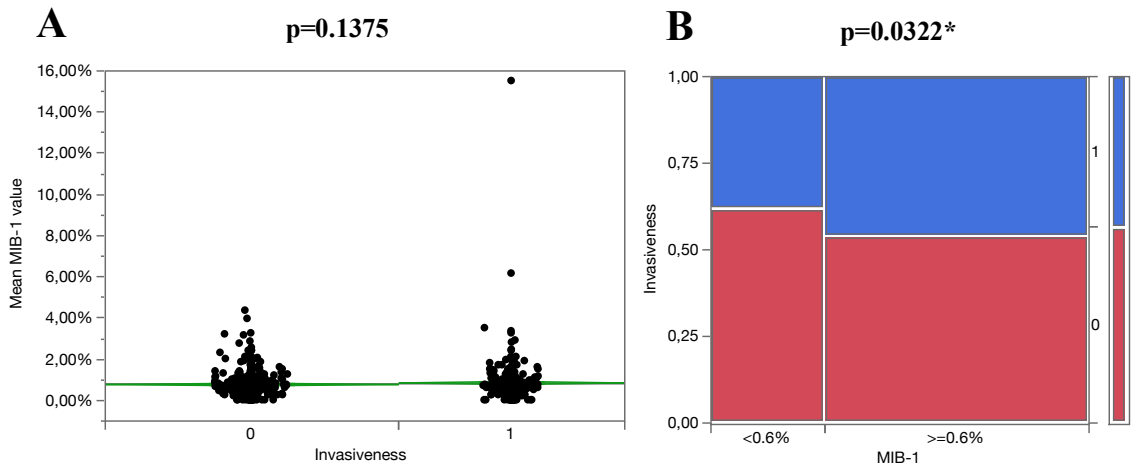

Figure 3.5.: MIB-1 ≥0.6% correlates with invasiveness.
A: The mean MIB-1 was higher in invasive adenomas.
B: Mosaic plot of invasiveness dependent on a CART-based MIB-1 cutoff of 0.6%. Adenoma invasion was significantly more frequent in cases with a MIB-1 ≥0.6%.
Asterisk (*) represents statistically significant differences (p<0.05).

3.2.4. H3K27me3 and H3K36me3

There were 889 adenomas in which H3K27me3 could be scored with a clear immunohistochemical loss in 38 cases. In 897 adenomas H3K36me3 was assessed with a clear loss in 30 cases.

More than half of adenomas had a H3K27me3 score of 4 (474 cases, 53.32%), which indicates at least 75% nuclear positivity (see Figure 3.6., Graph A). CART analyses defined a H3K27me3 score of 1 as the adequate cutoff for the analysis of intraoperative presence of invasiveness. There were only 25 adenomas in our cohort below this cutoff with less than 5% immunopositivity (2.81%). Application of this cutoff demonstrated that this loss of H3K27me3 correlates significantly with a higher occurrence of invasiveness (see Figure 3.6., Graph C). While 64% of adenomas (16 of 25 cases) with a H3K27me3 score <1 were invasive, invasiveness was found in 42.36% of adenomas (366 of 864 cases) with a higher H3K27me3 score (p=0.0312).

Almost two thirds of adenomas held a H3K36me3 score of 4 (587 cases, 65.44%), which equivalently stands for at least 75% positivity (see Figure 3.6., Graph B). A score of 4 was applied for the analysis of invasiveness, as this was the optimal cutoff found with a CART analysis. There was an insignificantly higher rate of invasive cases below the cutoff (see Figure 3.6., Graph D). Adenomas with less than 75% H3K36me3 positivity were invasive in 141 of 310 cases (45.48%), meanwhile 243 of 587 cases (41.40%) with a score of 4 showed invasive features intraoperatively (p=0.2394).

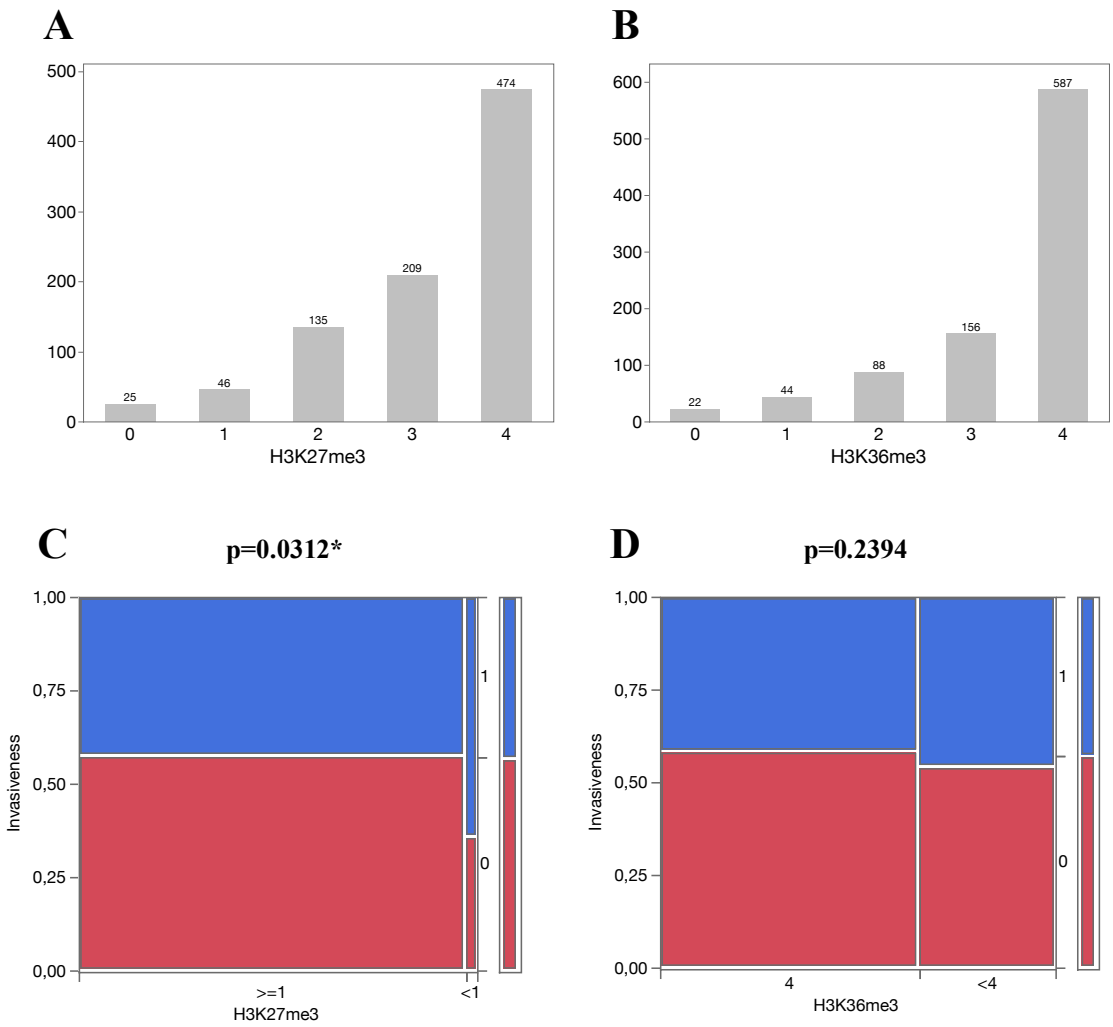

Figure 3.6.: Distribution of histone antibody scores and association of H3K27me3 <5% with invasion.

A, B: Distribution of H3K27me3 and H3K36me3 in whole-number scores from 0 to 4.
C: Mosaic plot of invasiveness dependent on a CART-based H3K27me3 cutoff of 1. Loss of H3K27me3 significantly correlated with invasiveness.
D: Mosaic plot of invasiveness dependent on a CART-based H3K36me3 cutoff of 4. Higher rate of invasive adenomas in the H3K36me3 <4 group.
Asterisk (*) represents statistically significant differences ($p<0.05$).

3.2.5. Osteonectin/SPARC

Most adenomas showed strong immunohistochemical staining signal for osteonectin (SPARC), as visualized in Figure 3.7., Graph A. Over half of adenomas had an osteonectin IRS of 8 or higher (508 cases, 56.63%) with an IRS of 12 existing in 350 adenomas alone (39.02%). About one fifth of cases exhibited low osteonectin scores of 3 or less (181 cases, 20.18%). An intermediate IRS of 6 was found in 111 cases (12.38%). While 652 cases (72.77%) stained exclusively cytoplasmatic, 243 cases (27.12%) had a membranous distribution pattern. Overall analysis of all scores without a cutoff did not detect any significant difference between invasive and noninvasive adenomas, as assessed intraoperatively (see Figure 3.7., Graph B). The mean IRS of invasive and of noninvasive cases was 7.81 and 7.61 respectively (p=0.2268). For the analysis of invasiveness, CART analysis was not able to produce an optimal cutoff.

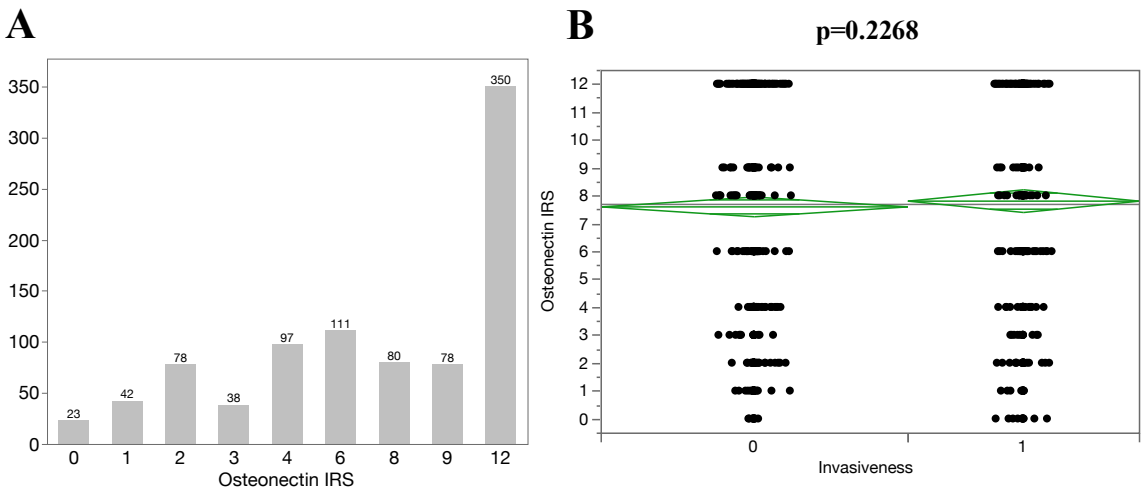

Figure 3.7.: Distribution of osteonectin IRS and its role on invasiveness.
A: Distribution of osteonectin in whole-number scores from 0 to 12.
B: Scatter diagram of osteonectin scores in dependance of invasiveness. Insignificantly higher IRS of invasive adenomas.
Asterisk (*) represents statistically significant differences ($p<0.05$).

3.3. Assessment of Radiological Invasiveness

Data on intraoperatively observed invasiveness was complemented with MRI findings of different radiographic signs of pituitary adenoma invasion. Adenomas were investigated for suprasellar growth and paranasal sinus invasion in 770 adenoma cases. Of this cohort, suprasellar growth was detected in 491 adenomas on MRI (63.77%). Less than 20 percent of tumors demonstrated paranasal sinus invasion on cranial MR imaging (147 cases, 19.09%).

The focus in this chapter is radiographic signs of cavernous sinus invasion.

The original Knosp classification was 5-tiered, however, we used the adapted version of Micko et al. with the recommended subdivision of grade 3 into two grades for more accurate acquisition of data on CSI (Knosp et al., 1993; Micko et al., 2015). The explanation of each grade is given and illustrated in Chapter 1.6.1. and Figure 1.1. By this means, the degree of CSI was graded in 764 tumors. For each adenoma, the CSI of the left as well as the right parasellar region was graded. To summarize these findings, in cases of different grades on the two sides, the higher grade was considered for further evaluation.

Table 3.5. provides an overview of the Knosp grades among our cohort. The most common grade was 0, which was prevalent in 300 adenomas (39.3%). 69 cases (9.0%) showed total enceasement of the ICA (= Knosp grade 4).

Following suggestions in the literature, the Knosp scale was dichotomized and while grades 0-2 were considered noninvasive, grades 3A-4 were considered to represent invasive cases (Mooney et al., 2017b; Dhandapani et al., 2016; Zoli et al., 2016; Micko et al., 2015). With the target variable of intraoperative invasion, a CART calculation proposed a second dichotomization in grades 0 and 1 (=noninvasive) and 2-4 (=invasive). The role of the clinical factors age, gender and adenoma subtypes as well as the immunohistochemical markers MIB-1, H3K27me3, H3K36me3 and osteonectin for CSI were investigated. For the numeric parameters age and the four antibodies, CART analyses were run to mathematically identify suitable cutoff values (see Table 3.6.).

Table 3.5.: Distribution of Knosp grades overall, by age and by rate of invasiveness.

Knosp grade	N (left CS)	N (right CS)	N (%) (combined)	Mean age	% invasiveness intra-op.
0	428	462	300 (39.3%)	48.5 years	22.3%
1	143	123	162 (21.2%)	56.0 years	35.2%
2	81	79	116 (15.2%)	57.3 years	50.0%
3A	58	43	87 (11.4%)	54.9 years	73.6%
3B	18	15	30 (3.9%)	57.6 years	66.7%
4	36	42	69 (9.0%)	53.8 years	84.0%

Table 3.6.: CART-proposed cutoffs for target variable cavernous sinus invasion by Knosp grade.

Parameter	CART-proposed cutoff	
	Knosp 0-2 & 3A-4 (literature-based cutoff)	Knosp 0-1 & 2-4 (CART-based cutoff)
Age	45 years	45 years
MIB-1	1.4%	3.4%
H3K27me3	3	3
H3K36me3	4	No adequate cutoff
Osteonectin	2	12

3.3.1. Age and Gender

There was no statistically significant difference of radiologically more distinct signs of CSI according to age at the literature-based Knosp cutoff. Patients with a Knosp grade 3A-4 adenoma had a mean age of 54.96 years, compared to a slightly younger mean age of 52.40 years of patients, whose tumors were graded 0-2 (p=0.0590, see Figure 3.8., Graph A). There was a significant age difference detected at the CART-proposed Knosp cutoff. While patients with a Knosp grade 2-4 tumor had a mean age of 55.84, patients with a Knosp 0 or 1 adenoma had a mean age of 51.17 years (p=0.0001, see Figure 3.9., Graph A).

CART analyses detected an age of 45 years at diagnosis as the optimal cutoff for the investigation of both Knosp dichotomizations. At both cutoffs, affiliation in the older age group was significantly associated with an increased rate of high Knosp grades (see Figure 3.8. and 3.9., Graph B). There were 41 of 239 patients aged under 45 years

(17.15%), compared to 145 of 525 patients ≥45 years old at diagnosis (27.62%) with an adenoma with Knosp grades 3A-4 (p=0.0018). At the other cutoff, Knosp grade 2-4 adenomas were prevalent in 68 of 239 patients <45 years of age (28.45%) and in 234 of 525 patients ≥45 years of age (44.57%, p=0.0001).

There was no gender-related statistical difference regarding the occurrence of high Knosp grades at both cutoffs (see Figure 3.8. and 3.9., Graph C). Knosp grade 2-4 tumors (p=0.1117) were found in 157 of 370 male patients (42.34%) and in 145 of 394 female patients (36.80%). 93 of 370 male patients (25.14%) and 93 of 394 female patients (23.60%) held an adenoma with Knosp grades 3A-4 (p=0.6222).

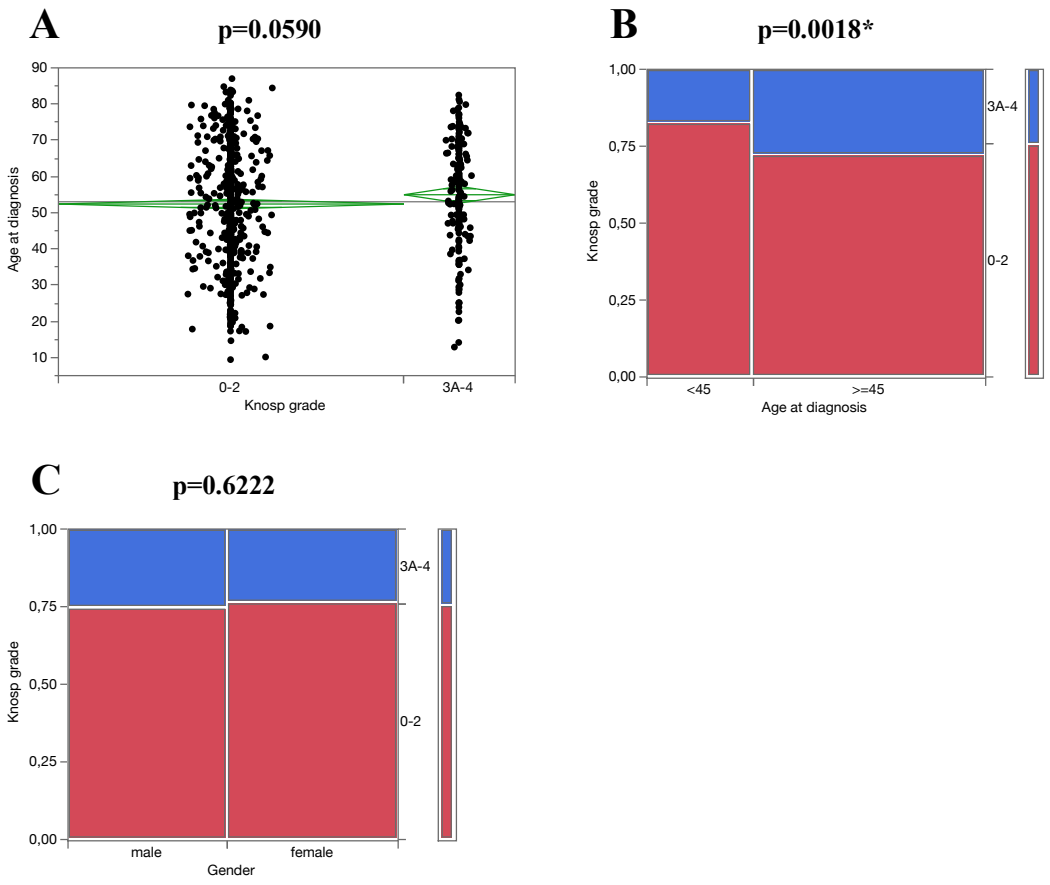

Figure 3.8.: Knosp grades 3A-4 independent of gender but associated with ≥45 years of age.
A: Scatter diagram of age at diagnosis depending on Knosp grade. Knosp 3A-4 adenomas were significantly older at diagnosis.
B: Mosaic plot of Knosp grades depending on age at a CART-based cutoff of 45 years. Knosp 3A-4 was prevalent significantly more often in patients ≥45 years.
C: Mosaic plot of Knosp grades depending on gender. No significant gender-dependency.
Asterisk (*) represents statistically significant differences (p<0.05).

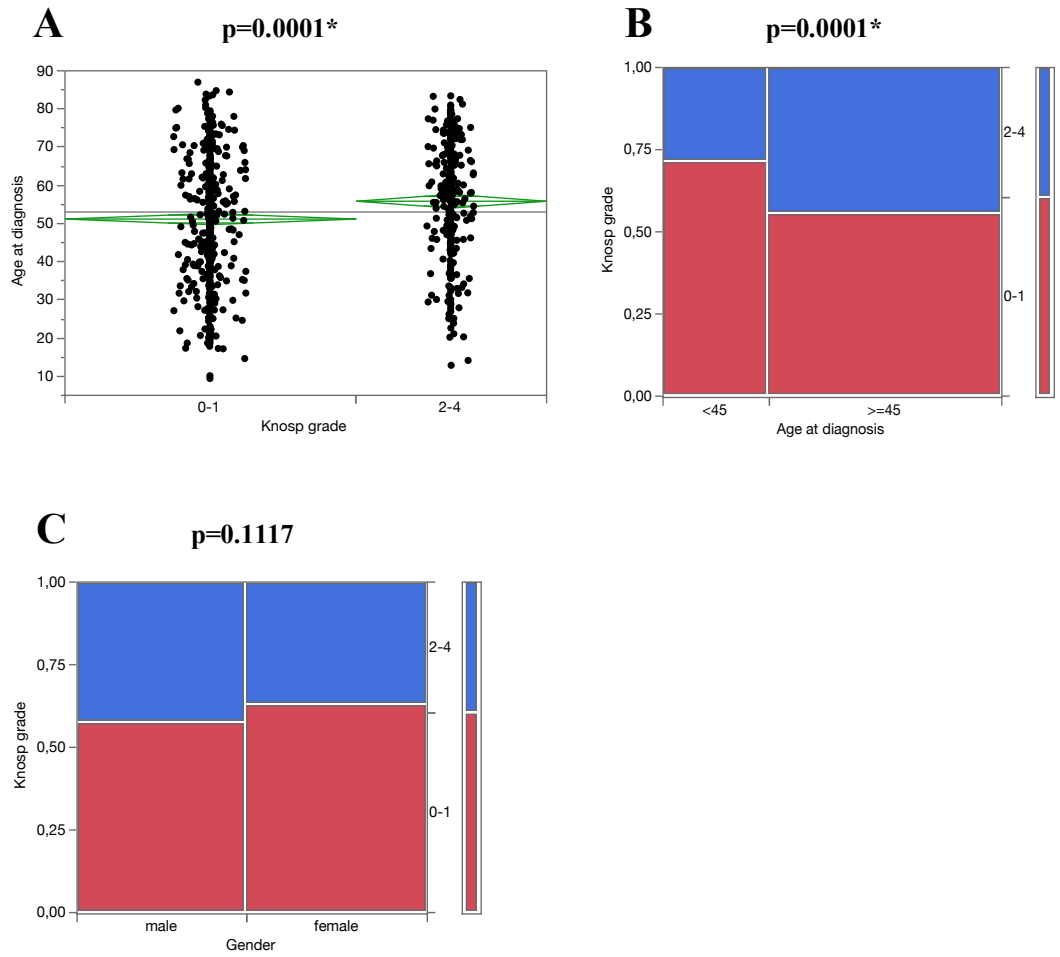

Figure 3.9.: Knosp grade 2-4 independent of gender but associated with ≥45 years of age.
A: Scatter diagram of age at diagnosis depending on Knosp grade. Knosp 2-4 adenomas were significantly older at diagnosis.
B: Mosaic plot of Knosp grades depending on age at a CART-based cutoff of 45 years. Knosp 2-4 was prevalent significantly more often in patients ≥45 years.
C: Mosaic plot of Knosp grades depending on gender. No significant gender-dependency.
Asterisk (*) represents statistically significant differences ($p<0.05$).

3.3.2. Adenoma Subtype

Identification of the subtype and MRI with Knosp grading of CSI was available in 701 cases of our cohort in total. For both Knosp grade cutoffs, each subtype was compared with the rest of the cohort regarding the rate of cases with the respective higher Knosp grades. Table 3.7. shows the results for the literature-based cutoff for CSI. Null cell adenomas (35.48% Knosp grade 3A-4 cases compared to 23.94%, p=0.0450) and SGCA (44.00% compared to 24.26%, p=0.0251) had a significantly higher rate of Knosp 3A-4 tumors than the rest of cases. The higher percentages of Knosp grade 3A-4 cases found in gonadotroph adenomas (28.38% compared to 22.47%, p=0.0742) and in SGSA (27.69% compared to 24.69%, p=0.5937) did not display a statistical difference.
Table 3.8. demonstrates the results accordingly for the other CART-based Knosp cutoff for CSI. By absolute numbers, most subtypes had more cases with affiliation in the Knosp 0-1 than the Knosp 2-4 group. Only SGCA (10 cases Knosp 0-1, 15 cases Knosp 2-4), gonadotroph adenomas (145 cases 0-1, 151 cases 2-4), and null cell adenomas (30 cases 0-1, 32 cases 2-4) had a greater number of cases with affiliation in the more distinctly CS-invasive group. A significant association with Knosp grades 2-4 was found for the gonadotroph adenoma subtype (51.01% compared to 33.83%, p=0.0001). Apart from that, despite the seeming preponderance of Knosp 2-4 tumors in SGSA (43.08% compared to 24.69%, p=0.7317), null cell adenomas (51.61% compared to 40.06%, p=0.0776), DGLA (44.44% compared to 41.04%, p=0.8366) and SGCA (60.00% compared to 40.38%, p=0.0503) in this study, there was no statistical significance and no correlation of these subtypes with Knosp grades 2-4.

Table 3.7.: Subtype-specific rate of CSI with literature-based Knosp cutoff in comparison to rest of cohort.

P values of univariate analysis of subtype compared with rest of cohort.
Asterisk (*) represents statistically significant difference ($p<0.05$).

Subtype	Knosp grade 3A-4		p value
	Subtype	Rest of cohort	(Pearson test)
	N (%)	N (%)	
Corticotroph			
- SGCA	11 of 25 (44.00%)	164 of 676 (24.26%)	0.0251*
- DGCA	13 of 62 (20.97%)	162 of 639 (25.35%)	0.4463
- Crooke	0 of 1 (0.00%)	175 of 700 (25.00%)	0.5638
Gonadotroph	84 of 296 (28.38%)	91 of 405 (22.47%)	0.0742
Lactotroph			
- SGLA	8 of 55 (14.55%)	167 of 646 (25.85%)	0.0629
- DGLA	1 of 9 (11.11%)	174 of 692 (25.14%)	0.3338
- ASCA	1 of 12 (8.33%)	174 of 689 (25.25%)	0.1794
Null Cell	22 of 62 (35.48%)	153 of 639 (23.94%)	0.0450*
Plurihormonal	1 of 15 (6.67%)	174 of 686 (25.36%)	0.0979
Somatotroph			
- SGSA	18 of 65 (27.69%)	157 of 636 (24.69%)	0.5975
- DGSA	10 of 59 (16.95%)	165 of 642 (25.70%)	0.1372
- MSA	1 of 15 (6.67%)	174 of 686 (25.36%)	0.0979
- Mixed SLA	4 of 17 (23.53%)	171 of 684 (25.00%)	0.8899
Thyreotroph	1 of 8 (12.50%)	174 of 693 (25.11%)	0.4126

p-values: * <0.05; ** <0.01

Table 3.8.: Subtype-specific rate of CSI with CART-based Knosp cutoff in comparison to rest of cohort.

P values of univariate analysis of subtype compared with rest of cohort.
Asterisk (*) represents statistically significant difference. Numbers in italics show that significance is result of preponderance of comparison group.

Subtype	Knosp grade 2-4		p value
	Subtype N (%)	Rest of Cohort N (%)	(Pearson test)
Corticotroph			
- SGCA	15 of 25 (60.00%)	273 of 676 (40.38%)	0.0503
- DGCA	15 of 62 (24.19%)	273 of 639 (42.72%)	*0.0046* *
- Crooke	0 of 1 (0.00%)	288 of 700 (41.14%)	0.4033
Gonadotroph	151 of 296 (51.01%)	137 of 405 (33.83%)	0.0001*
Lactotroph			
- SGLA	14 of 55 (25.45%)	274 of 646 (42.41%)	*0.0141**
- DGLA	4 of 9 (44.44%)	284 of 692 (41.04%)	0.8366
- ASCA	1 of 12 (8.33%)	287 of 689 (41.65%)	*0.0200**
Null Cell	32 of 62 (51.61%)	256 of 639 (40.06%)	0.0776
Plurihormonal	3 of 15 (20.00%)	285 of 686 (41.55%)	0.0934
Somatotroph			
- SGSA	28 of 65 (43.08%)	260 of 636 (40.88%)	0.7317
- DGSA	17 of 59 (28.81%)	271 of 642 (42.21%)	*0.0453**
- MSA	1 of 15 (6.67%)	287 of 686 (41.84%)	*0.0062**
- Mixed SLA	4 of 17 (23.53%)	284 of 684 (41.52%)	0.1364
Thyreotroph	3 of 8 (37.50%)	285 of 693 (41.13%)	0.8358

p-values: * <0.05; ** <0.01

3.3.3. MIB-1

MIB-1 values and MRI data on CSI according to the Knosp scale was available for 716 cases. At the literature-based Knosp cutoff and with all MIB-1 results combined without a cutoff, there was no significant difference of the mean MIB-1 value between the two groups (mean MIB-1 value of 0.82% of Knosp grade 3A-4 compared to a mean MIB-1

of 0.85% of Knosp grade 0-2 tumors, p=0.6219). For the further examination of the role of MIB-1 for radiological CSI, a CART analysis determined a MIB-1 value of 1.4% as an adequate cutoff. There was no significant correlation of MIB-1 with Knosp grades 3A-4 at this cutoff value (see Figure 3.10., Graph A). Knosp grades 3A-4 were found in 163 of 634 cases with a MIB-1 <1.4% (25.71%) and in 16 of 82 cases with a MIB-1 ≥1.4% (19.51%, p=0.2226).

The more invasive Knosp grades had a significantly higher mean MIB-1 value in the CART-based Knosp dichotomization. While Knosp grade 2-4 tumors had a mean MIB-1 level of 0.91%, Knosp 0-1 tumors had an average MIB-1 of 0.80% (p=0.0360). A CART analysis was conducted and proposed a MIB-1 level of 3.4% as an optimal cutoff. Among the cohort of 716 cases, there were only 5 cases in total with a MIB-1 value of ≥3.4%. While all 5 cases had a Knosp grade 2-4, these Knosp grades were found in 287 of 711 cases with MIB-1 levels <3.4% (40.37%). This result was statistically significant (p=0.0069, see Figure 3.10., Graph B).

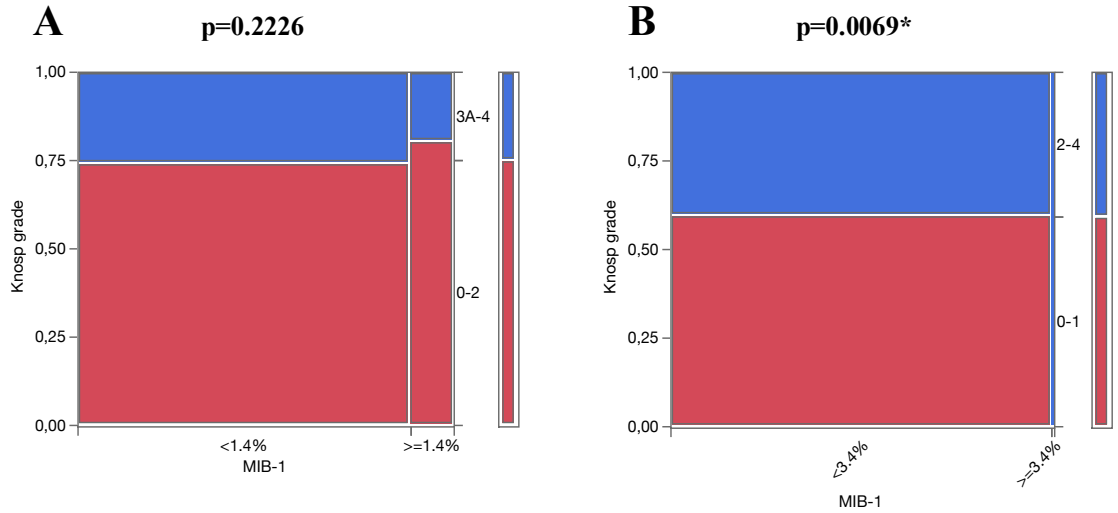

Figure 3.10.: CS invasion according to Knosp cutoffs depending on MIB-1.
A: Mosaic plot of Knosp grades at literature-based cutoff depending on a CART-based MIB-1cutoff of 1.4%. Knosp 3A-4 was observed insignificantly less often in adenomas with a MIB-1 ≥1.4%
B: Mosaic plot of Knosp grades at CART-based cutoff depending on a CART-based MIB-1 cutoff of 3.4%. Adenomas with a MIB-1 ≥3.4% all had a Knosp grade 2-4.
Asterisk (*) represents statistically significant differences (p<0.05).

3.3.4. H3K27me3 and H3K36me3

H3K27me3 scores and imaging data on CSI according to the Knosp scale were available in 736 cases. The histogram in Figure 3.11. illustrates the distribution of H3K27me3 scores by each of the six Knosp grades. A CART analysis was run to identify adequate cutoffs for both Knosp dichotomizations used in this study and proposed a score of 3, which represents 50-75% of nuclear positivity for H3K27me3 for both divisions. Adenomas with a H3K27me3 score <3 (<50% immunopositivity) had a higher rate of Knosp grades that were considered invasive.

For the literature-based Knosp cutoff, there was no significant association of H3K27me3 at its cutoff score with Knosp grades 3A-4 (see Figure 3.12., Graph A). While 135 of 583 adenomas with a H3K27me3 score ≥3 (23.16%) had a Knosp grade 3A-4, this was the case in 46 of 153 adenomas with a H3K27me3 score <3 (30.07%, p=0.0773).

A H3K27me3 score <3 significantly correlated with the invasive Knosp grades for the CART-based Knosp cutoff (see Figure 3.12., Graph B). Knosp grades 2-4 were detected in 221 of 583 tumors (37.91%) with a H3K27me3 score ≥3 and in 75 of 153 tumors with a H3K27me3 score <3 (49.02%, p=0.0126).

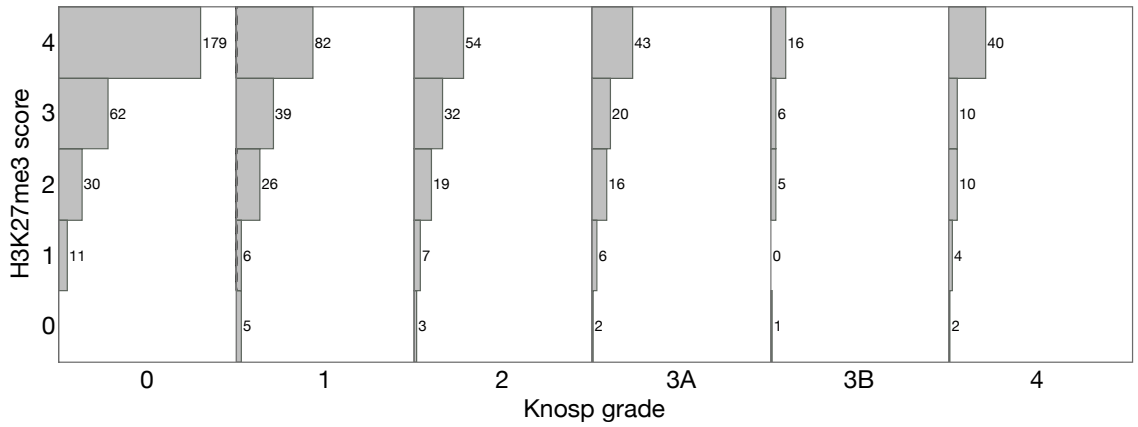

Figure 3.11.: Distribution of H3K27me3 scores by Knosp grade.

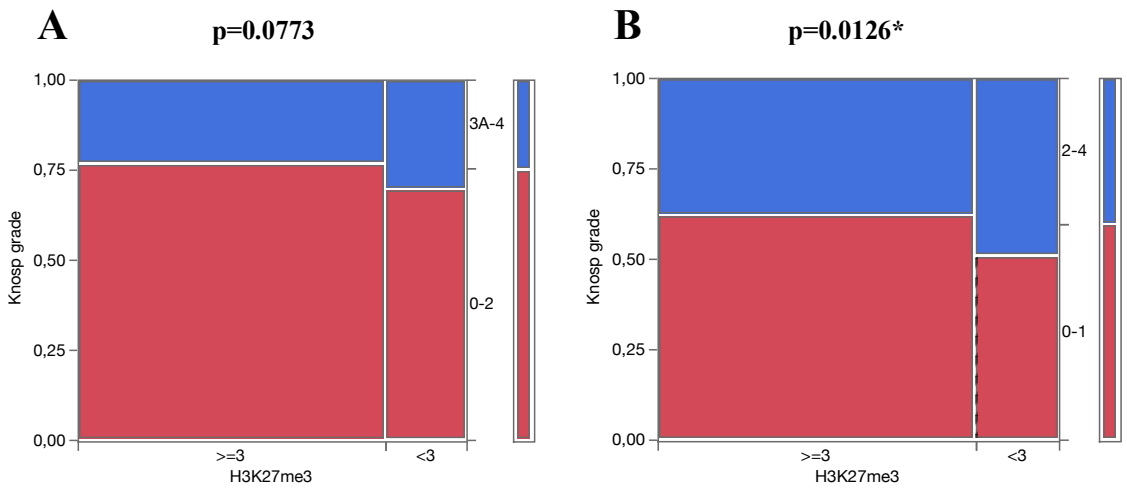

Figure 3.12.: Knosp grades 2-4 significantly more frequent in adenomas with H3K27me3 score <3.
Mosaic plots of Knosp grades depending on a CART-based H3K27me3 cutoff of 3.
A: No significant difference at literature-based Knosp cutoff.
B: At the CART-based Knosp cutoff, cases with a H3K27me3 score <3 had a significantly higher rate of Knosp grades 2-4.
Asterisk (*) represents statistically significant differences ($p<0.05$).

Availability of cases with both MRI data as well as data on the quantified expression of the antigen of interest was higher for H3K36me3 than for H3K27me3. In total, 743 cases were included in the following analysis. The distribution of H3K36me3 scores by each of the six Knosp grades is visualized in Figure 3.13. A CART analysis proposed a H3K36me3 cutoff score of 4 for the literature-based Knosp cutoff. Knosp grades 3A-4 were found more often in adenomas with a H3K36me3 score <4 (<75% immunopositivity), this difference reached statistical significance (see Figure 3.14.). Knosp grades 3A-4 were found in 117 of 518 tumors with a H3K36me3 score ≥4 (22.59%) and in 66 of 225 tumors with a H3K36me3 score <4 (29.33%, p=0.0499). For the CART-based Knosp cutoff, our CART analysis did not produce a suitable cutoff.

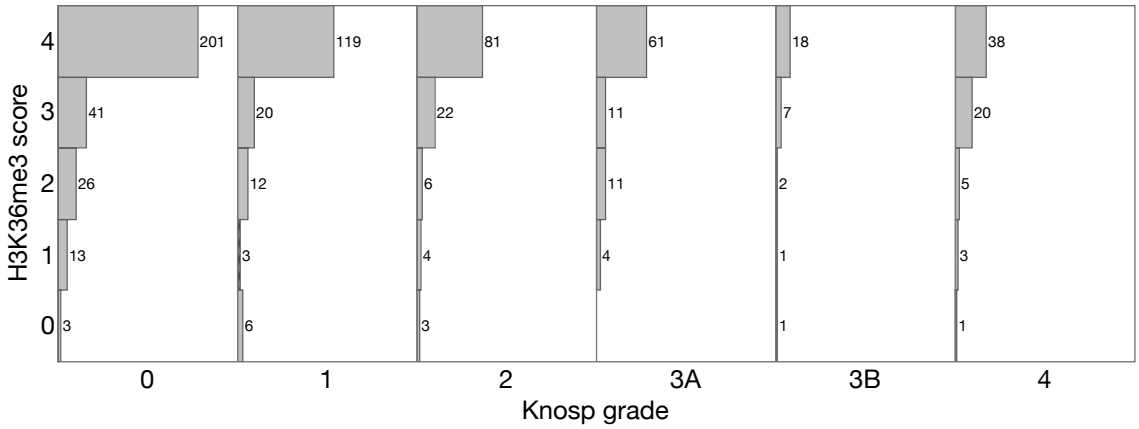

Figure 3.13.: Distribution of H3K36me3 scores by Knosp grade.

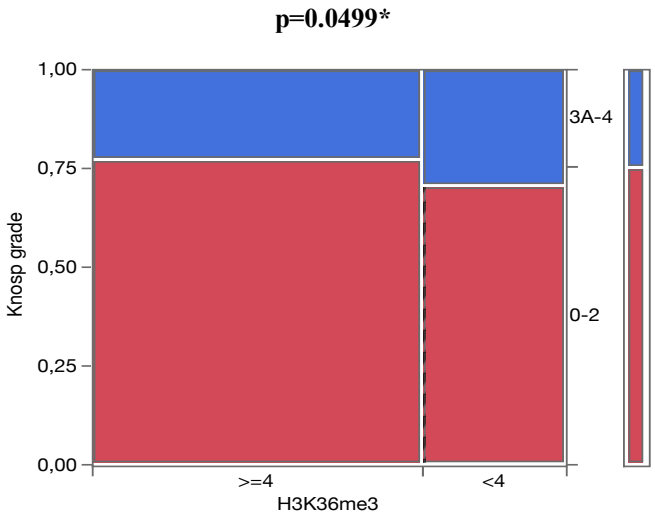

Figure 3.14.: H3K36me3 <4 associated with Knosp grades 3A-4.
Mosaic plot of Knosp grades with literature-based cutoff depending on a CART-based H3K36me3 cutoff of 4. Cases with a H3K36me3 score <4 showed Knosp grades 3A-4 significantly more often.
Asterisk (*) represents statistically significant differences ($p<0.05$).

3.3.5. Osteonectin/SPARC

Quantification of osteonectin (SPARC) expression with an immunoreactive score (IRS) and MRI data on CSI graded with the Knosp classification was available in 740 cases. As a means of finding the IRS with the most distinct difference between groups subdivided by different Knosp grades, CART analyses were conducted.

For the literature-based Knosp cutoff, an osteonectin IRS of 2 was suggested and applied as a cutoff. At this cutoff, there was no significant difference regarding the frequency of the Knosp grades that represent CSI (see Figure 3.15., Graph A). Knosp grades 3A-4 were found in 172 of 680 adenomas (25.29%) with an IRS ≥2 and in 10 of 60 adenomas with an IRS <2 (16.67%, p=0.1369). The CART analysis for the CART-based Knosp cutoff suggested an osteonectin IRS cutoff of 12. An IRS of <12 had a significantly higher rate of Knosp grades 2-4 (see Figure 3.15., Graph B). While they were present in 103 of 293 cases with an IRS ≥12 (35.15%), Knosp grades 2-4 were found in 195 of 447 cases with an IRS <12 (43.62%, p=0.0216).

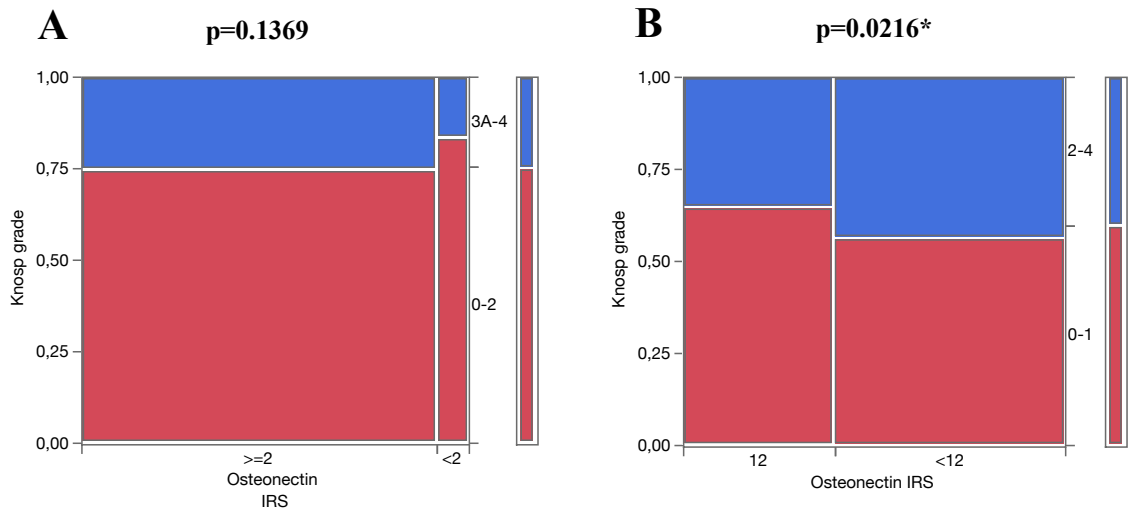

Figure 3.15.: CS invasion according to Knosp cutoffs depending on Osteonectin IRS.
A: Mosaic plot of Knosp grades with literature-based cutoff depending on a CART-based osteonectin IRS cutoff of 2. Without significance, Knosp grades 3A-4 occurred less frequent in adenomas with an IRS <2.
B: Mosaic plot of Knosp grades with CART-based cutoff depending on a CART-based osteonectin IRS cutoff of 12. Adenomas with an IRS <12 appeared as Knosp grade 2-4 significantly more often.
Asterisk (*) represents statistically significant differences (p<0.05).

3.4. Multivariate Analysis

A multivariate analysis (MVA) of the target variables intraoperative invasion as well as radiological CSI at both Knosp cutoffs was conducted separately. A logistic regression model was used. Only clinical factors and immunohistochemical markers with a significant association ($p<0.05$) or a statistical trend ($p<0.10$) in the univariate analysis were included.

3.4.1. Intraoperative Invasion

For intraoperative presence of invasion, significant results in the univariate analysis were found for an age ≥71 years at diagnosis (p=0.0255), as well as for MIB-1 expression ≥0.6% (p=0.0322) and a H3K27me3 score <1, which resembles below 5% immunopositivity (p=0.0312). A statistical trend was found for the clinical factor male gender (p=0.0604) and the subtypes SGCA (p=0.0517) and null cell adenoma (p=0.0954). All parameters that were included in the MVA are listed in Table 3.9.
The results of the MVA of intraoperative invasion are demonstrated in Table 3.10. Intraoperative invasion was independent from age and gender. While there was no association with null cell adenomas, a significant correlation was detected for SGCA, as intraoperative invasion was more than two times more likely to be found in this subtype. Regarding the immunohistochemical markers, a MIB-1 value ≥0.6% significantly correlated with invasion by intraoperative assessment and the latter was over 1.4 times more likely to exist in these adenomas. Adenomas with H3K27me3 scores <1 (expression below 5%) had a 2.67-fold higher chance to be invasive, making it an independent and significant predictor of intraoperative presence of pituitary adenoma invasion.

Table 3.9.: Parameters included in the MVA of intraoperative invasion.

Variable	Result in the univariate analysis
Age ≥71 years	p=0.0255 *
Male gender	p=0.0604
Null Cell Adenoma	p=0.0954
SGCA	p=0.0517
MIB-1 ≥ 0.6%	p=0.0322 *
H3K27me3 <1	p=0.0312 *

Table 3.10.: Results of the MVA of intraoperative invasion.

Variable	Coefficient	Standard error	Odds ratio	95% CI	p-value
Age ≥71 years	0.140900	0.100607	1.325514	-0.0568 – 0.3384	0.1614
Male gender	-0.121133	0.071150	1.274133	-0.2609 – 0.0182	0.0887
Null Cell Adenoma	0.219123	0.129867	1.549987	-0.0352 – 0.4758	0.0915
SGCA	0.430637	0.199005	2.366173	0.0463 – 0.8349	0.0305 *
MIB-1 ≥ 0.6%	0.180916	0.079101	1.435958	0.0268 – 0.3371	0.0222 *
H3K27me3 <1	0.492596	0.227633	2.678327	0.0567 – 0.9621	0.0305 *

p-values: * <0.05; ** <0.01

3.4.2. Radiographic Invasion according to the Literature-based Knosp cutoff

Clinical parameters with significant results in the univariate analysis of radiographic CSI according to the literature-based Knosp cutoff were an age ≥45 years at diagnosis (p=0.0018) as well as the subtypes SGCAs (p=0.0251) and null cell adenomas (p=0.0450). Gonadotroph adenomas had a statistical tendency (p=0.0742) towards CSI and were added to the MVA. The sole significant finding in the assessment of the immunohistochemical markers was a H3K36me3 score <4 (p=0.0499). Table 3.11. shows all parameters that were included in the MVA.

Radiographic CSI was age-dependent. An age of at least 45 years at diagnosis was independently associated with Knosp grades 3A-4. While an association with the gonadotroph adenoma subtype was absent, SGCA and null cell adenomas were significantly and independently predictive of CSI as it was more than two times more likely to exist in these two subtypes.

A H3K36me3 score <4 (expression below 75%) was an independent immunohistochemical marker with a significant association with radiographic invasion. Specifics on these results are provided in Table 3.12.

Table 3.11.: Parameters included in the MVA of CSI according to the literature-based Knosp cutoff.

Variable	Result in the univariate analysis
Age ≥45 years	p=0.0018 **
Null Cell Adenoma	p=0.0450 *
SGCA	p=0.0251 *
Gonadotroph A.	p=0.0742
H3K36me3 <4	p=0.0499 *

p-values: * <0.05; ** <0.01

Table 3.12.: Results of the MVA of CSI according to the literature-based Knosp cutoff.

Variable	Coefficient	Standard error	Odds ratio	95% CI	p-value
Age ≥45 years	0.236590	0.110385	1.605089	0.0237 – 0.4574	0.0321 *
Null Cell Adenoma	0.429667	0.154779	2.361589	0.1211 – 0.7302	0.0055 **
SGCA	0.543703	0.213492	2.966571	0.1146 – 0.9597	0.0109 *
Gonadotroph A.	0.186932	0.103223	1.453340	-0.0143 – 0.3909	0.0701
H3K36me3 <4	0.196592	0.094867	1.481692	0.0093 – 0.3817	0.0382 *

p-values: * <0.05; ** <0.01

3.4.3. Radiographic Invasion according to the CART-based Knosp cutoff

Statistical significance in the univariate analysis of radiographic CS invasion according to the CART-based Knosp cutoff was detected for the parameters age ≥45 years at diagnosis (p=0.0001), gonadotroph adenomas (p=0.0001) as well as the immunohistochemical marker scores H3K27me3 <3 (p=0.0126) and osteonectin <12 (p=0.0216). The result for MIB-1 expression ≥3.4% was excluded from further analysis due to its unequal cohort distribution. Due to their statistical trend, SGCAs (p= 0.0503) and null cell adenomas (p=0.0776) were added to the MVA for Knosp grades 2-4.

Age dependency of CSI was present at this Knosp cutoff as well. There was a significant correlation between an age of at least 45 years at diagnosis and Knosp grades 2-4. Gonadotroph and null cell adenomas were highly significantly correlated with Knosp grades 2-4, these grades were around two times more likely to occur in these subtypes. With an almost three times higher chance, radiographic invasion was even more likely in the SGCA subtype. This result makes SGCA the sole subtype in this study with significant results in the MVA of each target variable of invasion. Neither an osteonectin IRS <12 nor a H3K27me3 score <3 (below 50% expression) were associated with CSI at the CART-based Knosp cutoff. More detailed information on the results of the MVA of radiographic invasion at this Knosp cutoff is shown in Table 3.14.

Table 3.13.: Parameters included in the MVA of CSI according to the CART-based Knosp cutoff.

Variable	Result in the univariate analysis
Age ≥45 years	p=0.0001 **
Gonadotroph A.	p=0.0001 **
SGCA	p=0.0503
Null Cell Adenoma	p=0.0776
H3K27me3 <3	p=0.0126 *
Osteonectin <12	p=0.0216 *

p-values: * <0.05; ** <0.01

Table 3.14.: Results of the MVA of CSI according to the CART-based Knosp cutoff.

Variable	Coefficient	Standard error	Odds ratio	95% CI	p-value
Age ≥45 years	0.214180	0.094007	1.534737	0.0309 – 0.3999	0.0227 *
Gonadotroph	0.324071	0.099218	1.911984	0.1303 – 0.5197	0.0011 **
SGCA	0.531861	0.212794	2.897135	0.1161 – 0.9591	0.0124 *
Null Cell Adenoma	0.420040	0.147166	2.316551	0.1313 – 0.7100	0.0043 **
H3K27me3 <3	0.126227	0.098274	1.287181	-0.0669 – 0.3188	0.1990
Osteonectin <12	0.020994	0.089129	1.042882	-0.1541 – 0.1957	0.8138

p-values: * <0.05; ** <0.01

3.5. Prognostic Impact of Clinical Factors and Markers

Follow-up data consisted of postoperative MRI reports or medical reports of checkup examinations and was available in 1,121 cases (91.89%), 99 patients were lost to follow-up (8.11%). Mean follow-up duration was 2.64 years ranging from 0.06 – 15.20 years. This means that patients were on average followed up for about 2 years and 7 months after surgical removal of their pituitary adenoma.

For the following analyses, only the cohort of 927 patients, whose tumor samples underwent tissue analysis by TMA and immunohistochemical staining, were further considered. Of this cohort, follow-up data existed in 869 cases (see flow chart in Figure 3.1.). While in 694 of those cases (79.86%), there was no report or evidence of recurrence, a recurrent adenoma was documented in 175 patients (20.14%).

To complement the analysis of invasiveness, Kaplan-Meier analyses were conducted to determine recurrence-free survival rates. This allowed for an evaluation of the prognostic value of the previously examined clinical factors and immunohistochemical markers. The prognostic impact of the previous target variables intraoperative and radiological invasion themselves was assessed as well. Adequate cutoff values for the numeric parameter of age as well as the immunohistochemical markers MIB-1, H3K27me3, H3K36me3 and osteonectin were determined with the help of CART analyses and are shown in table 3.15.

Table 3.15.: Cutoffs for Kaplan-Meier analyses of recurrence-free survival time.

Parameter	CART-proposed cutoff
Age	49 years
MIB-1	0.6%
H3K27me3	3
H3K36me3	4
Osteonectin	2

3.5.1. Intraoperative and Radiological Invasion

Intraoperative existence of invasiveness itself had a negative prognostic impact, as invasive adenomas had a shorter mean recurrence-free survival time than noninvasive tumors (mean time 8.24 years of invasive, 11.058 years of noninvasive tumors). This result was statistically significant (p=0.0148).

Radiographic CSI was associated with a worse prognosis as well at both Knosp cutoffs. At the literature-based Knosp cutoff, adenomas with a Knosp grade 3A-4 had a shorter mean recurrence-free survival time than Knosp grade 0-2 adenomas (mean time 5.98 compared to 10.26 years). This difference was highly significant (p=0.0008). A difference with statistical significance (p=0.0010) was also found at the CART-based Knosp cutoff. With a mean time of 7.01 years compared to 11.06 years of Knosp grade 0-1 adenomas, there was a shorter recurrence free survival time of Knosp grade 2-4 adenomas. The negative prognostic impact of all three variables of invasion is depicted in Figure 3.16.

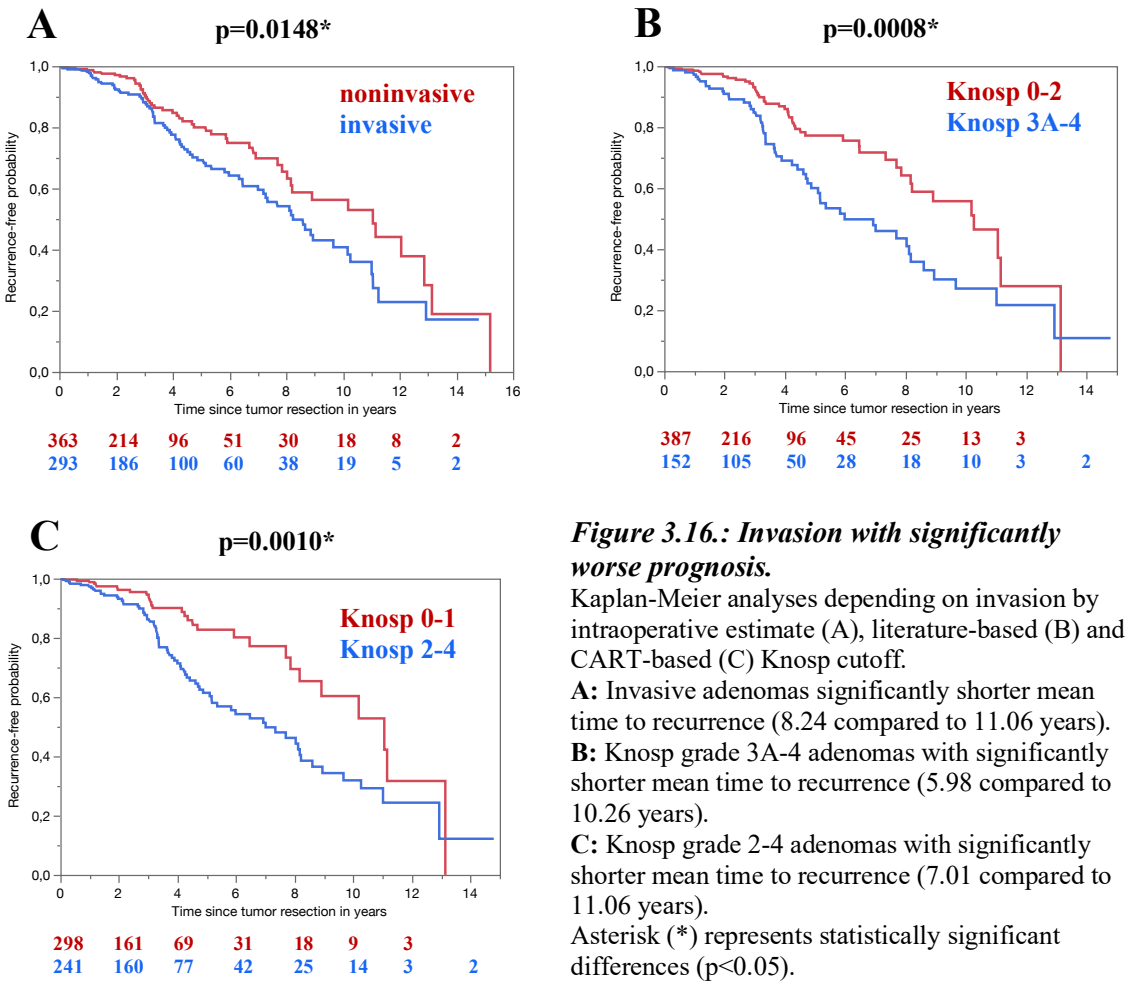

Figure 3.16.: Invasion with significantly worse prognosis.
Kaplan-Meier analyses depending on invasion by intraoperative estimate (A), literature-based (B) and CART-based (C) Knosp cutoff.
A: Invasive adenomas significantly shorter mean time to recurrence (8.24 compared to 11.06 years).
B: Knosp grade 3A-4 adenomas with significantly shorter mean time to recurrence (5.98 compared to 10.26 years).
C: Knosp grade 2-4 adenomas with significantly shorter mean time to recurrence (7.01 compared to 11.06 years).
Asterisk (*) represents statistically significant differences ($p<0.05$).

3.5.2. Age and Gender

Adenoma patients with a recorded recurrence on average were younger than patients who remained in full remission postoperatively (see Figure 3.17., Graph A). The mean age of patients with adenomas with postoperative recurrence was 51.19 years, compared to 54.30 years of patients without a recurrence (p=0.0402). A CART analysis of recurrence in dependance of age at diagnosis proposed an optimal cutoff at an age of 49 years. This cutoff was used for a Kaplan-Meier analysis of recurrence-free survival time. An age <49 years at diagnosis had a higher probability of recurrence and a shorter mean recurrence-free survival time of 8.21 compared to 10.17 years, this difference did not reach statistical significance (p=0.0862, see Figure 3.17. Graph B). Regarding patient gender, there was no statistical difference (p=0.4774), as a recurrent adenoma was detected in slightly more female (69 of 333, 20.72%) than male patients (60 of 324, 18.52%). While women on average had a recurrence-free survival time of 8.87 years, this duration was longer in men (mean time of 10.17 years), but without statistical significance (p=0.3764, see Figure 3.17., Graph C).

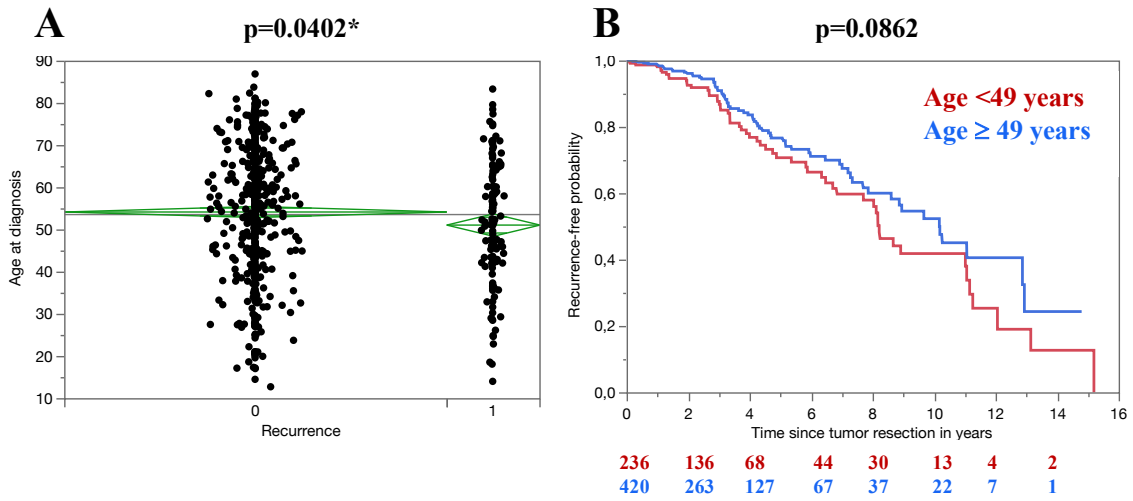

Figure 3.17.: Age and gender without significant difference.
A: Patients with recurrent tumor with significantly younger mean age than patients in full remission.
B: Kaplan-Meier analysis of recurrence-free survival with a CART-proposed cutoff of 49 years. No significant age-dependency.
C: Kaplan-Meier analysis of recurrence-free survival depending on gender without a significant difference.
Asterisk (*) represents statistically significant differences (p<0.05).

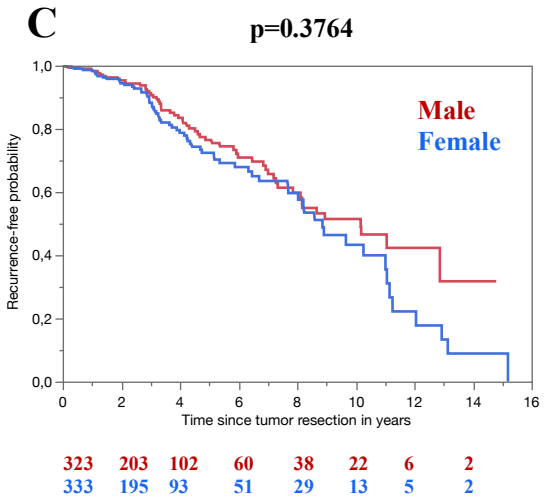

3.5.3. Adenoma Subtype

The recurrence rate of the entire cohort was 20.14% (175 of 869 cases, see Chapter 3.5.). Among the different histopathological subtypes, the rate of recurrent cases varied from 0.00-46.67%. The subtypes with the lowest incidence of recurrence were DGLAs (0 of 7 cases, 0.00%), ASCAs (1 of 10 cases, 10.00%) and MSAs (1 of 11 cases, 9.09%). More than one in five gonadotroph (65 of 230 cases, 22.03%) and mixed somatolactotroph (3 of 13, 23.08%) adenomas and almost half of SGCAs (7 of 15 cases, 46.67%) recurred postoperatively, making them the three subtypes with the highest risk of tumor recurrence. Each subtype was compared with the rest of the cohort and the results demonstrated that there was no significant correlation with postoperative recurrence for all but one subtype (see Table 3.16.). The diagnosis of a SGCA was significantly associated with a higher rate of recurrence postoperatively. While 113 of 605 (18.68%) tumors of other subtypes recurred, this was observed in 7 of 15 (46.67%) SGCAs (p=0.0067). Therefore, the SGCA subtype was undertaken a Kaplan-Meier analysis of recurrence-free survival time (see Figure 3.18.). With a mean time to recurrence of 7.28 years compared to a mean of 9.66 years of all other subtypes combined, SGCA demonstrated recurrence significantly earlier than other subtypes (p=0.0009).

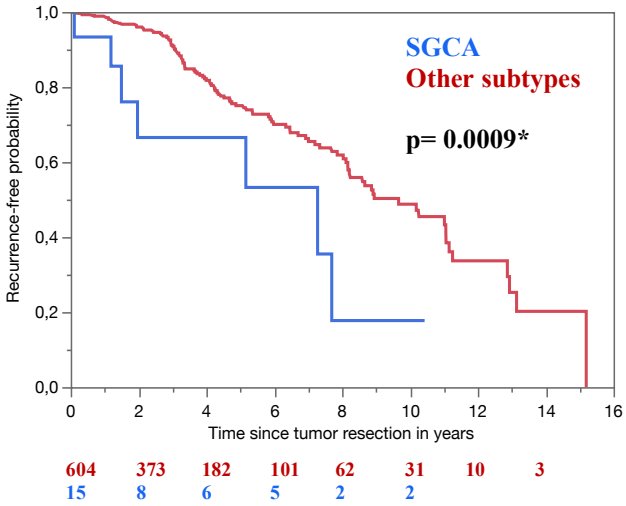

Figure 3.18.: SGCA subtype with significantly shorter recurrence-free survival time.
Kaplan-Meier analysis of recurrence-free survival time of the SGCA subtype.
The mean time to recurrence was significantly shorter in SGCA than in other adenoma subtypes (7.28 compared to 9.66 years).
Asterisk (*) represents statistically significant differences (p<0.05).

Table 3.16.: Subtype-specific rate of recurrence in comparison to rest of cohort.

Subtype	Recurrence		p value
	Subtype N (%)	Rest of cohort N (%)	(Pearson test)
Corticotroph			
- SGCA	7 of 15 (46.67%)	113 of 605 (18.68%)	0.0067 *
- DGCA	9 of 48 (18.75%)	111 of 572 (19.41%)	0.9121
- Crooke	0 of 0 (0.00%)	120 of 620 (19.35%)	
Gonadotroph	**65 of 295 (22.03%)**	**55 of 325 (16.92%)**	0.1077
Lactotroph			
- SGLA	8 of 39 (20.51%)	112 of 581 (19.28%)	0.8500
- DGLA	0 of 7 (0.00%)	120 of 613 (19.58%)	0.1924
- ASCA	1 of 10 (10.00%)	119 of 610 (19.51%)	0.4503
Null Cell	**10 of 53 (18.87%)**	**110 of 567 (19.40%)**	0.9252
Plurihormonal	**2 of 14 (14.29%)**	**118 of 606 (19.47%)**	0.6273
Somatotroph			
- SGSA	8 of 59 (13.56%)	112 of 561 (19.96%)	0.2362
- DGSA	6 of 49 (12.24%)	114 of 571 (19.96%)	0.1893
- MSA	1 of 11 (9.09%)	119 of 609 (19.54%)	0.3846
- Mixed SLA	3 of 13 (23.08%)	117 of 607 (19.28%)	0.7314
Thyreotroph	**0 of 7 (0.00%)**	**120 of 613 (19.58%)**	0.1924

p-values: * <0.05; ** <0.01

3.5.4. MIB-1

Recurrent adenomas had a slightly higher mean MIB-1 value of 0.81 compared to 0.76% of nonrecurrent adenomas, but without statistical significance (p=0.3327). A CART analysis for the target variable postoperative recurrence was conducted and defined a MIB-1 immunopositivity of 0.6% as an optimal cutoff, which was used for the Kaplan-Meier analysis. The results of the analyses with this MIB-1 cutoff are shown in Figure 3.19.

Subgroups of patients were unequally-sized, as there were 434 patients with a MIB-1 level ≥0.6% and 182 patients with values below the cutoff. While 28 cases in the latter subgroup recurred (15.38%), this rate was insignificantly higher in adenomas with a MIB-1 value ≥0.6% (96 cases or 22.12%, p=0.0535).

A MIB-1 value ≥0.6% significantly correlated with a shorter recurrence-free survival time. The mean time to recurrence of adenomas with a MIB-1 value ≥0.6% was about two years earlier than the mean duration of adenomas with MIB-1 values <0.6% (8.12 years as opposed to 10.26 years, p=0.0135).

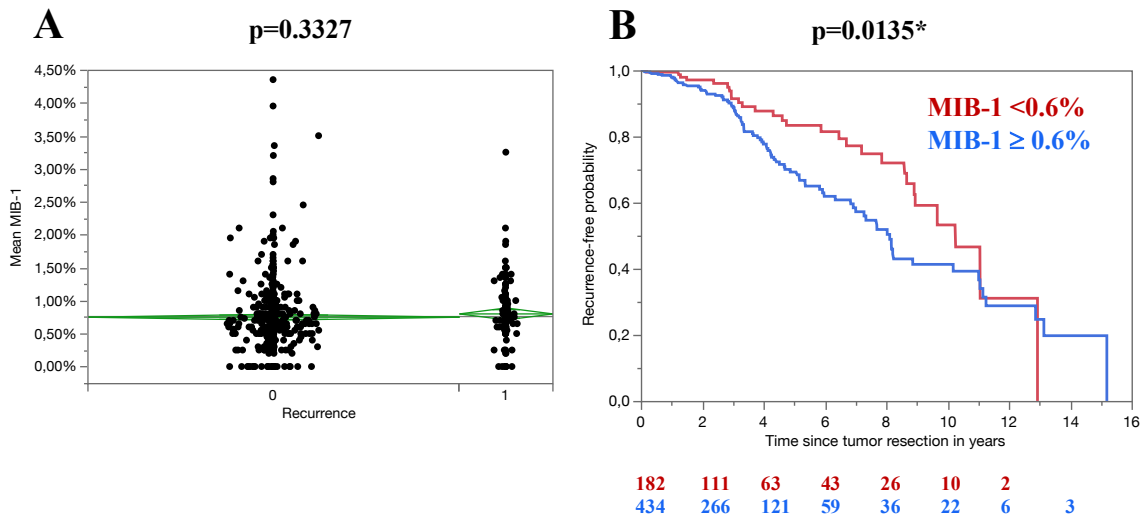

Figure 3.19.: MIB-1 values ≥0.6% with significantly earlier recurrence.
A: Scatter diagram of MIB-1 value dependent on recurrence. Higher mean MIB-1 value in recurrent cases without significance.
B: Kaplan-Meier analysis of recurrence-free survival time at a MIB-1 cutoff of 0.6%. Significantly shorter time to recurrence in cases with a MIB ≥0.6% (8.12 compared to 10.26 years).
Asterisk (*) represents statistically significant differences (p<0.05).

3.5.5. H3K27me3 and H3K36me3

For the assessment of recurrence risk dependent on H3K27me3, a CART analysis identified a cutoff at a score of 3 (50-75% positivity). A H3K27me3 expression below the cutoff (<50% immunopositivity) was associated with a significantly higher rate of recurrent tumors. While recurrence occurred in 40 of 156 adenomas (25.64%) with a H3K27me3 score <3, it was present in 82 of 471 adenomas (17.41%) with a score ≥3 (p=0.0236). In the Kaplan-Meier analysis a H3K27me3 score below the cutoff of 3 did not correlate significantly with recurrence-free survival time (see Figure 3.20., Graph A). In cases with a H3K27me3 score <3 the average time until tumors recurred was 8.67 years as opposed to 8.87 years in the comparison group (p=0.2173).

A CART-proposed cutoff of a score of 4 (≥75% immunopositivity) was used for the prognostic analysis of H3K36me3. A significantly higher rate of tumor recurrence was detected in adenomas with a H3K36me3 score <4. While 59 of 235 adenomas below this cutoff recurred (25.11%), 63 of 397 adenomas with a H3K36me3 score of 4 developed a recurrence (15.86%, p=0.0043). The Kaplan-Meier analysis of recurrence-free survival time was without a statistically significant difference at the H3K36me3 cutoff score of 4 (see Figure 3.20., Graph B). Adenomas with a H3K36me3 score below the cutoff had an average time to recurrence of 8.87 years, compared to 9.66 years of adenomas with a score of 4 (p=0.6978).

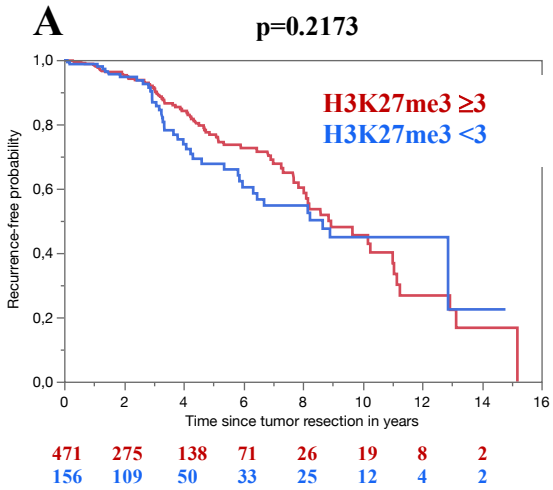

Figure 3.20.: No significant correlation of H3K27me3 <3 or H3K36me3 <4 and time to recurrence.
A: Kaplan-Meier analysis of recurrence-free survival at a H3K27me3 cutoff of 3. No significant correlation.
B: Kaplan-Meier analysis of recurrence-free survival at a H3K36me3 cutoff of 4. No significant correlation.

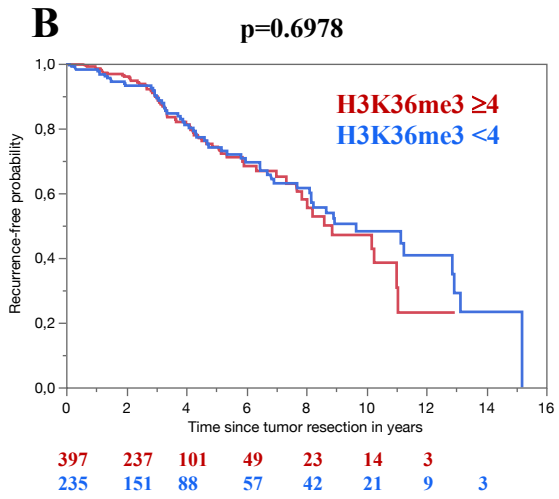

3.5.6. Osteonectin/SPARC

Among the osteonectin IRS ranging from 0 to 12, a CART analysis singled out low expression of osteonectin as suitable area to assess recurrence potential, as it proposed an IRS of 2 as the optimal cutoff for our cohort. There was a disparity by a factor of 10 regarding the size of the osteonectin subgroups at this cutoff, 49 cases with an IRS <2 were seen alongside 584 cases with an IRS above the cutoff. Cases with an IRS ≥2 had an insignificantly higher rate of recurrence than cases with an IRS <2 (117 cases or 20.03% compared to 7 cases or 14.29%, p=0.3327). As displayed in Figure 3.21., there was no statistical significance in the Kaplan-Meier analysis of tumors with lower and higher osteonectin IRS than the cutoff (mean recurrence-free survival time of 8.21 years and 8.91 years, respectively, p=0.6982).

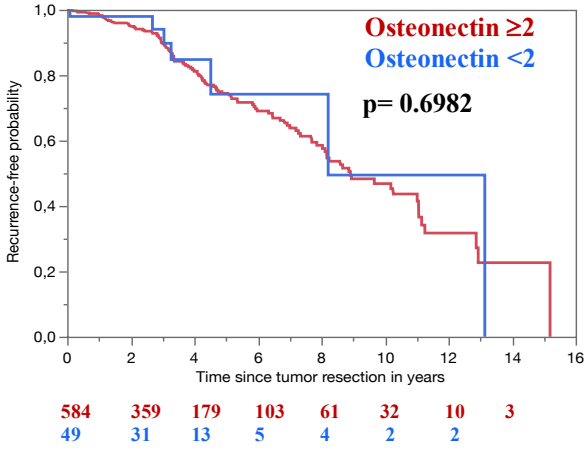

Figure 3.21.: No significant correlation of osteonectin IRS<2 and time to recurrence. **A:** Kaplan-Meier analysis of recurrence-free survival at an osteonectin cutoff of an IRS of 2 without a significant difference.

3.6. Multivariate Analysis

A cox regression analysis was created for the multivariate analysis of the target variable recurrence-free survival time. Only clinical factors or markers that demonstrated a significantly shorter mean time to recurrence ($p<0.05$) or a mentionable statistical trend ($p<0.10$) towards earlier recurrence were included in the proportional hazards model. In the univariate analysis, invasion by intraoperative observation ($p=0.0148$) as well as radiographic CSI corresponding to Knosp grades 3A-4 ($p=0.0008$) or Knosp grades 2-4 ($p=0.001$) were significantly associated with a shorter recurrence-free survival time. Separate MVAs were run for each of these variables. The univariate analysis also showed significant results for the SGCA subtype ($p=0.0009$) and a MIB-1 value ≥0.6% ($p=0.0135$). An age <49 years at diagnosis was demonstrated to have a statistical tendency towards early recurrence ($p=0.0862$). Table 3.17. lists all parameters included in the MVA, while the results of the cox regression analysis of these parameters are shown in Table 3.18.

Radiographic CSI was an independent negative prognostic factor as it was a significant predictor of earlier recurrence at both Knosp cutoffs. The time to recurrence was not influenced by invasion by intraoperative estimation and did not show age-dependency at a cutoff of 49 years at diagnosis, both variables lacked a significant prognostic impact.

The SGCA subtype and a MIB-1 score of ≥0.6% were independently and significantly associated with a worse prognosis in all analyses. Patients with an adenoma of the SGCA subtype were around 2.7-times more likely to suffer from an early recurrence in case radiographic CSI and 3 times more likely in case intraoperative invasion was the leading criteria used to define invasiveness.

No matter the definition of invasion applied, adenomas with MIB-1 scores of ≥0.6% had an over 1.5-fold higher risk of a shorter recurrence-free survival.

Table 3.17.: Parameters included in the MVA of recurrence-free survival time.

Variable	Result in the univariate analysis
Intraop. Invasion	p=0.0148 *
Knosp 3A-4	p=0.0008 **
Knosp 2-4	p=0.001 **
SGCA	p=0.0009 **
MIB-1 ≥0.6%	p=0.0135 *
Age < 49 years	p=0.0862

p-values: * <0.05; ** <0.01

Table 3.18.: Results of the Cox regression analysis.

Variable	Coefficient	Standard error	Hazard ratio	95% CI	p-value
Intraop. Invasion	-0.177960	0.096571	1.427494	-0.367237 – 0.011316	0.0654
Age <49	0.173454	0.095940	1.414686	-0.014585 – 0.361492	0.0706
SGCA	-0.556115	0.202964	3.041134	-0.953918 - -0.158312	0.0061 **
MIB-1 ≥0.6%	-0.228233	0.111568	1.578486	-0.446902 - -0.009564	0.0408 *

p-values: * <0.05; ** <0.01

Variable	Coefficient	Standard error	Hazard ratio	95% CI	p-value
Knosp 3A-4	-0.264575	0.105368	1.697490	-0.471568 - -0.057215	0.0126 *
Age <49	0.159193	0.106377	1.374909	-0.051164 - -0.036383	0.1369
SGCA	-0.491684	0.221335	2.673446	-0.887482 - -0.004715	0.0481 *
MIB-1 ≥0.6%	-0.280639	0.13019	1.752913	-0.549627 - -0.036383	0.0235 *

p-values: * <0.05; ** <0.01

Variable	Coefficient	Standard error	Hazard ratio	95% CI	p-value
Knosp 2-4	-0.326898	0.113625	1.922825	-0.549600 - -0.104197	0.0040 **
Age <49	0.161248	0.106708	1.380570	-0.047896 – 0.370392	0.1308
SGCA	-0.495326	0.219035	2.692991	-0.924627 - -0.066026	0.0237 *
MIB-1 ≥0.6%	-0.277278	0.130005	1.741167	-0.532084 - -0.022472	0.0329 *

p-values: * <0.05; ** <0.01

4. Discussion

4.1. Intraoperative and Radiological Assessment of Invasion

The two target variables in this study were intraoperative presence of invasion and radiological evidence of cavernous sinus invasion (CSI) on preoperative MR images. By intraoperative estimation, pituitary adenoma invasion was found in 395 of the 927 (42.61%) cases of all subtypes who underwent tissue analysis. As most surgeries were performed by the same neurosurgeon or under his supervision, inter-individual variation of this subjective evaluation of invasiveness was limited. Assessment of CSI based on the Knosp classification was obtained in 764 cases who underwent tissue analysis. In the literature-based dichotomization, Knosp grades 3A-4 were considered invasive when compared to the intraoperative assessment, which applied to 186 adenomas (24.35%). In the CART-based dichotomization, Knosp grades 2-4 were counted as invasive which applied to 302 cases (39.53%). The grading with the Knosp scale was conducted by a single interpreter which created uniformity for the second target variable as well.

Generally, the frequencies of invasive cases of our cohort appear in line with the literature as evidence of invasion was reported to be present in 30-50.41% of all adenomas in other studies (Trouillas et al., 2013; Zada et al., 2011; Miermeister et al., 2015; Tortosa & Webb, 2016). A meta-analysis of 40 studies featuring 3,295 cases that solely focused on CSI found this form of invasive growth in 22% of all adenomas (Dhandapani et al., 2016). A Portuguese study, which featured a total of 220 PAs, evaluated and found radiographic invasion in 13 of 28 (46.4%) atypical adenomas (Tortosa & Webb, 2016). Apart from the small cohort size, the atypical adenoma (APA) diagnosis is already abandoned due to lacking prognostic utility (Chesney et al., 2017). It would therefore have been more interesting to determine the rate of radiographic invasion among the whole cohort of 220 PAs in this study. Another series from Harvard Medical School featuring 121 typical and atypical adenomas detected a frequency of radiographic invasion of 50.41% (Zada et al., 2011). In a German comparative analysis of 98 APAs with 200 non-APAs and 10 pituitary carcinomas, an invasive growth pattern was present in 126 of 298 (42.28%) pituitary adenomas (Miermeister et al., 2015). Invasion was evaluated by the intraoperative estimate, existence on MRI or by histology. With a much higher rate,

invasion of the sphenoid sinus or CS by histological or radiographic estimate was detected in 68 of 120 (56.67%) cases in another study, however with limited general expressiveness for PAs as it featured only NFPAs (Lelotte et al., 2018). In a series with a relatively large cohort of 410 adenoma patients (Trouillas et al., 2013), radiological evidence of CS or sphenoid sinus invasion was present in 175 tumors (42.68%), this rate is very close to the rate of 42.61% of intraoperatively invasive cases in our study. The results in the literature were described this detailed to clarify that the criteria of invasion differ among studies. Besides, none of the mentioned retrospective studies encompassed a PA cohort with as many patients as our study cohort.

CSI was specifically addressed due to its therapeutic relevance, as it has been described as a possible risk factor for incomplete resection (Dhandapani et al., 2016; Sanmillán et al., 2017; Woodworth et al., 2014; Bao et al., 2016; Frank & Pasquini, 2006; Taniguchi et al., 2015). The original Knosp classification of 1993 has been widely used, but one major limitation is poor reliability of its middle scores (Micko et al., 2015; Mooney et al., 2017b). We used a dichotomized Knosp scale. This decision was based on a study with 6 different raters of 50 MRI scans of biopsy-proven pituitary adenomas that demonstrated only 5% interrater agreement for the middle scores and 10% for the full scale, but an increased interrater agreement rate of 60% for a commonly used dichotomization (Grades 0-2 vs. 3-4) (Mooney et al., 2017b). Another study of 137 macroadenomas proposed a subdivision into grades 3A and 3B (Micko et al., 2015). It was demonstrated that Grade 3 adenomas with extension beyond the lateral tangent of the internal carotid arteries (ICAs) were significantly more often invasive when they extended into the inferior CS compartment (grade 3B) than the superior CS compartment (grade 3A) (Micko et al., 2015). This subdivision was applied in our study. Instead of the original 5-tiered classification (Knosp et al., 1993), the updated scale with 6 scores was used.
Using this adapted Knosp scale, we observed concordance rates of ≥50% for the grades 2-4 and of ≥66.7% for the grades 3A-4 cutoff with intraoperatively present invasion. Data regarding the validity of the Knosp scale to predict CSI of pituitary adenomas is not fully unequivocal. One retrospective review of 106 cases found that extension beyond the lateral tangent of the ICAs which equates Knosp grade 3A or higher has a positive predictive value of 85% for the surgical finding of invasion (Cottier et al., 2000). On the

other hand, a meta-analysis encompassing 40 studies detected a considerable difference between the two modes of CSI detection. While CSI was reported to be prevalent in 18% of adenomas in studies using the intraoperative estimate, CSI was present in 43% of cases in series that used radiological criteria such as the Knosp scale (Dhandapani et al., 2016). At first, this finding seems contradictory to our result of a rate of 42.16% of intraoperative invasion and a rate of 24.35 (literature-based Knosp cutoff) and 39.53% (CART-based Knosp cutoff) of CSI. It is important to understand the difference between our intraoperative and radiographic definition of invasiveness, however. In our study the intraoperative definition included invasion of the sphenoid sinus and dural invasion. Radiographic CSI according to the Knosp scale was assumed whenever adenoma growth in the CS compartment with a certain relative position to the ICA was present on MRI. However, an adenoma with a high Knosp grade might also only have grown with a compressive instead of an invasive pattern into the CS space. The authors of the previously mentioned extensive review also stress that direct intraoperative observation of invasiveness is considered more accurate than invasion detected by radiology (Dhandapani et al., 2016). The different definitions of PA invasion are one possible explanation for the higher rate of intraoperative invasion than radiographic invasion in our study.

Some studies proposed other more certain, however less comparable criteria for CSI such as lack of visibility of venous CS compartments or at least 45 or 67% encasement of the ICA (Cottier et al., 2000; Vieira et al., 2006). Nevertheless, to date Knosp grades 3-4 are considered to be the best objective radiographic indicators of CSI (Dhandapani et al., 2016). As shown above, past studies have used different criteria for invasion which decreases comparability of scientific results. A solution of this problem for future research on this topic would be the use of standardized criteria for invasion by all authors. In this regard, a reliable and specific immunohistochemical marker for PA invasion with additional prognostic value would be a breakthrough.

4.2. Prognostic Evaluation of Recurrence Potential

As a means of considering another characteristic of PA aggressiveness besides the central aspect of invasiveness, the clinical factors and immunohistochemical markers discussed in this study underwent a complementary analysis of their prognostic impact. For this purpose, recurrence-free survival times were assessed by generation of Kaplan-Meier curves with specific cutoffs in 896 cases. Of the total of 1,220 cases included in this study, only 99 cases were lost to follow-up. Potential reasons for the lack of follow-up data are incompliance of patients by nonadherence to appointments or follow-up examinations at another medical center closer to home. In 175 of 869 adenomas (20.14%) a recurrence was detected during follow-up radiographic imaging or hormonal testing. Recurrence was defined as de novo growth following gross total resection, progression of a residual adenoma or anew hormonal elevation in laboratory tests in this series. Heterogeneity in studies is problematic and aggravates comparability of studies which focus on recurrence potential of pituitary adenomas. Firstly, while some sources defined recurrence the same way with inclusion of progressive residuals (Hasanov et al., 2019; Trouillas et al., 2013; Lelotte et al., 2018), in another large meta-analysis the definition of recurrence explicitly excluded regrowth of tumor remnants (Roelfsema et al., 2012). Recurrence rates reported in the literature vary greatly between 7.6 and 46% (Chacko et al., 2010; Meij et al., 2002; Chiloiro et al., 2014; Kim et al., 2016; Sadeghipour et al., 2017; Watts et al., 2017; Hasanov et al., 2019; Chen et al., 2012; Brochier et al., 2010). The finding of a meta-analysis of 19 studies, in which the case group without a remnant had a recurrence rate of 12% and the case group with residual tumors a rate of 46%, demonstrates that this variation can indeed be attributed to different definitions of recurrence (Chen et al., 2012). Apart from that, the recurrence rate depends on the adenoma characteristics. For instance, a series solely on macroadenomas had a much higher recurrence rate of 40% than our study (Brochier et al., 2010). Our median follow-up time of 31 months was shorter than in some studies with mean follow-up durations of 48 months (Lelotte et al., 2018; Watts et al., 2017), 9 (Dubois et al., 2007) or even 11.14 years (Trouillas et al., 2013), implicating that this study might not have considered possible long latency times until recurrence of some cases.

To assess their impact on the outcome, the central target variables of intraoperative invasion and radiographic CSI according to the literature- and CART-based Knosp cutoffs were included in the prognostic analysis. While in the Kaplan-Meier analyses all three definitions of PA invasion were significantly associated with a shorter mean recurrence-free survival time, in the multivariate cox regression analysis only CSI according to Knosp grade 3A-4 (p=0.0126) and Knosp grade 2-4 (p=0.0040) was a significant predictor of a worse progression-free survival. Invasion by intraoperative definition was not associated with an earlier recurrence in this study (p=0.0654). In fact, there is more evidence for a prognostic role of CSI in the literature as well. Invasion was found to be unrelated to recurrence in the meta-analysis of Roelfsema et al. which featured data from 143 studies (Roelfsema et al., 2012). While invasion was assessed macroscopically which equals our intraoperative estimate as well as microscopically, the meta-analysis used a different definition of recurrence compared to our study, as described in the passage above. In a Korean study of 167 PAs, cases with microscopic signs of invasion were not significantly associated with an increased risk of recurrence (Kim et al., 2016). The recurrence risk did also not depend on microscopic dural invasion in another, even larger series of 354 adenomas (Meij et al., 2002). Contrary to that, CSI was found to have a negative impact on recurrence risk by two studies featuring 142 and 275 cases (Brochier et al., 2010; Hwang et al., 2016). Apart from the limitation of the inclusion of solely NFPAs, recurrence risk was assessed with Kaplan-Meier analyses of recurrence-free survival times like in our study. Only the newer of the two studies assessed CSI with the adapted, 6-tiered Knosp classification and grades 3A, 3B and 4 were considered high-grade CS-invasive, which is equal with our literature-based Knosp cutoff. Without assessment of recurrence-free survival time, a series with a large cohort of 601 PAs of all subtypes observed a significantly higher frequency of recurrences in cases with CSI according to Knosp grades 2-4 (Hasanov et al., 2019), which matches our second, CART-based Knosp cutoff. The authors proposed a combination of both high Ki-67 and CSI as a predictor of recurrence. Indeed, since no multivariate analysis was conducted, a co-dependency of CSI on Ki-67 values could not be excluded. In a Japanese series, no correlation of CSI according to Knosp grades ≥3 with progression of a residual adenoma was detected, however only 39 PAs were included, and de novo regrowth was not considered as a form of recurrence (Matsuyama, 2012). In another retrospective

analysis of 343 adenomas, CSI was a significant factor for recurrence, while other forms of invasion were not (Chiloiro et al., 2015). As a matter of fact, based on the lack of a meaningful association in our study as well as the lack of evidence in the literature, intraoperatively reported invasion alone should not prompt to expect more frequent and earlier recurrence. The preponderance of findings of a significant prognostic role of CSI in the literature are in line with our study result and indicate that CSI according to high Knosp grades is of high prognostic value.

4.3. Age and Gender

On average, patients with invasive pituitary adenomas were older than noninvasive cases in this study for both the intraoperative and radiological estimate of invasiveness. An age at diagnosis above a cutoff of 71 years correlated with intraoperative observation of invasion in the univariate analysis, however this finding was not independently predictive. Radiologically detected CSI showed age dependency as an independent association of an age of at least 45 years at diagnosis with the higher Knosp grades was demonstrated. Neither radiographic CSI, nor intraoperatively existent invasion depended on gender.

Data in the literature regarding the role of the clinical factors patient age and gender on pituitary tumor invasion is limited. Only a few studies focusing on pituitary tumor invasion have evaluated specific age cutoff values.

Nevertheless, there is evidence in the literature that invasive adenomas might be more likely to affect the older age groups. In a Chinese study from 2014, patients with invasive adenomas were older at the time of surgery than patients with noninvasive adenomas, this difference was without statistical significance (Feng et al., 2014). Invasion was assessed in a similar way as in our study as all cases with Knosp grade 4 or Knosp grades 2-3 plus intraoperatively reported invasion were considered invasive. A drawback is that the study featured only 43 nonfunctioning adenomas. An older study from 2002 with a larger cohort of 354 patients also found that the mean age of invasive cases was higher than of noninvasive cases (Meij et al., 2002). This was even statistically significant, however it applied for intraoperatively observed dural invasion only. Regarding gender, the role on

adenoma invasion can only be speculated. One study of 153 adenomas of all subtypes reported the rate of invasion to be 56% in male patients (Scheithauer et al., 2006). Apart from that, past studies only observed that women tend to have smaller adenomas (Scheithauer et al., 2006; Meij et al., 2002). The role of age and gender on adenoma invasion is possibly also influenced by the adenoma subtype. For instance, the SCA subtype which was found to be significantly more invasive was also found to be significantly associated with sex with a female preponderance in a recent study (Jiang et al., 2021). Contrary to our and the findings of other authors, another relatively new study with data from 463 somatotroph adenomas found significantly higher rates of CSI in female patients and in younger age groups (premenopausal women and men <50 years of age) (Park et al., 2018). An insignificant finding in line with this is provided by another study. In a comparison of 55 adenoma patients >70 years of age with 30 patients aged 60-69 years and 289 patients aged <60 years, frequently more Knosp grade 3 and 4 cases were found in the younger age groups (Gondim et al., 2015).
To sum up against this background of scarce, but in part contrary results of other studies, we detected age dependency solely of CSI at both Knosp dichotomizations and only with a cutoff of 45 years at diagnosis. Without an age cutoff, patients suffering from an adenoma with CSI according to the Knosp grading only had a slightly higher mean age at diagnosis. The fact that the dependency is a strictly cutoff-based finding is impractical and therefore also has a questionable implication for the clinical routine.

Regarding recurrence potential, no statistically significant association was found. Patients with a recurrent adenoma were slightly younger than patients without a recurrence and slightly more female than male patients had a recurrent adenoma. However, neither an age below a cutoff of 49 years nor female gender had a significantly shorter mean recurrence-free survival time. In the literature, it is widely suggested that younger age at diagnosis may be associated with an increased risk of recurrence. However, it cannot be ruled out that this is influenced by the adenoma type. A meta-analysis on PA recurrence that analyzed data from 143 studies concluded that age and gender have prognostic significance mainly in studies on NFPAs, while these associations are absent in functional adenomas (Roelfsema et al., 2012). This is backed by results of Belgian (Lelotte et al., 2018), Italian (Losa et al., 2008) and Australian (Watts et al., 2017) studies that all

included follow-up-data of >120 NFPAs and demonstrated a younger age at diagnosis as an independent risk factor for recurrence. The latter study even found a significantly shorter mean time to recurrence at an age cutoff of 41 years, which is relatively close to our cutoff of 49 years. Despite the fact that evidence prevails for NFPAs, two studies also demonstrated a significantly higher rate of recurrence at a younger mean age in their cohorts of all subtypes (Trouillas et al., 2013; Kim et al., 2016). Other sources speculate that there is less aggressive potential and a lower incidence of regrowth in PA in the elderly (Gondim et al., 2015; Ferrante et al., 2002; Sheehan et al., 2008). Data on gender dependency of recurrence potential is more scarce than data for the factor age, but patient gender was found to be not a significant factor in several studies (Trouillas et al., 2013; Kim et al., 2019; Watts et al., 2017), which is in line with our results.

4.4. Adenoma Subtypes

In the subtype-specific analysis of invasiveness, null cell adenomas (NCAs), gonadotroph adenomas and sparsely granulated corticotroph adenomas (SGCAs) were the three entities that had striking findings. NCAs were associated with CSI for both Knosp dichotomizations, gonadotroph adenomas only correlated with CSI for the CART-based Knosp cutoff. SGCA were the sole subtype to be independently and significantly predictive of both criteria of pituitary adenoma invasion. CSI was almost three times and intraoperative presence of invasion more than two times more likely in SGCAs compared to other subtypes.

One possible logical explanation for why NCAs and gonadotroph adenomas were associated with radiological criteria of CSI in this study is the fact that both subtypes typically present as clinically nonfunctioning pituitary macroadenomas (NFPAs) at diagnosis. Consequently, patients usually become symptomatic because of tumor compression of surrounding structures. Due to their size, macroadenomas have an increased tendency to grow out of the sella into the supra- or parasellar compartment. A series of 294 adenomas of different subtypes backs this hypothesis as its distribution of Knosp grades demonstrated that there were significantly more NFPAs among the higher grades of the scale (Sanmillán et al., 2017). At times when the 2004 WHO classification

was still effective and before abandonment of the atypical adenoma diagnosis, NCAs and SGCAs were among the adenomas generally considered aggressive (Mete & Asa, 2012; Asa & Ezzat, 2009; Saeger et al., 2016; DeLellis, 2004). Since the 2017 WHO classification there has been a partial shift to the following adenoma types that are considered aggressive: sparsely granulated somatotroph adenomas (SGSA), lactotroph adenomas in men, Crooke's cell adenomas, silent corticotroph adenomas (SCAs) and PIT-1 positive plurihormonal adenomas (Saeger, 2021; Kontogeorgos, 2021; Liu et al., 2020; Pappy et al., 2019; Lloyd et al., 2017). Although aggressiveness is not equitable with invasiveness (Kontogeorgos, 2021), the connection between these two clinical behaviors prompted to the hypothesis that aggressive subtypes may also be more prone to be invasive. Indeed, in a Chinese study of 250 PAs, the incidence of invasive tumors in these five high-risk adenomas was significantly higher than in other subtypes (Liu et al., 2020). It is difficult to comment on the relation of Crooke's cell and plurihormonal adenomas with invasion in this series as these subtypes were very rare, accounting for 2 and 21 cases only, respectively. Besides, this study lacked a sex-specific assessment of lactotroph adenomas and any correlation of SGSA with invasion. Regarding the aggressive SCAs, there is a very likely connection with our finding that SGCA correlate with invasiveness. The necessity to differentiate the SCA subtype from other NFPAs has been long known (Mete & Asa, 2012) and is further justified because of its predisposition to hemorrhage (Saeger, 2021) and the fact that its frequency within NFPAs is higher than previously thought (Nishioka et al., 2015). While SCAs can be divided in type 1 which consists of DGCAs and type 2 consisting of SGCAs (Osamura et al., 2008), SGCAs are considered silent more often than DGCAs (Kontogeorgos, 2021). There has been a recent Chinese study of 371 and a Japanese study of 516 NFPAs where SCAs were significantly more frequently associated with CSI in comparison to other NFPA subtypes (Nishioka et al., 2015; Jiang et al., 2021). Fitting to these findings, in another Japanese series with NFPAs, CSI was most frequently present in SCAs (85%), ahead of NCAs (38%) and gonadotroph adenomas (11%) (Yamada et al., 2007). The study by Jiang et al. even demonstrated multiple-site invasion and direct intraoperative observation to occur significantly more frequently in SCAs (Jiang et al., 2021). However, while all previously mentioned studies only included NFPAs, our findings for SGCAs were based on the comparative analysis with all other adenoma subtypes. In our study, the strong correlation

of SGCA with radiological and intraoperative invasion is striking. However alternatively, another approach would have been an analysis of all SCAs including DGCAs, which is possible as nonfunctioning can be distinguished from functioning corticotroph adenomas with the help of the marker galectin-3 (Kontogeorgos, 2021). This is worth investigating for better comparability with the existing literature on SCA.

We were able to show in this study that the SGCA subtype is also predictive of a negative prognosis as it was significantly and over three times more likely to demonstrate an earlier recurrence. Similar to studies that focused on invasion, a prognostic analysis of a cohort that underwent exact subtyping according to the latest WHO criteria is missing in the literature so far. Another problem for comparability is that very few subtype-specific studies in the past worked with Kaplan-Meyer curves and multivariate prognostic analyses.

In a meta-analysis of 143 studies, prolactinomas and NFPAs had the highest recurrence rate, but NFPAs were not further subdivided into the particular type (Roelfsema et al., 2012). All other studies mentioned in this passage, which subdivided NFPAs, only included NFPAs but no other functional subtypes. The current European Guidelines for the management of aggressive pituitary adenomas also emphasize that lactotroph adenomas in men and silent corticotroph adenomas are more prone to earlier recurrence than silent gonadotrophs (Raverot et al., 2018; Delgrange et al., 2015; Cooper et al., 2010). Additionally, alongside with silent ACTH or GH/PRL adenomas, plurihormonal adenomas were also recognized to relapse more frequently than null cell adenomas and gonadotroph adenomas in a study of 142 macroadenomas (Brochier et al., 2010). Based on our study data, it is problematic to reliably comment on the prognostic implications of some of these subtypes. For instance, plurihormonal adenomas occurred very rarely and prolactinomas did not undergo a sex-specific analysis of recurrence risk. The most convincing findings exist for the SCA subtype. In a study of 501 adenomas, patients with SCAs had a significantly lower recurrence-free survival than other NFPA types (Pappy et al., 2019). In a different comparative analysis of 25 SCAs and 84 NFPAs, SCAs on average recurred 5 years earlier (Cooper et al., 2010). Since SGCA are thought to account for the majority of SCAs (Kontogeorgos, 2021), these findings fit with the result of our

prognostic analysis, where SGCAs were found to be independently and strongly predictive of a lower-recurrence free survival time.

4.5. MIB-1

In the analysis of all MIB-1 values combined, a significantly higher mean MIB-1 value of invasive cases was only found for CSI according to the CART-based Knosp cutoff. The mean MIB-1 value of adenomas with CSI at the literature-based Knosp cutoff was even slightly lower. For intraoperatively invasive adenomas, the mean value was only insignificantly higher. Using individual cutoffs for each target variable, solely for intraoperative invasion adenomas with a MIB-1 value ≥0.6% were independently and significantly more likely to be invasive. There was no correlation between MIB-1 and CSI based on the two Knosp grade cutoffs.

Immunohistochemical detection of dividing cells by staining of the antigen Ki-67 (also referred to as MIB-1) is established for decades in the histopathological assessment of tumors (Gerdes et al., 1984). However, its suitability as a marker of adenoma invasion is questionable. The mean MIB-1 value of 0.81% in this series seems relatively low compared to findings in the literature. Mean MIB-1 values in studies with a cohort size of at least 100 pituitary adenomas range from 1.00-3.73% (Chiloiro et al., 2014; Pizarro et al., 2004; Jaffrain-Rea et al., 2002; Chacko et al., 2010; Zhao, Tomono & Nose, 1999; Mastronardi, Guiducci & Puzzilli, 2001; Grimm et al., 2019; Monsalves & Larjani, 2014; Thapar et al., 1996a). This large variation of MIB-1 values might be attributable to methodological differences during tissue processing and counting of immunohistochemical activity (Chiloiro et al., 2014). We have used a standardized digital assessment tool to quantify immunopositivity and have therefore no interobserver bias as is believed to play a role in some retrospective analyses where histopathological reports were reviewed.

There is ambiguity regarding the correlation of Ki-67 with pituitary adenoma invasion. The creators of the Knosp classification linked higher Ki-67 values to histologically proven dural invasion (Knosp et al., 1989). While this definition of invasion differs from

ours, there is also another older study which used both radiological and intraoperative assessment criteria of invasion and found higher Ki-67 expression in invasive adenomas (Zhao et al., 1999). A Brazilian study of 159 adenomas, despite demonstrating significantly higher Ki-67 activity in invasive adenomas compared to macroadenomas, was not able to establish a suitable cutoff value to distinguish invasive from noninvasive lesions due to considerable overlap of MIB-1 values (Pizarro et al., 2004). In 1996 Thapar et al. proposed a Ki-67 cutoff of 3% that was able to distinguish invasive from noninvasive tumors with 97% specificity and 73% sensitivity (Thapar et al., 1996a). This cutoff was adopted by the 2004 WHO classification (DeLellis, 2004) and accepted by other authors to deserve special attention (Jaffrain-Rea et al., 2002), but it is greatly different from the 0.6% threshold that was significantly associated with intraoperatively present invasion in our study. A reason for this might be different methods of determination of Ki-67 LI. In their studies Thapar et al. and Jaffrain-Rea et al. both quantified Ki-67 by manual microscopic field enumeration of an average of 4,200 and 1,000 nuclei, respectively. Our usage of a standardized digital assessment tool, which considers every single adenoma nuclei of a sample, possibly is a more accurate quantification method. Some studies with other key issues (Scheithauer et al., 2006) or that featured only a small number of 44 macroadenomas (Paek et al., 2005) found no association between Ki-67 and radiological or intraoperative invasion at all. There are only few studies that work with cutoff values and generally, a question of relevance is dependency of the marker MIB-1 on other clinical factors. There is more evidence that there are indeed significant differences of MIB-1 values based on age, gender, medical pretreatment and functional or nonfunctional status (Monsalves & Larjani, 2014; Jaffrain-Rea et al., 2002; Zhao et al., 1999) than studies supporting that MIB-1 is not influenced by these factors (Chacko et al., 2010; Yuhan et al., 2021). MIB-1 does not seem to correlate with CSI in our study and in the majority of other studies. The apparently significant association of Ki-67 with CSI in some studies (Iuchi et al., 2000; Jaffrain-Rea et al., 2002) might only be caused by the fact that CSI is the result of faster growth or greater size of an adenoma and therefore higher Ki-67. This hypothesis is backed by the finding that in studies which featured only macroadenomas, there was no significant difference between Ki-67 level and Knosp grade (Micko et al., 2015; Paek et al., 2005). The argument against this hypothesis is the fact that different authors agreed that while

Ki-67 correlates with growth velocity, the actual tumor size is independent of Ki-67 expression (Honegger et al., 2003; Zhao et al., 1999; Mastronardi et al., 2001). A recent study in which Ki-67 was positively correlated with Knosp grades in NFPAs, but negatively correlated in FPAs, provides another explanatory approach as it claims that FPAs with high Ki-67 produce higher hormone levels and are subject to treatment at an earlier stage before even causing compression symptoms or invading the CS (Yuhan et al., 2021). In another study of 159 adenomas, Ki-67 significantly correlated with CSI, but the analysis of CSI was based on the Hardy classification and Cottiers criteria instead of the Knosp scale (Chacko et al., 2010). Until this study was made, due to inclusion of as much as 439 cases, the most important study on Ki-67 and CSI found no correlation of Ki-67 and CSI (Grimm et al., 2019). Differences to our study were that no Knosp grade cutoffs were used and instead of an exact calculation, there was only an estimation of the percentage of Ki-67 positive nuclei. To conclude, the lack of an association of Ki-67 and CSI found in our study seems likely when compared with the literature. We detected a significant correlation of adenomas with a MIB-1 value ≥0.6% and intraoperative invasion in this study. Further research for verification of this result with the same software-based quantification method as ours needs to be conducted as well as research on possible confounding factors, given past findings (Monsalves & Larjani, 2014; Jaffrain-Rea et al., 2002; Zhao et al., 1999).

The same shortcomings of the Ki-67 antibody also incurred in prognostic studies. The result of our analysis of recurrence-free survival time was a significantly and 1.6-fold higher risk of an earlier recurrence of adenomas with a MIB-1 value ≥0.6%. The MIB-1 cutoff of 0.6% and the mean MIB-1 value of 0.81% of recurrent cases also seem low compared to the findings in other prognostic adenoma studies. Just like in studies which focus on invasion, Ki-67 appears as the most frequently examined antibody in prognostic analyses. Its mean value in recurrent adenomas ranges from 1.11-4.09% (Sadeghipour et al., 2017; Yao et al., 2017; Kim et al., 2016; Trouillas et al., 2013; Chacko et al., 2010; Dubois et al., 2007; Paek et al., 2005; Hentschel et al., 2003; Jaffrain-Rea et al., 2002; Noh et al., 2009). Regarding confounding factors, some authors found an influence of the factors patient age, medical pretreatment and functional characteristic of the tumor on the MIB-1 value. In the mentioned study of 132 pituitary adenomas, a significant association

between Ki-67 value and recurrence was also not existent (Jaffrain-Rea et al., 2002). Interestingly, other researchers also demonstrated that the MIB-1 value might depend on the duration until recurrence occurs, as it was found to be significantly higher in early recurrence (<4 years post-surgery) compared to late recurrence (≥ 4 years) (Noh et al., 2009). In multiple studies, no significant correlation of Ki-67 values with recurrence was detected. Some of these series included exclusively and less than 100 NFPAs (Hentschel et al., 2003; Dubois et al., 2007; Yao et al., 2017), but there are also sources with >150 pituitary adenomas of all subtypes which did not detect any significant association (Sadeghipour et al., 2017; Chacko et al., 2010). In contrast to these studies, there are series which found Ki-67 to be significantly associated with recurrence and even proposed cutoffs which were predictive for shorter recurrence-free survival. Two almost equally-sized studies of 167 (Kim et al., 2016) and 166 (Righi et al., 2012) pituitary adenomas found a Ki-67 index >3% to be associated with recurrence. This is twice the percentage of Chiloiro et al., who proposed a 1.5% cutoff for the prediction of a worse disease-free survival time and even demonstrated that this finding is independent from several cofactors (Chiloiro et al., 2014). According to the latest and largest series which featured follow-up data of 601 adenomas, an intermediate cutoff at 1.5% is predictive for recurrence (Hasanov et al., 2019). It is striking, that the proposed cutoffs in all of these studies are much higher than the 0.6% cutoff we applied. Again, this might be caused by the different methods of Ki-67 LI determination compared to ours. While only Righi et al. quantified Ki-67 in a similar fashion, using a digital camera and image analysis software, all other previously mentioned authors did manual counting of 1,000 nuclei on numerous high-power microscopic fields. This method has already been identified as a potential source of intra- and interobserver variability (Righi et al., 2012). In general, the variety of different study findings, and especially of different cutoff values, reveals the necessity to work with a standardized MIB-1 quantification method in the future.

In this study, we were able to show that a MIB-1 value ≥0.6% is an independent negative prognostic factor associated with early recurrence. Our finding stands in contrast to a past review that claimed Ki-67 disqualifies as a definitely independent and sole predictor of pituitary adenoma prognosis (Aguiar et al., 2010). However, no other past study included such a high number of adenoma cases, which enhances the statistical power of our finding.

4.6. Histone Antibodies

Strong immunopositivity was detected in the majority of adenoma cases for both histone trimethylations. Of note, a major issue of histone antibodies is low target-specificity. There are reports of an inability to detect methylation status (mono-, di- or trimethylation) or of off-target recognition, as well as cross-reactivity between H3K27me3 antibodies and H3K4me3 peptides (Katz et al., 2018; Rothbart et al., 2015). In this study, we also observed the phenomenon of very weak staining intensity of tissue samples older than ten years. It is therefore possible, that some cases were falsely graded with a low histone immunopositivity score. Indeed, in a reviewal of all H3K27me3 stains by a neuropathologist (Prof. Dr. med. Schittenhelm) in our research group, of the 25 adenomas with a score of 1, only 5 cases undoubtedly demonstrated total H3K27me3 loss.

4.6.1. H3K27me3

There was no association between H3K27me3 scores and CSI. A H3K27me3 score <1, which resembled less than 5% immunopositivity and applied for only 25 cases, was an independent and significant predictor of intraoperatively observed pituitary adenoma invasion.

There are findings contradictory to our result that <5% H3K27me3 immunopositivity correlate with intraoperative adenoma invasion. While loss of H3K27me3 by H3K27M mutation is indeed associated with more aggressive pediatric gliomas (Sturm et al., 2012; Khuong-Quang et al., 2012; Venneti et al., 2014), a review of epigenetic modifications hints at increased H3K27me3 expression in pituitary adenomas (Shariq & Lines, 2019). Enhancer of zeste homologue 2 (EZH2) is the enzyme known for trimethylation of H3K27me3 (Nichol et al., 2016; Schuettengruber et al., 2011; Schult et al., 2015) and its expression was demonstrated to be elevated in 163 PAs and to correlate with Ki-67, but it was not associated with an invasive growth pattern of PAs (Schult et al., 2015). However, a newer study, which compared 50 invasive PAs with 53 noninvasive PAs, found enhanced H3K27me methylation in invasive adenomas (Xue et al., 2017). Besides the selection bias of this study, H3K27 methylation was assessed by enzyme-linked

immunosorbent assay (ELISA) of DNA extracted from frozen adenoma tissue sections instead of immunohistochemical detection of H3K27me3. The comparability with our study is therefore low. An explanation for a correlation of higher H3K27me with more invasive pituitary tumors might be the finding that methylated H3K27 is able to silence microRNAs, which usually target HMGA, a protein possibly involved in pituitary tumor development (Kitchen et al., 2015). These findings stand in opposition to our result of a loss of H3K27me3 expression in invasive pituitary adenomas. However, given the observation and correlation with a negative outcome in other brain tumors such as meningiomas as well as pediatric ependymomas and gliomas (Jung et al., 2021; Katz et al., 2018; Behling et al., 2021; Panwalkar et al., 2017; Sturm et al., 2012; Khuong-Quang et al., 2012; Venneti et al., 2014), it would biologically make sense if a loss of H3K27me3 was associated with unfavorable characteristics in PAs. In case of a H3K27me3 score <1 (immunopositivity <5%), it is spoken of a loss, because endothelial cells within an adenoma typically still stain positive, while adenohypophyseal tumor cells are negative. In fact, this serves as control for the antibody. As mentioned before (see Chapter 4.6.), only 5 cases in our study had definite H3K27me3 loss in the tumor cells with simultaneous positive endothelial staining.

The analysis of the prognostic role of H3K27me3 did not have a definite trendsetting result in this study. Adenomas with a H3K27me3 score <3 (immunopositivity <50%) were significantly more frequently recurrent than cases above the cutoff. However, this did not imply a more rapid dynamic, as the mean time to recurrence of adenomas with a H3K27me3 score <3 was not significantly shorter in the Kaplan-Meier analysis. In the literature, studies that examined the prognostic role of H3K27me3 in pituitary adenomas are still absent. The only existing notion is the previously described study of Schult et al. where the methylating enzyme of H3K27me3, EZH2, was found to be upregulated in pituitary adenomas and to be correlated with Ki-67 and therefore more proliferative adenomas (Schult et al., 2015). A speculative hypothesis derived from this result is that this increased proliferation might have a rather negative impact regarding recurrence potential of pituitary adenomas. Concerning the role of H3K27me3 in solid tumors, different effects were detected. On the one hand, in pediatric pontine gliomas a K27M mutation on histone H3.3 leading to H3K27me3 loss was found to be predictive of shorter

survival compared to wildtype-tumors (Sturm et al., 2012; Khuong-Quang et al., 2012; Venneti et al., 2014). Similarly, complete loss of H3K27me3 immunohistochemical staining was found to correlate with earlier recurrence and overall worse prognosis in cohorts of 141 (Jung et al., 2021), 232 (Katz et al., 2018) and 1,103 (Behling et al., 2021) meningiomas. In childhood posterior fossa ependymomas a global H3K27me3 reduction was demonstrated to be predictive of a poor prognosis in an immunohistochemical analysis of 230 of these tumors (Panwalkar et al., 2017). Low H3K27me3 was also detected to be an independent predictor of shorter survival in breast, ovarian and pancreatic cancer in another immunohistochemical study, while it was not associated with EZH2 (Wei et al., 2008). In contrast to these findings of a prognostic effect of low H3K27me3 staining, high H3K27me3 expression was positively correlated with EZH2 and linked to shorter progression-free and overall survival in esophageal squamous cell carcinomas by different researchers (He et al., 2009; Cai et al., 2011; Tzao et al., 2009). All in all, it can only be speculated which effect H3K27me3 has on pituitary adenoma prognosis as it is also elusive in other tumor types with highly variable expression patterns.

4.6.2. H3K36me3

H3K36me3, the second histone modification analyzed in this study, is thought to be important for DNA damage repair by regulation of RNA splicing, mismatch repair and detection of double strand breaks (Sun et al., 2020). A correlation between H3K36me3 and intraoperative invasion was not found. Regarding CSI, a H3K36me3 score <4, which resembles less than 75% immunopositivity, occurred significantly more frequently in Knosp grade 3A-4 adenomas. To date, there are no other studies that immunohistochemically analyzed H3K36me3 expression in pituitary adenomas. For other tumor entities like chrondroblastomas, giant cell bone tumors or soft tissue sarcomas, a correlation between reduced H3K36me3 by H3K36M mutation and malignant transformation was shown (Behjati et al., 2013; Lu et al., 2016) and it is generally assumed that H3K36me3 deficiency leads to increased spontaneous mutations and microsatellite instability (Sun et al., 2020; Li et al., 2013; Huang et al., 2018). Based

on these findings, an association of reduced H3K36me3 activity with more aggressive brain tumors does not seem improbable.

Similar to the prognostic analysis of the other histone antibody, the results for H3K36me3 did not point to a clear correlation with a worse prognosis. On the one hand, a significantly higher frequency of recurrence was detected in cases with a H3K36me3 score <4. On the other hand, no statistical difference of the duration until recurrence was observed. A H3K36me3 score <4 was not correlated with earlier recurrence in the Kaplan-Meier analysis.

There are few cancer studies dealing with H3K36me3 and its role on the clinical outcome and no previous prognostic analyses of H3K36me3 in PAs at all. However, it is generally thought that H3K36 methylation has antagonistic functions to H3K27me3 and while the latter works as a gene silencer, H3K36me3 is a gene activator (Varier & Timmers, 2011; Sun et al., 2020). Fittingly, in a mouse model a K36M mutation on histone H3.3 led to increased H3K27me3 and reduced H3K36me3 expression, which, by generating a differentiation arrest, was causative for undifferentiated sarcomas with a poor prognosis (Lu et al., 2016). Reduced H3K36me3 expression caused by a loss-of-function mutation of its trimethyltransferase SETD2 was also detected in pediatric high-grade gliomas. However, this finding was not linked to clinical outcome measures (Fontebasso et al., 2013). In a methodologically sound retrospective analysis of 1,454 renal clear cell carcinoma specimens, that even adjusted its results for age and a validated prognostic scoring system, loss of H3K36me3 expression was significantly correlated with worse overall survival and progression-free survival (Ho et al., 2016). In contrast to that, in another immunohistochemical analysis of 152 hepatocellular cancer (HCC) specimens, H3K36me3 positivity was an independent predictor of poor prognosis as it was linked to lower 5-year-disease-free survival and 5-year overall survival (Lien et al., 2018). The authors also used percent ranges for the scoring of H3K36me3 and, instead of the 5% cutoff we applied, a cutoff of a positivity of 1% was chosen to dichotomize between retained and lost H3K36me3 expression. Increased H3K36me3 expression was also found in breast cancer, however with undetermined clinical consequence (Rivenbark et al., 2009). Similar to findings for H3K27me3, the expression pattern of H3K36me3 and its influence on patient outcome vary greatly depending on the tumor type.

4.7. Osteonectin/SPARC

By intraoperative assessment, there was no significant difference between invasive and noninvasive adenomas for all osteonectin scores combined and no suitable cutoff detectable by CART analysis. Significantly more Knosp grade 2-4 adenomas were found below an osteonectin IRS <12, but multivariate analysis demonstrated that, in fact, there was no association between osteonectin and radiological CSI in in our study.

Contrary to these findings, a role of osteonectin on tumor cell invasion of solid cancers was demonstrated by multiple in vivo and in vitro studies, some also using immunohistochemistry of TMAs. Especially in gastrointestinal tumor entities such as esophageal squamous cell carcinoma (Zhang et al., 2020), colorectal cancer (Drev et al., 2019), hepatocellular carcinoma (Deng et al., 2016), gastric cancer (Yin et al., 2010) and pancreatic cancer (Rossi et al., 2016; Guweidhi et al., 2005) downregulation of SPARC by small interfering RNAs (siRNAs) significantly decreased tumor invasion. Although the SPARC-dependency of invasion was detected in breast cancer (Gilles et al., 1998) and different bone cancers (Amaral et al., 2018) as well, a possible explanation for why this oncogenic effect of SPARC was especially intensely present in gastrointestinal cancers is the fact that SPARC expression is restricted to areas of high extracellular matrix turnover (Bradshaw & Sage, 2001; Chlenski & Cohn, 2010). SPARC possibly gained interest for neurooncological research because of its affection of metalloproteinases and its binding capacity of collagen IV, the main component of the dura mater (Brekken & Sage, 2000; Bradshaw & Sage, 2001). Indeed, strong in vitro and in vivo evidence exists that highly invasive gliomas have significantly higher SPARC-expression (Rich et al., 2003; Schultz et al., 2002) and a more recent series even indicated that SPARC is an essential requirement for tumor invasion into white matter structures (Wirthschaft et al., 2019). Fittingly, an immunohistochemical analysis with TMAs of 43 craniopharyngiomas also detected a significant correlation of SPARC expression with central nervous system infiltration (Ebrahimi et al., 2013). There are contradictory findings in meningioma research. While SPARC expression was present in invasive, but absent in noninvasive meningiomas in a relatively old study (Rempel et al., 1999), two methodologically superior immunohistochemical analyses with greater cohorts found no statistically

significant association between SPARC expression and invasive potential of meningiomas (Rooprai et al., 2020; Schittenhelm et al., 2006).
Knowledge about the functional effect of SPARC in pituitary adenomas is still sparse. To date, there is only one study that compared 25 noninvasive with 15 invasive pituitary adenomas according to the Hardy classification and that found no significant difference of SPARC expression (Onoz et al., 2015). The same scoring system by Remmele and Stenger (Remmele et al., 1986), that was used in our study, was applied. During our microscopic evaluation of the osteonectin IRS, we noted a high frequency of cases where osteonectin did not stain exclusively cytoplasmatic, but also nuclear. While indeed the translocation of osteonectin into the nucleus has been observed and described elsewhere previously (Yan et al., 2005), it is completely unknown what effects this has on tumor behavior, if at all. Another unanswered question is the role of the expression pattern, which can be either cytoplasmatic or perimembranous (Rempel et al., 1999). Both observations were not analyzed by us. Nevertheless, the result of this study is in line with the sole co-existing series on SPARC in pituitary adenomas and there is no evidence that SPARC has an implication on PA invasiveness.

No statistical association was detected between SPARC expression and the rate of recurrence as well as time to recurrence. Many findings in the research literature of different human malignancies indicate that high SPARC expression is linked to a worse prognosis. In a study on HCC, the downregulation of a microRNA named miR-211 was associated with significantly shorter overall survival (Deng et al., 2016). The link to simultaneous higher SPARC expression in such cases is only of indirect nature, as it was further demonstrated that SPARC is repressed by miR-211 and consequently low miR-211 results in an increase of SPARC expression. Direct in vivo evidence of high SPARC expression and a resulting prognostic worsening was shown in a mouse model with glioma cells of 27 patients, where high SPARC expression correlated with shorter survival and silencing of SPARC-increased survival (Wirthschaft et al., 2019). Another clue is provided by a TMA-based immunohistochemical study of 466 colorectal cancer specimens. High SPARC expression merely showed a statistical trend towards reduced 5-year-disease-free survival in the entire cohort and only in the subset of 27 recurrent cases this finding was an independent predictor of worse survival (Drev et al., 2019).

Furthermore, in a retrospective analysis of 43 craniopharyngiomas, high SPARC correlated with a higher rate of recurrence, however the influence on time to recurrence was not assessed (Ebrahimi et al., 2013). An interesting aspect was brought to light by a study on pancreatic ductal adenocarcinomas, where high SPARC expression in stromal cells was associated with shortened overall survival, while the expression of SPARC in the cancer cells themselves was unassociated (Rossi et al., 2016). This result indicates that the non-tumorous tissue in tumor samples might be worth to be included in the analysis of SPARC expression. In this series of pituitary adenomas, scoring of SPARC expression was only done in adenoma cells.

4.8. The Patient Collective

This study featured surgical and patient demographical data of 1,220 pituitary adenoma cases. 1,181 of 1,220 adenomas (96.80%) were operated using a transsphenoidal approach. This conforms with the literature, where it is stated that this surgical approach is sufficient for the management of 96-99% of pituitary adenomas (Wilson, 1984; Youssef et al., 2005). In our study cohort, a complete macroscopic resection rate of 79.53% (948 of 1,220 cases) was achieved. This rate appears to be slightly higher compared to data in the literature. Gross total resection rates of two Italian single center surgical series with smaller cohort sizes were 77% of 173 adenomas (Frank & Pasquini, 2006) and 63% of 491 adenomas (Losa et al., 2008). Meta-analyses with data from a similar, or even larger amount of adenoma cases than our study reported gross total resection rates of around 60-70% for both the endoscopic and microscopic surgical approach (Gao et al., 2014; Goudakos et al., 2011) . Regarding age, patients of our cohort had a mean age at diagnosis of 51.98 years, and female patients were significantly younger at diagnosis than male patients (49.85 compared to 54.41 years). Other surgical series typically focus on surgical results or postoperative complications instead of epidemiological data, which is why multiple European cross-sectional population studies had to be used for comparison. While in these large-scale multicentric studies women on average were also 6-17 years younger at diagnosis and there was also an overall female preponderance, a median age at diagnosis that ranged from 37 to 44 years is reported

(Daly et al., 2006; Agustsson et al., 2015; Raappana et al., 2010; Fernandez, Karavitaki & Wass, 2010; Gruppetta, Mercieca & Vassallo, 2013). The mean age at diagnosis is higher in our study, possibly due to the fact, that our study is a surgical series and the recorded age at diagnosis was always postsurgical at histological conformation of the study. Tumors may have been radiologically diagnosed at an earlier age. The gender distribution in our study was an overall female preponderance with a male-to-female incidence ratio of 0.87, which is comparable to a male-to-female incidence ratio of 0.67 in Iceland (Agustsson et al., 2015) and of 0.82 in the United States (Ostrom et al., 2020). Concerning subtypes, in the inquiry from Iceland NFPA (gonadotroph and null cell adenomas combined) were more common than prolactinomas (Agustsson et al., 2015), but in all other European population-based studies (Daly et al., 2006; Raappana et al., 2010; Fernandez, Karavitaki & Wass, 2010; Gruppetta, Mercieca & Vassallo, 2013) prolactinomas were the most prevalent subtype. Contrary to that, gonadotroph adenomas were the most common subtype in our study and prolactinomas were only the fourth most frequent subtype. This is most likely caused by the fact that this is a surgical series and the first line therapy of prolactinomas is medicinal. All in all, while some clinical aspects of our patient collective are in line with the findings in the literature, differences exist in the form of an older average age of patients and differences of subtype distribution.

4.9. Strengths and Limitations of this Study

4.9.1. The Study Design

Limitations of this series are mainly of methodological nature, since the immunohistochemical markers were not assessed with full objectivity. Apart from that, another drawback is the retrospective design of the study. The strengths of this study lie in the huge cohort size of almost 1,000 pituitary adenomas, which assured sufficient statistical power. Besides, with the target variables of invasion and recurrence, two main aspects of aggressiveness were addressed simultaneously and invasion was assessed by two different approaches, with the radiographic and the intraoperative estimate.

Two aspects served for the purpose of quality control. Firstly, preselection of cases was done by reviewing of all available matching HE sections of the 1,220 cases with available surgical reports by the same neuropathologist with an area of expertise on this field (Prof. Dr. med. Jens Schittenhelm, University Hospital of Tübingen). This verified sufficiency of tumor cell amount within a sample, which served to increase validity of the results for pituitary adenoma tissue. Increasement of uniformity was also achieved by the fact that the majority of surgeries of the pituitary adenoma cases included in this study were done by the same neurosurgeon (Prof. Dr. Jürgen Honegger, University Hospital of Tübingen).

4.9.2. The TMA Method

The TMA technique was first described in 1998 by a research group (Kononen et al., 1998) and has since been widely used in cancer research. Advantages of the method are its tissue-saving and high-throughput nature, that allows for the comparative analysis of theoretically thousands of tumors on only a few array sections. The technique itself and the direct comparison of multiple staining results on one slide simultaneously accounts for identical conditions, and therefore, a high degree of standardization (Sauter & Mirlacher, 2002; Camp et al., 2000). The main point of criticism is possible insufficient representability of the 0.6-2mm tumor biopsy cores for a whole tissue sample due to tumor heterogeneity (Sauter & Mirlacher, 2002; Hoos & Cordon-Cardo, 2001). A common approach to tackle this issue are multiple tissue cores for each case (Parsons & Grabsch, 2009; Sauter & Mirlacher, 2002; Voduc et al., 2008). In studies, there were concordance rates of >95% with full sections in case of two existing cores per case (Camp et al., 2000) and of 98% in case of three existing cores per case (Gulmann & O'Grady, 2003). While it was possible to obtain two or more cores in most cases in our study, a small number only had one core represented on TMA slides. These cases were still considered for further analysis for the sake of a preferably extensive cohort. Besides, due to size-dependent representativity of a core, in this study a rather big core-biopsy diameter of 1mm was used on samples with previously checked sufficient tumor cell amount (see Chapter 4.9.1). Nevertheless, cases with only one core might be only insufficiently representative of whole tissue sections which might hinder validity of the

immunohistochemical staining results of these cases. This is especially relevant given the fact that PA are a very heterogenous disease entity. However, it is speculated that false negative results can at least partly be compensated by the high number of included cases in TMA studies (Torhorst et al., 2001). More cores per case are advisable nonethelessto account for the case loss during processing. In a series of renal cell tumors, reducing the number of cores per case by one doubled the percentage of excluded cases (Hager et al., 2009). In another TMA study, 15% of cases were lost during processing (Gulmann & O'Grady, 2003). Besides our effort to obtain multiple cores, a cutoff for the amount of viable tissue of at least one fifth of a cores' diameter was established and only tumor samples above this cutoff were immunohistochemically evaluated.

4.9.3. Immunohistochemistry

Immunohistochemistry was fully automated in our study. By this method, improvement of reproducibility and reliability can be achieved (Gustavson et al., 2009). It is well known that age of analyzed tissue samples is a possible confounding factor for the quality of immunohistochemical staining, as increasing time between sample preparation and staining can lead to loss of antigen immunoreactivity (Kim et al., 2016; Hoos & Cordon-Cardo, 2001; Sauter & Mirlacher, 2002). Due to this circumstance, we tried to minimize time between microtomy of our TMA sections and staining. The influence of the factor age of the tumor samples we processed on our results can only be speculated. In case of antigen immunoreactivity of the histones H3K27me3 and H3K36me3, we observed a tendency that older samples stained with less intensity, which might have aggravated and distorted interpretation of the staining results. Generally, quantification of histone immunopositivity was subjective, as it was done according to visual estimate only. To minimize inter-individual variation of results, a score that encoded relatively broad percent ranges was used. We followed the argument that a single interpreter can reduce inter- and intraindividual variation (Tzankov et al., 2005) to increase consistency of results. Nevertheless, we trained and discussed quantification of histones in a team of three interpreters prior to interpretation by a single person. Consistency of interpretation of staining results was also increased by the fact that all evaluations of antibody

expression were done with the same microscope. Calculation of MIB-1 immunopositivity had high objectivity and reproducibility as it was conducted by a software. Osteonectin or SPARC expression was assessed with an adapted version of an immunoreactive score (IRS) that was previously used in other immunohistochemical studies (Boltze et al., 2009; Remmele et al., 1986; Ebrahimi et al., 2013). The score range from 0-12 is a potential disadvantage. Too many possible variations of a score can lead to different interpretation between researchers, which is why a maximum of five or six score levels is recommended for immunohistochemical studies (Kim et al., 2016). To counteract this potential drawback, we followed the recommendation to work with cutoff values (Kim et al., 2016).

5. Conclusion

A patient age of ≥45 years at diagnosis and the NCA subtype are factors associated with cavernous sinus invasion. A H3K36me3 expression <75% is not a definite marker for CSI, correlating with CSI according to the literature-based Knosp cutoff only. A loss of H3K27me3 is associated with intraoperative invasion. Both histone antibodies are not of prognostic value. While cavernous sinus invasion leads to a shorter progression-free survival, the intraoperative estimate of invasion does not result in earlier recurrence.
The SGCA subtype is an independent risk factor of radiological and intraoperative presence of invasive growth and of a worse prognosis regarding progression-free survival. Increased MIB-1 expression of ≥0.6% is an independent marker of intraoperative invasion and of an earlier recurrence of pituitary adenomas.

For the management of pituitary adenomas in the clinical routine, an accurate, software-based assessment of MIB-1 expression might serve as a valuable tool to single out more aggressive cases. Besides, as a substantial subset is prone to an aggressive behavior, special attention should be given to corticotroph adenomas. Especially when silent, patients with these tumors deserve close monitoring.

6. Summary

Introduction:

Pituitary adenomas make up 15% of all intracranial neoplasms. A fraction of adenoma cases is considered aggressive which poses huge therapeutic challenges. Aggressiveness encompasses the subcriteria of invasive growth, high and early recurrence potential and therapy refractiveness. To date, no immunohistochemical marker has been shown to be able to predict aggressive adenoma behavior. In this study, the impact of several clinical and immunohistochemical markers on invasiveness and prognosis was assessed in a cohort of 927 pituitary adenomas.

Materials and Methods:

In this study, 927 cases of pituitary adenoma underwent TMA analysis and immunohistochemical staining with the markers MIB-1, H3K27me3, H3K36me3 and osteonectin. All cases were treated with transsphenoidal or transcranial surgery. Invasiveness was assessed by intraoperative estimation as well as by grading of MRIs with the Knosp scale of cavernous sinus invasion. Follow-up data was collected. Where applicable, adequate cutoff values were chosen with CART analyses. The role of age at diagnosis, patient gender and adenoma subtype as well as the expression of the markers on intraoperative and radiological invasion was assessed by Pearson Chi^2 tests and by multivariate analysis (logistic regression). For the prognostic analysis of the mentioned parameters, Kaplan-Meier analyses of recurrence-free survival time and a multivariate analysis (Cox regression) were applied.

Results:

An age at diagnosis ≥71 years (p=0.0255), a MIB-1 score ≥0.6% (p=0.0320) and a H3K27me3 immunopositivity <5% (p=0.0312) significantly correlated with intraoperative invasion. The SGCA (p=0.0517) and NCA (p=0.0954) subtype only showed a statistical tendency. Both subtypes were significantly correlated with Knosp grades 3A-4 as a parameter of radiological invasion (SGCA p=0.0251, NCA p=0.0450), as well as <75% H3K36me3 expression (p=0.0499). The gonadotroph adenoma (p=0.0001) and SGCA (p=0.0503) subtypes as well as a H3K27me3 immunopositivity

<50% (p=0.0126) and osteonectin IRS <12 (p=0.0216) significantly correlated with Knosp grades 2-4. An age ≥45 years was significant for both criteria of CSI (p=0.0018 for Knosp grades 3A-4, p=0.0001 for Knosp grades 2-4).

By multivariate analysis, an age ≥45 years and the NCA subtype was predictive for radiographic CSI, regarding the markers, this was the case for <75% H3K36me3 staining only for Knosp grades 3A-4. MIB-1 ≥0.6% and H3K27me3 expression <5% were independent markers of intraoperative invasion. The SGCA subtype was shown to be a significant independent predictor of all criteria of invasion.

Prognostically, CSI (p=0.0040 for Knosp grades 2-4, p=0.0126 for Knosp grades 3A-4), the SGCA subtype (p=0.0009) and a MIB-1 value ≥0.6% (p=0.0135) were significantly associated with earlier recurrence and significant independent prognostic markers in the cox regression analysis.

Conclusion:

H3K27me3 <5% was a marker for intraoperative invasion and H3K36me3 <50% for radiological Knosp grades 3A-4. Given methodological disadvantages of the histone antibodies and conflicting study findings, these results have to be handled with caution and further research needs to be conducted. The SGCA subtype was the sole examined parameter that was predictive of radiographic and intraoperative invasion as well as a worse prognosis and can therefore be considered aggressive. A MIB-1 value ≥0.6% was a significant and independent predictor of intraoperative invasion and recurrence. CSI according to two Knosp grade cutoffs was associated with an increased recurrence risk.

For the clinician, data on MIB-1 expression might serve as a valuable tool to single out more aggressive pituitary adenomas. To account for an aggressive subset of corticotroph adenomas, close monitoring is appropriate in all patients with silent tumors of this type.

Zusammenfassung

Einleitung:

Hypophysenadenome stellen 15% aller intrakraniellen Neoplasien dar. Ein Teil wird als aggressiv angesehen, was große therapeutische Herausforderungen birgt. Aggressivität als Überbegriff umfasst dabei die Kriterien invasives Wachstumsverhalten, ausgeprägte und frühzeitige Rezidivneigung sowie Therapierefraktärität. Bis heute ist noch kein einzelner immunhistochemischer Marker etabliert, der zuverlässig aggressives biologisches Verhalten von Hypophysenadenomen vorherzusagen vermag. In dieser Studie wurden daher neben dem Einfluss von verschiedenen klinischen Faktoren insbesondere der Einfluss von immunohistochemischen Antikörpern auf Invasivität und schlechtere Prognose an einer Kohorte von 927 Hypophysenadenomen untersucht.

Material und Methoden:

Die eingeschlossenen 927 Fälle wurden in dieser Studie mittels Tissue Microarray-Verfahren und anschließender immunhistochemischer Anfärbung mit den Antikörpern MIB-1, H3K27me3, H3K36me3 und Osteonectin bearbeitet. Alle Fälle wurden mit transsphenoidaler oder transkranieller Resektion operativ versorgt. Die Zielvariable Invasivität wurde auf zwei verschiedene Arten erfasst: zum einen anhand Angaben des Operateurs in OP-Berichten (=intraoperative Invasion), außerdem anhand des Grades der Invasion in den Sinus cavernosus nach der Klassifikation nach Knosp auf präoperativen MRT-Bildern (=radiologische Invasion). Daten von postoperativen Verlaufsuntersuchungen hinsichtlich Remissionserhalt oder Rezidiv wurden gesammelt. Die zu untersuchenden Parameter wurden mit Cut-off-Werten dichotomisiert. Für quantitative Parameter (Alter, immunhistochemische Marker) wurde zur Bestimmung geeigneter Cut-off-Werte der CART-Algorithmus herangezogen. Die Rolle von Patientenalter bei Diagnose, Patientengeschlecht, Adenom-Subtyp, sowie die Expression der immunhistochemischen Marker auf intraoperatives oder radiologisches Vorhandensein von Invasion wurde mittels Pearson Chi^2-Tests und multivariater Analyse (logistische Regression) untersucht. Die prognostische Analyse der genannten Parameter und der intraoperativen und radiologischen Invasion erfolgte mit Kaplan-Meier-Analysen des rezidivfreien Überlebens und ebenfalls mit multivariater Analyse (Cox Regression).

Ergebnisse:

Ein Patientenalter bei Diagnose von ≥71 Jahren (p=0.0255), ein MIB-1 Wert ≥0.6% (p=0.0320) und H3K27me3 Expression <5% (p=0.0312) korrelierte signifikant mit intraoperativer Invasion. Die Subtypen spärlich granuliertes kortikotrophes Adenom (SGCA) (p=0.0251) und Nullzell-Adenom (NCA) (p=0.0450) waren signifikant mit den Knosp Graden 3A-4 assoziiert, ebenso wie <75% Expression von H3K36me3 (p=0.0499). Für die Knosp Grade 2-4 als radiographische Invasion ergaben sich signifikante Ergebnisse für die Subtypen gonadotrophes Adenom (p=0.0001) und SGCA (p=0.0503), sowie für <50% H3K27me3 Expression (p=0.0126) und einen immunoreaktiven Osteonectin-Score (IRS) <12 (p=0.0216). Ein Patientenalter bei Diagnose von ≥45 Jahren war signifikant für Invasion nach beiden Knosp-Einteilungen (p=0.0018 für Knosp Grade 3A-4, p=0.0001 für Knosp Grade 2-4). In der multivariaten Analyse waren das Patientenalter bei Diagnose von ≥45 Jahren und der NCA-Subtyp prädiktiv für radiographische Invasion in den Sinus cavernosus. Hinsichtlich der immunhistochemischen Marker war dies lediglich für <75% H3K36me3 Expression, und lediglich für die Knosp Grade 3A-4, der Fall. Die Expression von MIB-1 ≥0.6% und von H3K27me3 <5% waren unabhängige Marker der intraoperativen Invasion. Es zeigte sich, dass der SGCA-Subtyp ein signifikanter, unabhängiger Prädiktor für Invasion, sowohl nach intraoperativem als auch radiologischem Befund, war.

Prognostisch waren Invasion in den Sinus cavernosus (p=0.0040 für die Knosp Grade 2-4, p=0.0126 für die Knosp Grade 3A-4), der SGCA-Subtyp (p=0.0009) und ein MIB-1 Wert ≥0.6% (p=0.0135) signifikant mit einem früheren Auftreten eines Rezidivs vergesellschaftet und auch in der Cox Regressionsanalyse signifikante, unabhängige prognostische Marker.

Schlussfolgerung:

Die Expression von H3K27me3 <5% war ein unabhängiger Marker der intraoperativen Invasion, während H3K36me3 <50% dies für die Knosp Grade 3A-4 war. Angesichts methodologischer Nachteile der Histon-Antikörper und widersprüchlicher Studienergebnisse müssen diese Ergebnisse vorsichtig bedacht werden und weitere Forschung ist vonnöten. Der SGCA Subtyp war der einzige untersuchte Parameter, der prädiktiv sowohl für radiologische und intraoperative Invasion als auch für eine

schlechtere Prognose war und kann somit als aggressiv angesehen werden. Ein MIB-1 Wert ≥0.6% war ein signifikanter und unabhängiger Prädiktor von intraoperativer Invasion und Rezidivneigung. Invasion in den Sinus cavernosus war mit erhöhtem Rezidivrisiko assoziiert.

Für den Kliniker können Daten zur MIB-1 Expression eine wertvolle Möglichkeit sein, um Hypophysenadenome mit aggressiverem Verlauf zu detektieren. Um einen aggressiven Teil der kortikotrophen Adenome adäquat zu berücksichtigen, ist engmaschige Überwachung in allen klinisch stummen Tumoren dieses Typs angezeigt.

7. Bibliography

Aguiar, P.H.P. de, Aires, R., Laws, E.R., Isolan, G.R., Logullo, A., Patil, C. & Katznelson, L. (2010) Labeling index in pituitary adenomas evaluated by means of MIB-1: is there a prognostic role? A critical review. *Neurological research*. 32 (10), 1060–1071. doi:10.1179/016164110x12670144737855.

Agustsson, T.T., Baldvinsdottir, T., Jonasson, J.G., Olafsdottir, E., Steinthorsdottir, V., Sigurdsson, G., Thorsson, A.V., Carroll, P.V., Korbonits, M. & Benediktsson, R. (2015) The epidemiology of pituitary adenomas in Iceland, 1955-2012: a nationwide population-based study. *European Journal of Endocrinology*. 173 (5), 655–664. doi:10.1530/eje-15-0189.

Ajithkumar, T. & Brada, M. (2016) *Pituitary radiotherapy*. Oxford University Press. Oxford University Press. https://books.google.com/books?hl=en&lr=&id=9R-RAAAAQBAJ&oi=fnd&pg=PA176&dq=Pituitary+radiotherapy+ajithkumar&ots=vCFkfbTBCF&sig=sZYw-bP5YVkTiagD9PqV50Vi6rY.

Albani, A., Pérez-Rivas, L.G., Dimopoulou, C., Zopp, S., Colón-Bolea, P., Roeber, S., Honegger, J., Flitsch, J., Rachinger, W., Buchfelder, M., Stalla, G.K., Herms, J., Reincke, M. & Theodoropoulou, M. (2018) The USP8 mutational status may predict long-term remission in patients with Cushing's disease. *Clinical Endocrinology*. 89 (4), 454–458. doi:10.1111/cen.13802.

Al-Shraim, M. & Asa, S.L. (2006) The 2004 World Health Organization classification of pituitary tumors: What is new? *Acta Neuropathologica*. 111 (1), 1–7. doi:10.1007/s00401-005-1093-6.

Alzhrani, G., Sivakumar, W., Park, M.S., Taussky, P. & Couldwell, W.T. (2018) Delayed Complications After Transsphenoidal Surgery for Pituitary Adenomas. *World Neurosurgery*. 109, 233–241. doi:10.1016/j.wneu.2017.09.192.

Amar, A.P., DeArmond, S.J., Spencer, D.R., Coopersmith, P.F., Ramos, D.M. & Rosenblum, M.L. (1994) Development of an in vitro extracellular matrix assay for studies of brain tumor cell invasion. *Journal of neuro-oncology*. 20 (1), 1–15. doi:10.1007/bf01057956.

Amaral, C.B., Leite, J. da S., Fonseca, A.B.M. & Ferreira, A.M.R. (2018) Vimentin, osteocalcin and osteonectin expression in canine primary bone tumors: diagnostic and prognostic implications. *Molecular biology reports*. 45 (5), 1289–1296. doi:10.1007/s11033-018-4285-6.

Angelis, M. de & Cappabianca, P. (2014) Thyrotropin pituitary adenomas. *World Neurosurgery*. 82 (6), 1026–1027. doi:10.1016/j.wneu.2014.06.037.

Arafah, B.M. & Nasrallah, M.P. (2001) Pituitary tumors: pathophysiology, clinical manifestations and management. *Endocrine-Related Cancer*. 8, 287–305.

Asa, S.L. (1998) Tumors of the Pituitary Gland. *Atlas of Tumor Pathology*. 3. https://books.google.com/books?hl=en&lr=&id=wgCaX7WzWkMC&oi=fnd&pg=PA1&dq=Tumors+of+the+pituitary+gland&ots=NoiCB_ZwGm&sig=kVdJTAIgEvUahos1ZPjtJcZA1B8.

Asa, S.L. & Ezzat, S. (2009) The Pathogenesis of Pituitary Tumors. *The Annual Review of Pathology Mechanism of Disease*. 4 (1), 97–126. doi:10.1146/annurev.pathol.4.110807.092259.

Asa, S.L. & Mete, O. (2018) What's new in pituitary pathology? *Histopathology*. 72 (1), 133–141. doi:10.1111/his.13295.

Balogun, J.A., Monsalves, E., Juraschka, K., Parvez, K., Kucharczyk, W., Mete, O., Gentili, F. & Zadeh, G. (2015) Null cell adenomas of the pituitary gland: an institutional review of their clinical imaging and behavioral characteristics. *Endocrine Pathology*. 26 (1), 63–70. doi:10.1007/s12022-014-9347-2.

Bando, H., Sano, T., Ohshima, T., Zhang, C.Y., Yamasaki, R., Matsumoto, K. & Saito, S. (1992) Differences in pathological findings and growth hormone responses in patients with growth hormone-producing pituitary adenoma. *Endocrinologia japonica*. 39 (4), 355–363. doi:10.1507/endocrj1954.39.355.

Bao, X., Deng, K., Liu, X., Feng, M., Chen, C.C., Lian, W., Xing, B., Yao, Y. & Wang, R. (2016) Extended transsphenoidal approach for pituitary adenomas invading the cavernous sinus using multiple complementary techniques. *Pituitary*. 19 (1), 1–10. doi:10.1007/s11102-015-0675-0.

Beck-Peccoz, P., Brucker-Davis, F., Persani, L., Smallridge, R.C. & Weintraub, B.D. (1996) Thyrotropin-secreting pituitary tumors. *Endocrine reviews*. 17 (6), 610–638. doi:10.1210/edrv-17-6-610.

Béguelin, W., Popovic, R., Teater, M., Jiang, Y., Bunting, K.L., et al. (2013) EZH2 Is Required for Germinal Center Formation and Somatic EZH2 Mutations Promote Lymphoid Transformation. *Cancer Cell*. 23 (5), 677–692. doi:10.1016/j.ccr.2013.04.011.

Behjati, S., Tarpey, P.S., Presneau, N., Scheipl, S., Pillay, N., et al. (2013) Distinct H3F3A and H3F3B driver mutations define chondroblastoma and giant cell tumor of bone. *Nature Genetics*. 45 (12), 1479–1482. doi:10.1038/ng.2814.

Behling, F., Fodi, C., Gepfner-Tuma, I., Kaltenbach, K., Renovanz, M., Paulsen, F., Skardelly, M., Honegger, J., Tatagiba, M., Meningiomas, I.C. on, Schittenhelm, J. & Tabatabai, G. (2021) H3K27me3 loss indicates an increased risk of recurrence in the Tübingen meningioma cohort. *Neuro-Oncology*. 23 (8), 1273–1281. doi:10.1093/neuonc/noaa303.

Bengtsson, D., Schrøder, H.D., Andersen, M., Maiter, D., Berinder, K., Rasmussen, U.F., Rasmussen, A.K., Johannsson, G., Hoybye, C., Lely, A.J. van der, Petersson, M.,

Ragnarsson, O. & Burman, P. (2015) Long-term outcome and MGMT as a predictive marker in 24 patients with atypical pituitary adenomas and pituitary carcinomas given treatment with temozolomide. *The Journal of Clinical Endocrinology & Metabolism*. 100 (4), 1689–1698. doi:10.1210/jc.2014-4350","keywords":["immunohistochemistry","carcinoma","pituitary.

Benveniste, R.J., King, W.A., Walsh, J., Lee, J.S., Delman, B.N. & Post, K.D. (2005) Repeated transsphenoidal surgery to treat recurrent or residual pituitary adenoma. *Journal of neurosurgery*. 102 (6), 1004–1012. doi:10.3171/jns.2005.102.6.1004.

Bevan, J.S. (2005) The antitumoral effects of somatostatin analog therapy in acromegaly. *The Journal of Clinical Endocrinology & Metabolism*. 90 (3), 1856–1863. doi:10.1210/jc.2004-1093","keywords":["acromegaly","insulin-like.

Bhayana, S., Booth, G.L., Asa, S.L., Kovacs, K. & Ezzat, S. (2005) The implication of somatotroph adenoma phenotype to somatostatin analog responsiveness in acromegaly. *The Journal of Clinical Endocrinology and metabolism*. 90 (11), 6290–6295. doi:10.1210/jc.2005-0998.

Bi, W.L., Greenwald, N.F., Ramkissoon, S.H., Abedalthagafi, M., Coy, S.M., Ligon, K.L., Mei, Y., MacConaill, L. & Ducar, M. (2017) Clinical identification of oncogenic drivers and copy-number alterations in pituitary tumors. *Endocrinology*. 158, 2284–2291. doi:10.1210/en.2016-1967","inlanguage":"en","copyrightholder":"endocrine.

Boguszewski, C.L., Musolino, N.R. de C. & Leandro Kasuki (2019) Management of pituitary incidentaloma. *Best Practice & Research Clinical Endocrinology & Metabolism*. 33 (2), 101268. doi:10.1016/j.beem.2019.04.002.

Boltze, C., Riecke, A., Ruf, C.G., Port, M., Nizze, H., Kügler, C., Miethke, C., Wiest, N. & Abend, M. (2009) Sporadic and radiation-associated papillary thyroid cancers can be distinguished using routine immunohistochemistry. *Oncology Reports*. 22 (3), 459–467. doi:10.3892/or_00000457.

Brada, M., Rajan, B., Traish, D., Ashley, S., Sellors, P.J.H., Nussey, S. & Uttley, D. (1993) The long-term efficacy of conservative surgery and radiotherapy in the control of pituitary adenomas. *Clinical Endocrinology*. 38 (6), 571–578. doi:10.1111/j.1365-2265.1993.tb02137.x.

Bradshaw, A.D. & Sage, E.H. (2001) SPARC, a matricellular protein that functions in cellular differentiation and tissue response to injury. *The Journal of Clinical Investigation*. 107 (9), 1049–1054. doi:10.1172/jci12939.

Brat, D.J., Scheithauer, B.W., Eberhart, C.G. & Burger, P.C. (2001) Extraventricular neurocytomas: pathologic features and clinical outcome. *The American journal of surgical pathology*. 25 (10), 1252–1260. doi:10.1097/00000478-200110000-00005.

Brekken, R.A. & Sage, E.H. (2000) SPARC, a matricellular protein: at the crossroads of cell–matrix. *Matrix Biology*. 19 (7), 569–580. doi:10.1016/s0945-053x(00)00105-0.

Brochier, S., Galland, F., Kujas, M., Parker, F., Gaillard, S., Raftopoulos, C., Young, J., Alexopoulou, O., Maiter, D. & Chanson, P. (2010) Factors predicting relapse of nonfunctioning pituitary macroadenomas after neurosurgery: a study of 142 patients. *European Journal of Endocrinology*. 163 (2), 193–200. doi:10.1530/eje-10-0255.

Bronstein, M.D. (2005) Prolactinomas and Pregnancy. *Pituitary*. 8 (1), 31–38. doi:10.1007/s11102-005-5083-4.

Brucker-Davis, F., Oldfield, E.H., Skarulis, M.C., Doppman, J.L. & Weintraub, B.D. (1999) Thyrotropin-secreting pituitary tumors: diagnostic criteria, thyroid hormone sensitivity, and treatment outcome in 25 patients followed at the National Institutes of Health. *The Journal of Clinical Endocrinology and metabolism*. 84 (2), 476–486. doi:10.1210/jcem.84.2.5505.

Buchfelder, M. (2002) Thyrotroph Pituitary Adenomas. *The Endocrinologist*. 12 (2), 117–125. doi:10.1097/00019616-200203000-00010.

Cahill, D.P., Levine, K.K., Betensky, R.A., Codd, P.J., Romany, C.A., Reavie, L.B., Batchelor, T.T., Futreal, P.A., Stratton, M.R., Curry, W.T., Iafrate, A.J. & Louis, D.N. (2007) Loss of the Mismatch Repair Protein MSH6 in Human Glioblastomas Is Associated with Tumor Progression during Temozolomide Treatment. *Clinical Cancer Research*. 13 (7), 2038–2045. doi:10.1158/1078-0432.ccr-06-2149.

Cai, M.-Y., Tong, Z.-T., Zhu, W., Wen, Z.-Z., Rao, H.-L., Kong, L.-L., Guan, X.-Y., Kung, H.-F., Zeng, Y.-X. & Xie, D. (2011) H3K27me3 protein is a promising predictive biomarker of patients' survival and chemoradioresistance in human nasopharyngeal carcinoma. *Molecular medicine (Cambridge, Mass.)*. 17 (11–12), 1137–1145. doi:10.2119/molmed.2011.00054.

Caimari, F. & Korbonits, M. (2016) Novel Genetic Causes of Pituitary Adenomas. *Clinical Cancer Research*. 22 (20), 5030–5042. doi:10.1158/1078-0432.ccr-16-0452.

Camp, R.L., Charette, L.A. & Rimm, D.L. (2000) Validation of Tissue Microarray Technology in Breast Carcinoma. *Laboratory investigation; a journal of technical methods and pathology*. 80 (12), 1943–1949. doi:10.1038/labinvest.3780204.

Cardinal, T., Rutkowski, M.J., Micko, A., Shiroishi, M., Liu, C.-S.J., Wrobel, B., Carmichael, J. & Zada, G. (2020) Impact of tumor characteristics and pre- and postoperative hormone levels on hormonal remission following endoscopic transsphenoidal surgery in patients with acromegaly. *Neurosurgical Focus*. 48 (6), E10. doi:10.3171/2020.3.focus2080.

Chacko, G., Chacko, A.G., Kovacs, K., Scheithauer, B.W., Mani, S., Muliyil, J.P. & Seshadri, M.S. (2010) The clinical significance of MIB-1 labeling index in pituitary adenomas. *Pituitary*. 13 (4), 337–344. doi:10.1007/s11102-010-0242-7.

Chakraborti, S., Mandal, M., Das, S., Mandal, A. & Chakraborti, T. (2003) Regulation of matrix metalloproteinases: An overview. *Molecular and Cellular Biochemistry*. 253 (1), 269–285. doi:10.1023/a:1026028303196.

Chang, E.F., Sughrue, M.E., Zada, G., Wilson, C.B., Blevins, L.S. & Kunwar, S. (2010) Long term outcome following repeat transsphenoidal surgery for recurrent endocrine-inactive pituitary adenomas. *Pituitary*. 13 (3), 223–229. doi:10.1007/s11102-010-0221-z.

Chatzellis, E., Alexandraki, K.I., Androulakis, I.I. & Kaltsas, G. (2015) Aggressive Pituitary Tumors. *Neuroendocrinology*. 101 (2), 87–104. doi:10.1159/000371806.

Chaudhary, S.B.V. (2011) Imaging of the pituitary: Recent advances. *Indian Journal of Endocrinology and Metabolism*. 15 (Suppl3), S216-23. doi:10.4103/2230-8210.84871.

Chen, Y., Wang, C.D., Su, Z.P., Chen, Y.X., Cai, L., Zhuge, Q.C. & Wu, Z.B. (2012) Natural history of postoperative nonfunctioning pituitary adenomas: a systematic review and meta-analysis. *Neuroendocrinology*. 96 (4), 333–342. doi:10.1159/000339823.

Chesney, K., Memel, Z., Pangal, D.J., Donoho, D., Hurth, K., Mathew, A., Carmichael, J.D. & Zada, G. (2017) Variability and Lack of Prognostic Value Associated With Atypical Pituitary Adenoma Diagnosis: A Systematic Review and Critical Assessment of the Diagnostic Criteria. *Neurosurgery*. 0 (0), 1–9. doi:10.1093/neuros/nyx541.

Chiloiro, S., Bianchi, A., Doglietto, F., Waure, C. de, Giampietro, A., Fusco, A., Iacovazzo, D., Tartaglione, L., Nardo, F.D., Signorelli, F., Lauriola, L., Anile, C., Rindi, G., Maira, G., Pontecorvi, A. & Marinis, L.D. (2014) Radically resected pituitary adenomas: prognostic role of Ki 67 labeling index in a monocentric retrospective series and literature review. *Pituitary*. 17 (3), 267–276. doi:10.1007/s11102-013-0500-6.

Chiloiro, S., Doglietto, F., Trapasso, B., Iacovazzo, D., Giampietro, A., Nardo, F.D., Waure, C. de, Lauriola, L., Mangiola, A., Anile, C., Maira, G., Marinis, L.D. & Bianchi, A. (2015) Typical and Atypical Pituitary Adenomas: A Single-Center Analysis of Outcome and Prognosis. *Neuroendocrinology*. 101 (2), 143–150. doi:10.1159/000375448.

Chinezu, L., Vasiljevic, A., Trouillas, J., Lapoirie, M., Jouanneau, E. & Raverot, G. (2017) Silent somatotroph tumour revisited from a study of 80 patients with and without acromegaly and a review of the literature. *European Journal of Endocrinology*. 176 (2), 195–201. doi:10.1530/eje-16-0738.

Chlenski, A. & Cohn, S.L. (2010) Modulation of matrix remodeling by SPARC in neoplastic progression. *Seminars in Cell & Developmental Biology*. 21 (1), 55–65. doi:10.1016/j.semcdb.2009.11.018.

Ciric, I., Ann, R., Craig, B. & Debi, P. (1997) Complications of transsphenoidal surgery: results of a national survey, review of the literature, and personal experience.

Neurosurgery. 40 (2), 225–237. doi:10.1097/0006123-199702000-00001","keywords":["surgical.

Colao, A., Bronstein, M.D., Freda, P., Gu, F., Shen, C.C., Gadelha, M., Fleseriu, M., Lely, A.J. van der, Farrall, A.J., Résendiz, K.H., Ruffin, M., Chen, Y. & Sheppard, M. (2014) Pasireotide versus octreotide in acromegaly: a head-to-head superiority study. *The Journal of Clinical Endocrinology & Metabolism*. 99 (3), 791–799. doi:10.1210/jc.2013-2480","keywords":["acromegaly","insulin-like.

Colao, A. & Savastano, S. (2011) Medical treatment of prolactinomas. *Nature Reviews Endocrinology*. 7 (5), 267–278. doi:10.1038/nrendo.2011.37.

Colin, P., Jovenin, N., Delemer, B., Caron, J., Grulet, H., Hecart, A.-C., Lukas, C., Bazin, A., Bernard, M.-H., Scherpereel, B., Peruzzi, P., Nakib, I., Redon, C. & Rousseaux, P. (2005) Treatment of pituitary adenomas by fractionated stereotactic radiotherapy: A prospective study of 110 patients. *International Journal of Radiation Oncology*Biology*Physics*. 62 (2), 333–341. doi:10.1016/j.ijrobp.2004.09.058.

Cooper, O., Ben-Shlomo, A., Bonert, V., Bannykh, S., Mirocha, J. & Melmed, S. (2010) Silent corticogonadotroph adenomas: clinical and cellular characteristics and long-term outcomes. *Hormones & cancer*. 1 (2), 80–92. doi:10.1007/s12672-010-0014-x.

Cordeiro, D., Xu, Z., Mehta, G.U., Ding, D., Vance, M.L., et al. (2019) Hypopituitarism after Gamma Knife radiosurgery for pituitary adenomas: a multicenter, international study. *Journal of neurosurgery*. 131 (4), 1188–1196. doi:10.3171/2018.5.jns18509.

Cottier, J.-P., Destrieux, C., Brunereau, L., Bertrand, P., Moreau, L., Jan, M. & Herbreteau, D. (2000) Cavernous Sinus Invasion by Pituitary Adenoma: MR Imaging1. *Radiology*. 215 (2), 463–469. doi:10.1148/radiology.215.2.r00ap18463.

Daly, A.F., Rixhon, M., Adam, C., Dempegioti, A., Tichomirowa, M.A. & Beckers, A. (2006) High Prevalence of Pituitary Adenomas: A Cross-Sectional Study in the Province of Liège, Belgium. *The Journal of Clinical Endocrinology and metabolism*. 91 (12), 4769–4775. doi:10.1210/jc.2006-1668.

Dehdashti, A.R. & Gentili, F. (2007) Current state of the art in the diagnosis and surgical treatment of Cushing disease: early experience with a purely endoscopic endonasal technique. *Neurosurgical Focus*. 23 (3), 1–8. doi:10.3171/foc.2007.23.3.11.

Dehghani, M., Davoodi, Z., Bidari, F., Moghaddam, A.M., Khalili, D., Bahrami-Motlagh, H., Jamali, E., Alamdari, S., Hosseinpanah, F., Hedayati, M. & Valizadeh, M. (2021) Association of different pathologic subtypes of growth hormone producing pituitary adenoma and remission in acromegaly patients: a retrospective cohort study. *BMC Endocrine Disorders*. 21 (1), 1–11. doi:10.1186/s12902-021-00850-2.

DeLellis, R.A. (2004) *Pathology and Genetics of Tumours of Endocrine Organs*. https://books.google.de/books?id=id-AL7mFv8IC.

Delgrange, E., Daems, T., Verhelst, J., Abs, R. & Maiter, D. (2009) Characterization of resistance to the prolactin-lowering effects of cabergoline in macroprolactinomas: a study in 122 patients. *European Journal of Endocrinology*. 160, 747–752. https://eje.bioscientifica.com/downloadpdf/journals/eje/160/5/747.pdf?pdfJsInlineViewToken=1548562187&inlineView=true.

Delgrange, E., Vasiljevic, A., Wierinckx, A., François, P., Jouanneau, E., Raverot, G. & Trouillas, J. (2015) Expression of estrogen receptor alpha is associated with prolactin pituitary tumor prognosis and supports the sex-related difference in tumor growth. *European Journal of Endocrinology*. 172 (6), 791–801. doi:10.1530/eje-14-0990.

Deng, B., Qu, L., Li, J., Fang, J., Yang, S., Cao, Z., Mei, Z. & Sun, X. (2016) MiRNA-211 suppresses cell proliferation, migration and invasion by targeting SPARC in human hepatocellular carcinoma. *Scientific Reports*. 6 (1), 26679–12. doi:10.1038/srep26679.

Deutschbein, T., Jaursch-Hancke, C. & Fassnacht, M. (2020) Hormoninaktive Hypophysentumoren – Kurzpräsentation der ersten deutschen Leitlinie. *DMW - Deutsche Medizinische Wochenschrift*. 145 (20), 1444–1449. doi:10.1055/a-0958-0138.

Dhandapani, S., Singh, H., Negm, H.M., Cohen, S., Anand, V.K. & Schwartz, T.H. (2016) Cavernous Sinus Invasion in Pituitary Adenomas: Systematic Review and Pooled Data Meta-Analysis of Radiologic Criteria and Comparison of Endoscopic and Microscopic Surgery. *World Neurosurgery*. 96 (C), 36–46. doi:10.1016/j.wneu.2016.08.088.

Donovan, J.L. & Nesbit, G.M. (1996) Distinction of masses involving the sella and suprasellar space: specificity of imaging features. *Am Roentgen Ray Soc*. 167, 597–603. https://www.ajronline.org/doi/pdf/10.2214/ajr.167.3.8751659.

Drev, D., Harpain, F., Beer, A., Stift, A., Gruber, E.S., Klimpfinger, M., Thalhammer, S., Reti, A., Kenner, L., Bergmann, M. & Marian, B. (2019) Impact of Fibroblast-Derived SPARC on Invasiveness of Colorectal Cancer Cells. *Cancers*. 11 (10), 1421. doi:10.3390/cancers11101421.

Dubois, S., Guyetant, S., Menei, P., Rodien, P., Illouz, F., Vielle, B. & Rohmer, V. (2007) Relevance of Ki-67 and prognostic factors for recurrence/progression of gonadotropic adenomas after first surgery. *European Journal of Endocrinology*. 157 (2), 141–147. doi:10.1530/eje-07-0099.

Ebrahimi, A., Honegger, J., Schluesener, H. & Schittenhelm, J. (2013) Osteonectin Expression in Surrounding Stroma of Craniopharyngiomas: Association With Recurrence Rate and Brain Infiltration. *International Journal of Surgical Pathology*. 21 (6), 591–598. doi:10.1177/1066896913486695.

Edal, A.L., Skjödt, K. & Nepper-Rasmussen, H.J. (1997) SIPAP: A new MR classification for pituitary adenomas: *Acta Radiologica*. 38 (1), 30–36. doi:10.1080/02841859709171238.

Erickson, D., Scheithauer, B., Atkinson, J., Horvath, E., Kovacs, K., Lloyd, R.V. & Jr, W.F.Y. (2009) Silent subtype 3 pituitary adenoma: a clinicopathologic analysis of the Mayo Clinic experience. *Clinical Endocrinology*. 71 (1), 92–99. doi:10.1111/j.1365-2265.2008.03514.x.

Eschbacher, J.M. & Coons, S.W. (2006) Cytokeratin CK20 is a sensitive marker for Crooke's cells and the early cytoskeletal changes associated with hypercortisolism within pituitary corticotrophs. *Endocrine Pathology*. 17 (4), 365–376. doi:10.1007/s12022-006-0008-y.

Ezzat, S., Asa, S.L., Couldwell, W.T., Barr, C.E., Dodge, W.E., Vance, M.L. & McCutcheon, I.E. (2004) The prevalence of pituitary adenomas. *Cancer*. 101 (3), 613–619. doi:10.1002/cncr.20412.

Faglia, G., Beck-Peccoz, P., Ambrosi, B., Tavaglini, P. & Spada, A. (1991) *Pituitary Adenomas: New Trends in Basic and Clinical Research*. Elsevier. Elsevier.

Famini, P., Maya, M.M. & Melmed, S. (2011) Pituitary magnetic resonance imaging for sellar and parasellar masses: ten-year experience in 2598 patients. *The Journal of Clinical Endocrinology & Metabolism*. 96 (6), 1633–1641. doi:10.1210/jc.2011-0168","keywords":["magnetic.

Feng, J., Hong, L., Wu, Y., Li, C., Wan, H., Li, G., Sun, Y., Yu, S., Chittiboina, P., Montgomery, B., Zhuang, Z. & Zhang, Y. (2014) Identification of a subtype-specific ENC1 gene related to invasiveness in human pituitary null cell adenoma and oncocytomas. *Journal of neuro-oncology*. 119 (2), 307–315. doi:10.1007/s11060-014-1479-1.

Fernandez, A., Karavitaki, N. & Wass, J.A.H. (2010) Prevalence of pituitary adenomas: a community-based, cross-sectional study in Banbury (Oxfordshire, UK). *Clinical Endocrinology*. 72 (3), 377–382. doi:10.1111/j.1365-2265.2009.03667.x.

Ferrante, L., Trillò, G., Ramundo, E., Celli, P., Jaffrain-Rea, M.-L., Salvati, M., Esposito, V., Roperto, R., Osti, M.F. & Minniti, G. (2002) Surgical Treatment of Pituitary Tumors in the Elderly: Clinical Outcome and Long-term Follow-up. *Journal of neuro-oncology*. 60 (2), 185–191. doi:10.1023/a:1020652604014.

Filippella, M., Galland, F., Kujas, M., Young, J., Faggiano, A., Lombardi, G., Colao, A., Meduri, G. & Chanson, P. (2006) Pituitary tumour transforming gene (PTTG) expression correlates with the proliferative activity and recurrence status of pituitary adenomas: a clinical and immunohistochemical study. *Clinical Endocrinology*. 65 (4), 536–543. doi:10.1111/j.1365-2265.2006.02630.x.

Fontebasso, A.M., Schwartzentruber, J., Khuong-Quang, D.-A., Liu, X.-Y., Sturm, D., et al. (2013) Mutations in SETD2 and genes affecting histone H3K36 methylation target hemispheric high-grade gliomas. *Acta Neuropathologica Communications*. 125 (5), 659–669. doi:10.1007/s00401-013-1095-8.

Fougner, S.L., Casar-Borota, O., Heck, A., Berg, J.P. & Bollerslev, J. (2012) Adenoma granulation pattern correlates with clinical variables and effect of somatostatin analogue treatment in a large series of patients with acromegaly. *Clinical Endocrinology*. 76 (1), 96–102. doi:10.1111/j.1365-2265.2011.04163.x.

Fountas, A., Lavrentaki, A., Subramanian, A., Toulis, K.A., Nirantharakumar, K. & Karavitaki, N. (2018) Recurrence in silent corticotroph adenomas after primary treatment: A systematic review and meta-analysis. *The Journal of Clinical Endocrinology and metabolism*. doi:10.1210/jc.2018-01956.

Frank, G. & Pasquini, E. (2006) Endoscopic Endonasal Cavernous Sinus Surgery, with Special Reference to Pituitary Adenomas E.R. Laws & S.J.P. Laws (eds.). *Frontiers of Hormone Research*. 34, 64–82. doi:10.1159/000091573.

Freda, P.U., Chung, W.K., Matsuoka, N., Walsh, J.E., Kanibir, M.N., Kleinman, G., Wang, Y., Bruce, J.N. & Post, K.D. (2007) Analysis of GNAS mutations in 60 growth hormone secreting pituitary tumors: correlation with clinical and pathological characteristics and surgical outcome based on highly sensitive GH and IGF-I criteria for remission. *Pituitary*. 10 (3), 275–282. doi:10.1007/s11102-007-0058-2.

Freda, P.U., Katznelson, L., Lely, A.J. van der, Reyes, C.M., Zhao, S. & Rabinowitz, D. (2005) Long-acting somatostatin analog therapy of acromegaly: a meta-analysis. *The Journal of Clinical Endocrinology & Metabolism*. 90 (8), 4465–4473. doi:10.1210/jc.2005-0260","keywords":["acromegaly","insulin-like.

Friedman, T., Zuckerbraun, E., Lee, M., Kabil, M. & Shahinian, H. (2007) Dynamic Pituitary MRI has High Sensitivity and Specificity for the Diagnosis of Mild Cushing's Syndrome and should be Part of the Initial Workup. *Hormone and metabolic research = Hormon- und Stoffwechselforschung = Hormones et metabolisme*. 39 (6), 451–456. doi:10.1055/s-2007-980192.

Gao, Y., Zhong, C., Wang, Y., Xu, S., Guo, Y., Dai, C., Zheng, Y., Wang, Y., Luo, Q. & Jiang, J. (2014) Endoscopic versus microscopic transsphenoidal pituitary adenoma surgery: a meta-analysis. *World Journal of Surgical Oncology*. 12 (1), 1–12. doi:10.1186/1477-7819-12-94.

Gerdes, J., Lemke, H., Baisch, H., Wacker, H.H., Schwab, U. & Stein, H. (1984) Cell cycle analysis of a cell proliferation-associated human nuclear antigen defined by the monoclonal antibody Ki-67. *The Journal of Immunology*. 133 (4), 1710–1715. https://www.jimmunol.org/content/133/4/1710.short.

Gilles, C., Bassuk, J.A., Pulyaeva, H., Sage, E.H., Foidart, J.M. & Thompson, E.W. (1998) SPARC/osteonectin induces matrix metalloproteinase 2 activation in human breast cancer cell lines. *Cancer Research*. 58 (23), 5529–5536. https://cancerres.aacrjournals.org/content/58/23/5529.short.

Gilliot, O., Khalil, T., Irthum, B., Zasadny, X., Verrelle, P., Tauveron, I. & Pontvert, D. (2007) Radiotherapy of pituitary adenomas: state of the art. *Annales d'Endocrinologie*. 68 (5), 337–348. doi:10.1016/j.ando.2007.03.012.

Giustina, A., Arnaldi, G., Bogazzi, F., Cannavò, S., Colao, A., Marinis, L.D., Menis, E.D., Uberti, E.D., Giorgino, F., Grottoli, S., Lania, A.G., Maffei, P., Pivonello, R. & Ghigo, E. (2017) Pegvisomant in acromegaly: an update. *Journal of Endocrinological Investigation*. 40 (6), 577–589. doi:10.1007/s40618-017-0614-1.

Gomez-Hernandez, K., Ezzat, S., Asa, S.L. & Mete, O. (2015) Clinical Implications of Accurate Subtyping of Pituitary Adenomas: Perspectives from the Treating Physician. *Turk patoloji dergisi*. 31 Suppl 1, 4–17. doi:10.5146/tjpath.2015.01311.

Gondim, J.A., Almeida, J.P., Albuquerque, L.A. de, Gomes, E., Schops, M. & Mota, J.I. (2015) Endoscopic endonasal transsphenoidal surgery in elderly patients with pituitary adenomas. *Journal of neurosurgery*. 123, 31–38. doi:10.3171/2014.10.jns14372.

Gong, J., Zhao, Y., Abdel-Fattah, R., Amos, S., Xiao, A., Lopes, M.B.S., Hussaini, I.M. & Laws, E.R. (2008) Matrix metalloproteinase-9, a potential biological marker in invasive pituitary adenomas. *Pituitary*. 11 (1), 37–48. doi:10.1007/s11102-007-0066-2.

Goudakos, J.K., Markou, K.D. & Georgalas, C. (2011) Endoscopic versus microscopic trans-sphenoidal pituitary surgery: a systematic review and meta-analysis. *Clinical Otolaryngology*. 36 (3), 212–220. doi:10.1111/j.1749-4486.2011.02331.x.

Greenman, Y. & Melmed, S. (1996) Diagnosis and management of nonfunctioning pituitary tumors. *Annual review of medicine*. 47 (1), 95–106. doi:10.1146/annurev.med.47.1.95.

Grimm, F., Maurus, R., Beschorner, R., Naros, G., Stanojevic, M., Gugel, I., Giese, S., Bier, G., Bender, B. & Honegger, J. (2019) Ki-67 labeling index and expression of p53 are non-predictive for invasiveness and tumor size in functional and nonfunctional pituitary adenomas. *Acta neurochirurgica*. 161 (6), 1149–1156. doi:10.1007/s00701-019-03879-4.

Gruppetta, M., Mercieca, C. & Vassallo, J. (2013) Prevalence and incidence of pituitary adenomas: a population based study in Malta. *Pituitary*. 16 (4), 545–553. doi:10.1007/s11102-012-0454-0.

Gulmann, C. & O'Grady, A. (2003) Tissue microarrays: an overview. *Current Diagnostic Pathology*. 9 (3), 149–154. doi:10.1016/s0968-6053(02)00094-7.

Gültekin, G.D., Çabuk, B., Vural, Ç. & Ceylan, S. (2015) Matrix metalloproteinase-9 and tissue inhibitor of matrix metalloproteinase-2: Prognostic biological markers in invasive prolactinomas. *Journal of Clinical Neuroscience*. 22 (8), 1282–1287. doi:10.1016/j.jocn.2015.02.021.

Gustavson, M.D., Bourke-Martin, B., Reilly, D., Cregger, M., Williams, C. & Mayotte, J. (2009) Standardization of HER2 immunohistochemistry in breast cancer by automated quantitative analysis. *Archives of Pathology Laboratory Medicine*. 133 (9), 1413–1419. https://meridian.allenpress.com/aplm/article-abstract/133/9/1413/64034.

Guweidhi, A., Kleeff, J., Adwan, H., Giese, N.A., Wente, M.N., Giese, T., Büchler, M.W., Berger, M.R. & Friess, H. (2005) Osteonectin Influences Growth and Invasion of Pancreatic Cancer Cells. *Annals of Surgery*. 242 (2), 224–234. doi:10.1097/01.sla.0000171866.45848.68.

Haas, L.F. (2002) *Harvey Williams Cushing (1869-1939).* Journal of neurology, neurosurgery, and psychiatry. J. Neurol. Neurosurg. Psychiatry. doi:10.1136/jnnp.73.5.596.

Hager, M., Kolbitsch, C., Tiefenthaler, W., Haufe, H., Kemmerling, R. & Moser, P.L. (2009) Tissue microarrays from renal cell tumors: Exclusion criteria and rate of exclusion. *Scandinavian Journal of Urology and Nephrology*. doi:10.1080/00365590701520552.

Hague, K., Post, K.D. & Morgello, S. (2000) Absence of peritumoral Crooke's change is associated with recurrence in surgically treated Cushing's disease. *Surgical Neurology*. 53 (1), 77–81. doi:10.1016/s0090-3019(99)00159-7.

Hardy, J. & Vezina, J.L. (1976) Transsphenoidal neurosurgery of intracranial neoplasm. *Advances in Neurology*. 15, 261–273. https://europepmc.org/abstract/med/945663.

Hasanov, R., Aydoğan, B.İ., Kiremitçi, S., Erden, E. & Güllü, S. (2019) The Prognostic Roles of the Ki-67 Proliferation Index, P53 Expression, Mitotic Index, and Radiological Tumor Invasion in Pituitary Adenomas. *Endocrine Pathology*. 30 (1), 49–55. doi:10.1007/s12022-018-9563-2.

He, L.-R., Liu, M.-Z., Li, B.-K., Rao, H.-L., Liao, Y.-J., Guan, X.-Y., Zeng, Y.-X. & Xie, D. (2009) Prognostic impact of H3K27me3 expression on locoregional progression after chemoradiotherapy in esophageal squamous cell carcinoma. *BMC Cancer*. 9 (1), 1–9. doi:10.1186/1471-2407-9-461.

Heck, A., Ringstad, G., Fougner, S.L., Casar-Borota, O., Nome, T., Ramm-Pettersen, J. & Bollerslev, J. (2012) Intensity of pituitary adenoma on T2-weighted magnetic resonance imaging predicts the response to octreotide treatment in newly diagnosed acromegaly. *Clinical Endocrinology*. 77 (1), 72–78. doi:10.1111/j.1365-2265.2011.04286.x.

Hegi, M.E., Diserens, A.-C., Gorlia, T., Hamou, M.-F., Tribolet, N. de, Weller, M., Kros, J.M., Hainfellner, J.A., Mason, W., Mariani, L., Bromberg, J.E.C., Hau, P., Mirimanoff, R.O., Cairncross, J.G., Janzer, R.C. & Stupp, R. (2009) MGMT Gene Silencing and Benefit from Temozolomide in Glioblastoma. *The New England Journal of Medicine*. 352 (10), 997–1003. doi:10.1056/nejmoa043331.

Hentschel, S.J., McCutcheon, lan E., Moore, W. & Durity, F.A. (2003) P53 and MIB-1 immunohistochemistry as predictors of the clinical behavior of nonfunctioning pituitary adenomas. *Canadian Journal of Neurological Sciences*. 30 (3), 215–219. doi:10.1017/s0317167100002614.

Hirohata, T., Asano, K., Ogawa, Y., Takano, S., Amano, K., Isozaki, O., Iwai, Y., Sakata, K., Fukuhara, N., Nishioka, H., Yamada, S., Fujio, S., Arita, K., Takano, K. & Tominaga, A. (2013) DNA mismatch repair protein (MSH6) correlated with the responses of atypical pituitary adenomas and pituitary carcinomas to temozolomide: the national cooperative …. *The Journal of Clinical Endocrinology & Metabolism*. 98 (3), 1130–1136. doi:10.1210/jc.2012-2924","keywords":["immunohistochemistry","pituitary.

Ho, D.M., Hsu, C.Y., Ting, L.T. & Chiang, H. (2001) Plurihormonal pituitary adenomas: immunostaining of all pituitary hormones is mandatory for correct classification. *Histopathology*. 39 (3), 310–319. doi:10.1046/j.1365-2559.2001.01204.x.

Ho, T.H., Kapur, P., Joseph, R.W., Serie, D.J., Eckel-Passow, J.E., Tong, P., Wang, J., Castle, E.P., Stanton, M.L., Cheville, J.C., Jonasch, E., Brugarolas, J. & Parker, A.S. (2016) Loss of histone H3 lysine 36 trimethylation is associated with an increased risk of renal cell carcinoma-specific death. *Modern Pathology*. 29 (1), 34–42. doi:10.1038/modpathol.2015.123.

Hofstetter, C.P., Nanaszko, M.J., Mubita, L.L., Tsiouris, J., Anand, V.K. & Schwartz, T.H. (2012) Volumetric classification of pituitary macroadenomas predicts outcome and morbidity following endoscopic endonasal transsphenoidal surgery. *Pituitary*. 15 (3), 450–463. doi:10.1007/s11102-011-0350-z.

Honegger, J., Ernemann, U., Psaras, T. & Will, B. (2007) Objective criteria for successful transsphenoidal removal of suprasellar nonfunctioning pituitary adenomas. A prospective study. *Acta neurochirurgica*. 149 (1), 21–29. doi:10.1007/s00701-006-1044-6.

Honegger, J., Nasi-Kordhishti, I. & Giese, S. (2019) Hypophysenadenome. *Der Nervenarzt*. 1–8. doi:10.1007/s00115-019-0708-4.

Honegger, J., Prettin, C., Feuerhake, F., Petrick, M., Schulte-Mönting, J. & Reincke, M. (2003) Expression of Ki-67 antigen in nonfunctioning pituitary adenomas: correlation with growth velocity and invasiveness. *Journal of neurosurgery*. 99 (4), 674–679. doi:10.3171/jns.2003.99.4.0674.

Hoos, A. & Cordon-Cardo, C. (2001) Tissue microarray profiling of cancer specimens and cell lines: opportunities and limitations. *Laboratory investigation; a journal of technical methods and pathology*. 81 (10), 1331–1338. doi:10.1038/labinvest.3780347.

Horvath, E., Kovacs, K., Smyth, H.S., Killinger, D.W., Scheithauer, B.W., Randall, R., Laws, E.R. & Singer, W. (1988) A novel type of pituitary adenoma: morphological

features and clinical correlations. *The Journal of Clinical Endocrinology and metabolism*. 66 (6), 1111–1118. doi:10.1210/jcem-66-6-1111.

Huang, Y., Gu, L. & Li, G.-M. (2018) H3K36me3-mediated mismatch repair preferentially protects actively transcribed genes from mutation. *Journal of Biological Chemistry*. 293 (20), 7811–7823. doi:10.1074/jbc.ra118.002839.

Hussaini, I.M., Trotter, C., Zhao, Y., Abdel-Fattah, R., Amos, S., Xiao, A., Agi, C.U., Redpath, G.T., Fang, Z., Leung, G.K.K., Lopes, M.B.S. & Jr, E.R.L. (2007) Matrix Metalloproteinase-9 Is Differentially Expressed in Nonfunctioning Invasive and Noninvasive Pituitary Adenomas and Increases Invasion in Human Pituitary Adenoma Cell Line. *The American Journal of Pathology*. 170 (1), 356–365. doi:10.2353/ajpath.2007.060736.

Hwang, J., Seol, H.J., Nam, D.-H., Lee, J.-I., Lee, M.H. & Kong, D.-S. (2016) Therapeutic Strategy for Cavernous Sinus-Invading Non-Functioning Pituitary Adenomas Based on the Modified Knosp Grading System. *Brain Tumor Research and Treatment*. 4 (2), 63–69. doi:10.14791/btrt.2016.4.2.63.

Iglesias, P., Arcano, K., Berrocal, V.R., Bernal, C., Villabona, C. & Díez, J.J. (2018) Giant Prolactinoma in Men: Clinical Features and Therapeutic Outcomes. *Hormone and metabolic research = Hormon- und Stoffwechselforschung = Hormones et metabolisme*. 50 (11), 791–796. doi:10.1055/a-0752-0741.

Iuchi, T., Saeki, N., Osato, K. & Yamaura, A. (2000) Proliferation, vascular endothelial growth factor expression and cavernous sinus invasion in growth hormone secreting pituitary adenomas. *Acta neurochirurgica*. 142 (12), 1345–1351. doi:10.1007/s007010070003.

Jaffrain-Rea, M.L., Stefano, D.D., Minniti, G., Esposito, V., Bultrini, A., Ferretti, E., Santoro, A., Scucchi, L.F., Gulino, A. & Cantore, G. (2002) A critical reappraisal of MIB-1 labelling index significance in a large series of pituitary tumours: secreting versus non-secreting adenomas. *Endocrine-Related Cancer*. 9 (2), 103–113. doi:10.1677/erc.0.0090103.

Jiang, S., Zhu, J., Feng, M., Yao, Y., Deng, K., Xing, B., Lian, W., Wang, R. & Bao, X. (2021) Clinical profiles of silent corticotroph adenomas compared with silent gonadotroph adenomas after adopting the 2017 WHO pituitary classification system. *Pituitary*. 1–10. doi:10.1007/s11102-021-01133-8.

Johnsen, D.E., Woodruff, W.W., Allen, I.S., Cera, P.J., Funkhouser, G.R. & Coleman, L.L. (1991) MR imaging of the sellar and juxtasellar regions. *RadioGraphics*. 11 (5), 727–758. doi:10.1148/radiographics.11.5.1947311.

Jr, J.O.V., Cukiert, A. & Liberman, B. (2006) Evaluation of magnetic resonance imaging criteria for cavernous sinus invasion in patients with pituitary adenomas: logistic regression analysis and correlation with surgical findings. *Surgical Neurology*. 65 (2), 130–135. doi:10.1016/j.surneu.2005.05.021.

Jr., W.F.Y., Scheithauer, B.W., Kovacs, K.T., Horvath, E., Davis, D.H. & Randall, R.V. (1996) Gonadotroph Adenoma of the Pituitary Gland: A Clinicopathologic Analysis of 100 Cases. *Mayo Clinic Proceedings*. 71 (7), 649–656. doi:10.1016/s0025-6196(11)63002-4.

Jung, M., Kim, S.-I., Lim, K.Y., Bae, J., Park, C.-K., Choi, S.H., Park, S.-H. & Won, J.-K. (2021) The substantial loss of H3K27me3 can stratify risk in grade 2, but not in grade 3 meningioma. *Human pathology*. 26 (115), 96–103. doi:10.1016/j.humpath.2021.06.005.

Kanapathipillai, M. (2018) Treating p53 Mutant Aggregation-Associated Cancer. *Cancers*. 10 (6), 154. doi:10.3390/cancers10060154.

Karamouzis, I., Caputo, M., Mele, C., Nuzzo, A., Zavattaro, M., Car, P., Panzarasa, G., Prodam, F., Marzullo, P. & Aimaretti, G. (2018) Transsphenoidal surgery for pituitary adenomas: early results from a single center. *HORMONES*. 17 (4), 551–556. doi:10.1007/s42000-018-0082-9.

Karow, T. & Lang-Roth, R. (2020) *Allgemeine und Spezielle Pharmakologie und Toxikologie 2020*. Thomas Karow. Thomas Karow. http://scholar.google.comjavascript:void(0).

Katz, L.M., Hielscher, T., Liechty, B., Silverman, J., Zagzag, D., et al. (2018) Loss of histone H3K27me3 identifies a subset of meningiomas with increased risk of recurrence. *Acta Neuropathologica Communications*. 135 (6), 955–963. doi:10.1007/s00401-018-1844-9.

Kawamoto, H., Uozumi, T., Kawamoto, K., Arita, K., Yano, T. & Hirohata, T. (1996) Type IV collagenase activity and cavernous sinus invasion in human pituitary adenomas. *Acta neurochirurgica*. 138 (4), 390–395. doi:10.1007/bf01420300.

Khuong-Quang, D.-A., Buczkowicz, P., Rakopoulos, P., Liu, X.-Y., Fontebasso, A.M., et al. (2012) K27M mutation in histone H3.3 defines clinically and biologically distinct subgroups of pediatric diffuse intrinsic pontine gliomas. *Acta Neuropathologica Communications*. 124 (3), 439–447. doi:10.1007/s00401-012-0998-0.

Kim, J., Yoon, S.J., Moon, J.H., Ku, C.R., Kim, S.H., Lee, E.J., Kim, S.H. & Kim, E.H. (2019) Clinical Significance of Radical Surgery in the Treatment of Silent Corticotroph Adenoma. *Journal of Korean Neurosurgical Society*. 62 (1), 114–122. doi:10.3340/jkns.2018.0027.

Kim, J.S., Lee, Y.S., Jung, M.J. & Hong, Y.K. (2016) The Predictive Value of Pathologic Features in Pituitary Adenoma and Correlation with Pituitary Adenoma Recurrence. *Journal of Pathology and Translational Medicine*. 50 (6), 419–425. doi:10.4132/jptm.2016.06.30.

Kim, S.W., Roh, J. & Park, C.S. (2016) Immunohistochemistry for Pathologists: Protocols, Pitfalls, and Tips. *Journal of Pathology and Translational Medicine*. 50, 411–418. doi:10.4132/jptm.2016.08.08&domain=pdf&date_stamp=2016-11-15.

Kirkman, M.A., Jaunmuktane, Z., Brandner, S., Khan, A.A., Powell, M. & Baldeweg, S.E. (2014) Active and silent thyroid-stimulating hormone-expressing pituitary adenomas: presenting symptoms, treatment, outcomes, and recurrence. *World Neurosurgery*. 82 (6), 1224–1231. doi:10.1016/j.wneu.2014.03.031.

Kitchen, M.O., Yacqub-Usman, K., Emes, R.D., Richardson, A., Clayton, R.N. & Farrell, W.E. (2015) Epidrug mediated re-expression of miRNA targeting the HMGA transcripts in pituitary cells. *Pituitary*. 18 (5), 674–684. doi:10.1007/s11102-014-0630-5.

Klingmüller, D., Saller, B. & Quabbe, H.-J. (2001) Diagnostik von Hypophysenadenomen. *Deutsches Ärzteblatt*. 96 (46), 3053–3059.

Knosp, E., Kitz, K. & Perneczky, A. (1989) Proliferation activity in pituitary adenomas: measurement by monoclonal antibody Ki-67. *Neurosurgery*. 25 (6), 927–930. http://eutils.ncbi.nlm.nih.gov/entrez/eutils/elink.fcgi?dbfrom=pubmed&id=2601824&retmode=ref&cmd=prlinks.

Knosp, E., Steiner, E., Kitz, K. & Matula, C. (1993) Pituitary adenomas with invasion of the cavernous sinus space: a magnetic resonance imaging classification compared with surgical findings. *Neurosurgery*. 33 (4), 610–618. doi:10.1097/00006123-199310000-00008","keywords":["magnetic.

Kononen, J., Bubendorf, L., Kallionimeni, A., Bärlund, M., Schraml, P., Leighton, S., Torhorst, J., Mihatsch, M.J., Sauter, G. & Kallionimeni, O.-P. (1998) Tissue microarrays for high-throughput molecular profiling of tumor specimens. *Nature Medicine*. 4 (7), 844–847. doi:10.1038/nm0798-844.

Kontogeorgos, G. (2021) Update on pituitary adenomas in the 2017 World Health Organization classification: innovations and perspectives. *HORMONES*. 20 (2), 287–291. doi:10.1007/s42000-020-00269-9.

Kontogeorgos, G., Asa, S.L., Kovacs, K., Smyth, H.S. & Singer, W. (1993) Production of alpha-subunit of glycoprotein hormones by pituitary somatotroph adenomas in vitro. *Acta endocrinologica*. 129 (6), 565–572. doi:10.1530/acta.0.1290565.

Kontogeorgos, G. & Thodou, E. (2016) The gonadotroph origin of null cell adenomas. *HORMONES*. 1–6. doi:10.14310/horm.2002.1652.

Kottler, M.L., Seret-Bégué, D., Lahlou, N., Assayag, M., Carré, M.C., Lagarde, J.P., Ajzenberg, C., Christin-Maitre, S., Bouchard, P., Mikol, J., Counis, R. & Warnet, A. (1998) The GnRH receptor gene is preferentially expressed in functioning gonadotroph adenomas and displays a Mae III polymorphism site. *Clinical Endocrinology*. 49 (1), 115–123. doi:10.1046/j.1365-2265.1998.00500.x.

Koutourousiou, M., Fernandez-Miranda, J.C., Snyderman, C.H. & Gardner, P.A. (2012) Endoscopic Endonasal Approach for Giant Pituitary Adenomas: Advantages and Limitations. *Journal of Neurological Surgery Part B: Skull Base*. 73 (S 01), A140. doi:10.1055/s-0032-1312188.

Kuga, D., Toda, M., Ozawa, H., Ogawa, K. & Yoshida, K. (2019) Endoscopic Endonasal Approach Combined with a Simultaneous Transcranial Approach for Giant Pituitary Tumors. *World Neurosurgery*. 121, 173–179. doi:10.1016/j.wneu.2018.10.047.

Lane, D.P. (1992) p53, guardian of the genome. *Nature*. 358 (6381), 15–16. https://doi.org/10.1038/358015a0.

Langlois, F., Lim, D.S.T., Varlamov, E., Yedinak, C.G., Cetas, J.S., McCartney, S., Dogan, A. & Fleseriu, M. (2017) Clinical profile of silent growth hormone pituitary adenomas; higher recurrence rate compared to silent gonadotroph pituitary tumors, a large single center experience. *Endocrine*. 58 (3), 528–534. doi:10.1007/s12020-017-1447-6.

Langlois, F., Woltjer, R., Cetas, J.S. & Fleseriu, M. (2018) Silent somatotroph pituitary adenomas: an update. *Pituitary*. 21 (2), 194–202. doi:10.1007/s11102-017-0858-y.

Laron, Z. (2001) Insulin-like growth factor 1 (IGF-1): a growth hormone. *Molecular pathology : MP*. 54 (5), 311–316. doi:10.1136/mp.54.5.311.

Lelotte, J., Mourin, A., Fomekong, E., Michotte, A., Raftopoulos, C. & Maiter, D. (2018) Both invasiveness and proliferation criteria predict recurrence of non-functioning pituitary macroadenomas after surgery: a retrospective analysis of a monocentric cohort of 120 patients. *European Journal of Endocrinology*. 178 (3), 237–246. doi:10.1530/eje-17-0965.

Li, F., Mao, G., Tong, D., Huang, J., Gu, L., Yang, W. & Li, G.-M. (2013) The histone mark H3K36me3 regulates human DNA mismatch repair through its interaction with MutSα. *Cell*. 153 (3), 590–600. doi:10.1016/j.cell.2013.03.025.

Li, Y., Zhou, L.-P., Ma, P., Sui, C.-G., Meng, F.-D., Tian, X., Fu, L.-Y. & Jiang, Y.-H. (2014) Relationship of PTTG expression with tumor invasiveness and microvessel density of pituitary adenomas: a meta-analysis. *Genetic testing and molecular biomarkers*. 18 (4), 279–285. doi:10.1089/gtmb.2013.0447.

Lien, H.-C., Jeng, Y.-M., Jhuang, Y.-L. & Yuan, R.-H. (2018) Increased Trimethylation of histone H3K36 associates with biliary differentiation and predicts poor prognosis in resectable hepatocellular carcinoma. *PloS one*. 13 (10), e0206261. doi:10.1371/journal.pone.0206261.

Liu, H.-Y., Gu, W.-J., Wang, C.-Z., Ji, X.-J. & Mu, Y.-M. (2016) Matrix metalloproteinase-9 and -2 and tissue inhibitor of matrix metalloproteinase-2 in invasive pituitary adenomas. *Medicine*. 95 (24), e3904-10. doi:10.1097/md.0000000000003904.

Liu, J., He, Y., Zhang, X., Yan, X. & Huang, Y. (2020) Clinicopathological analysis of 250 cases of pituitary adenoma under the new WHO classification. *Oncology Letters*. 19 (3), 1890–1898. doi:10.3892/ol.2020.11263.

Liu, W., Matsumoto, Y., Okada, M., Miyake, K., Kunishio, K., Kawai, N., Tamiya, T. & Nagao, S. (2005) Matrix metalloproteinase 2 and 9 expression correlated with cavernous sinus invasion of pituitary adenomas. *The Journal of Medical Investigation*. 52 (3,4), 151–158. doi:10.2152/jmi.52.151.

Lloyd, R.V., Osamura, R.Y., Grossman, A., Korbonits, M., Kovacs, K., lopes, M.B.S., Matsuno, A. & Trouillas, J. (2017) *WHO Classification of Tumours of Endocrine Organs* R.V. Lloyd, R.Y. Osamura, G. Klöppel, & J. Rosai (eds.). 13–64.

Loeffler, J.S. & Shih, H.A. (2011) Radiation Therapy in the Management of Pituitary Adenomas. *The Journal of Clinical Endocrinology & Metabolism*. 96 (7), 1992–2003. doi:10.1210/jc.2011-0251.

Lopes, M.B.S. (2017) The 2017 World Health Organization classification of tumors of the pituitary gland: a summary. *Acta Neuropathologica Communications*. 134 (4), 521–535. doi:10.1007/s00401-017-1769-8.

Losa, M., Mortini, P., Barzaghi, R., Ribotto, P., Terreni, M.R., Marzoli, S.B., Pieralli, S. & Giovanelli, M. (2008) Early results of surgery in patients with nonfunctioning pituitary adenoma and analysis of the risk of tumor recurrence. *Journal of neurosurgery*. 108 (3), 525–532. doi:10.3171/jns/2008/108/3/0525.

Losa, M., Mortini, P., Pagnano, A., Detomas, M., Cassarino, M.F. & Giraldi, F.P. (2019) Clinical characteristics and surgical outcome in USP8-mutated human adrenocorticotropic hormone-secreting pituitary adenomas. *Endocrine*. 63 (2), 240–246. doi:10.1007/s12020-018-1776-0.

Lu, C., Jain, S.U., Hoelper, D., Bechet, D., Molden, R.C., et al. (2016) Histone H3K36 mutations promote sarcomagenesis through altered histone methylation landscape. *Science (New York, N.Y.)*. 352 (6287), 844–849. doi:10.1126/science.aac7272.

Luo, Q., Beaver, J.M., Liu, Y. & Zhang, Z. (2017) Dynamics of p53: A Master Decider of Cell Fate. *Genes*. 8 (2), 66. doi:10.3390/genes8020066.

Ma, Z.-Y., Song, Z.-J., Chen, J.-H., Wang, Y.-F., Li, S.-Q., et al. (2015) Recurrent gain-of-function USP8 mutations in Cushing's disease. *Cell Research*. 25 (3), 306–317. doi:10.1038/cr.2015.20.

Maiter, D. (2019) Management of Dopamine Agonist-Resistant Prolactinoma. *Neuroendocrinology*. 109 (1), 42–50. doi:10.1159/000495775.

Malik, M.T. & Kakar, S.S. (2006) Regulation of angiogenesis and invasion by human Pituitary tumor transforming gene (PTTG) through increased expression and secretion

of matrix metalloproteinase-2 (MMP-2). *Molecular Cancer*. 5 (1), 1–13. doi:10.1186/1476-4598-5-61.

Mastronardi, L., Guiducci, A. & Puzzilli, F. (2001) Lack of correlation between Ki-67 labelling index and tumor size of anterior pituitary adenomas. *BMC Cancer*. 1 (1), 12–15. doi:10.1186/1471-2407-1-12.

Matsuyama, J. (2012) Ki-67 Expression for Predicting Progression of Postoperative Residual Pituitary Adenomas: Correlations With Clinical Variables. *Neurologia medico-chirurgica*. 52 (8), 563–569. doi:10.2176/nmc.52.563.

McCabe, C.J., Boelaert, K., Tannahill, L.A., Heaney, A.P., Stratford, A.L., Khaira, J.S., Hussain, S., Sheppard, M.C., Franklyn, J.A. & Gittoes, N.J.L. (2002) Vascular endothelial growth factor, its receptor KDR/Flk-1, and pituitary tumor transforming gene in pituitary tumors. *The Journal of Clinical Endocrinology and metabolism*. 87 (9), 4238–4244. doi:10.1210/jc.2002-020309.

McCabe, C.J., Khaira, J.S., Boelaert, K., Heaney, A.P., Tannahill, L.A., Hussain, S., Mitchell, R., Oliff, J., Sheppard, M.C. & Franklyn, J. (2003) Expression of pituitary tumour transforming gene (PTTG) and fibroblast growth factor-2 (FGF-2) in human pituitary adenomas: relationship to clinical tumor behaviour. *Clinical Endocrinology*. 58, 141–150. http://scholar.google.comjavascript:void(0).

McGrath, G.A., Goncalves, R.J., Udupa, J.K., Grossman, R.I., Pavlou, S.N., Molitch, M.E., Rivier, J., Vale, W.W. & Snyder, P.J. (1993) New technique for quantitation of pituitary adenoma size: use in evaluating treatment of gonadotroph adenomas with a gonadotropin-releasing hormone antagonist. *The Journal of Clinical Endocrinology and metabolism*. 76 (5), 1363–1368. doi:10.1210/jcem.76.5.8496331.

Meij, B.P., Lopes, M.B.S., Ellegala, D.B., Alden, T.D. & Laws, E.R. (2002) The long-term significance of microscopic dural invasion in 354 patients with pituitary adenomas treated with transsphenoidal surgery. *Journal of neurosurgery*. 96 (2), 195–208. doi:10.3171/jns.2002.96.2.0195.

Melmed, S., Casanueva, F.F., Hoffman, A.R., Kleinberg, D.L., Montori, V.M., Schlechte, J.A. & Wass, J. (2011) Diagnosis and treatment of hyperprolactinemia: an Endocrine Society clinical practice guideline. *The Journal of Clinical Endocrinology & Metabolism*. 96 (2), 273–288. doi:10.1210/jc.2010-1692","inlanguage":"en","copyrightholder":"oxford.

Messerer, M., battista, J.C.D., Raverot, G., Kassis, S., Dubourg, J., Lapras, V., Trouillas, J., Perrin, G. & Jouanneau, E. (2011) Evidence of improved surgical outcome following endoscopy for nonfunctioning pituitary adenoma removal: Personal experience and review of the literature. *Neurosurgical Focus*. 30 (4), E11. doi:10.3171/2011.1.focus10308.

Mete, O. & Asa, S.L. (2012) Clinicopathological Correlations in Pituitary Adenomas. *Brain Pathology*. 22 (4), 443–453. doi:10.1111/j.1750-3639.2012.00599.x.

Mete, O. & Asa, S.L. (2013) Therapeutic implications of accurate classification of pituitary adenomas. *Seminars in diagnostic pathology*. 30 (3), 158–164. doi:10.1053/j.semdp.2013.06.002.

Mete, O., Ezzat, S. & Asa, S.L. (2012) Biomarkers of aggressive pituitary adenomas. *Journal of Molecular Endocrinology*. 49 (2), R69–R78. doi:10.1530/jme-12-0113.

Mete, O., Gomez-Hernandez, K., Kucharczyk, W., Ridout, R., Zadeh, G., Gentili, F., Ezzat, S. & Asa, S.L. (2016) Silent subtype 3 pituitary adenomas are not always silent and represent poorly differentiated monomorphous plurihormonal Pit-1 lineage adenomas. *Nature Publishing Group*. 29 (2), 131–142. doi:10.1038/modpathol.2015.151.

Mete, O. & Lopes, M.B. (2017) Overview of the 2017 WHO Classification of Pituitary Tumors. *Endocrine Pathology*. 28 (3), 228–243. doi:10.1007/s12022-017-9498-z.

Meyer, S., Valdemarsson, S. & Larsson, E.-M. (2011) Classification of pituitary growth hormone producing adenomas according to SIPAP: application in clinical practice: *Acta Radiologica*. 52 (7), 796–801. doi:10.1258/ar.2011.110014.

Micko, A.S.G., Wöhrer, A., Wolfsberger, S. & Knosp, E. (2015) Invasion of the cavernous sinus space in pituitary adenomas: endoscopic verification and its correlation with an MRI-based classification. *Journal of neurosurgery*. 122 (4), 803–811. doi:10.3171/2014.12.jns141083.

Miermeister, C.P., Petersenn, S., Buchfelder, M., Fahlbusch, R., Lüdecke, D.K., Hölsken, A., Bergmann, M., Knappe, H.U., Hans, V.H., Flitsch, J., Saeger, W. & Buslei, R. (2015) Histological criteria for atypical pituitary adenomas – data from the German pituitary adenoma registry suggests modifications. *Acta Neuropathologica Communications*. 3 (1), 1–11. doi:10.1186/s40478-015-0229-8.

Mindermann, T. & Wilson, C.B. (1993) Thyrotropin-producing pituitary adenomas. *Journal of neurosurgery*. 79 (4), 521–527. doi:10.3171/jns.1993.79.4.0521.

Minniti, G., Clarke, E., Scaringi, C. & Enrici, R.M. (2016) Stereotactic radiotherapy and radiosurgery for non-functioning and secreting pituitary adenomas. *Reports of Practical Oncology and Radiotherapy*. 21 (4), 370–378. doi:10.1016/j.rpor.2014.09.004.

Mohr, G., Hardy, J., Comtois, R. & Beauregard, H. (1990) Surgical Management of Giant Pituitary Adenomas. *Canadian Journal of Neurological Sciences*. 17 (1), 62–66. doi:10.1017/s0317167100030055.

Molitch, M.E. (2006) Pituitary Disorders During Pregnancy. *Endocrinology and Metabolism Clinics*. 35 (1), 99–116. doi:10.1016/j.ecl.2005.09.011.

Molitch, M.E. (1997) Pituitary incidentalomas. *Endocrinology and Metabolism Clinics*. 26 (4), 725–740. doi:10.1016/s0889-8529(05)70279-6.

Monsalves, E., Larjani, S. & B Loyola Godoy (2014) Growth patterns of pituitary adenomas and histopathological correlates. *The Journal of Clinical Endocrinology & Metabolism*. 99 (4), 1330–1338. doi:10.1210/jc.2013-3054.

Mooney, M., Hardesty, D., Sheehy, J., Bird, C., Chapple, K., White, W. & Little, A. (2017a) Rater Reliability of the Hardy Classification for Pituitary Adenomas in the Magnetic Resonance Imaging Era. *Journal of Neurological Surgery Part B: Skull Base*. 78 (05), 413–418. doi:10.1055/s-0037-1603649.

Mooney, M.A., Hardesty, D.A., Sheehy, J.P., Bird, R., Chapple, K., White, W.L. & Little, A.S. (2017b) Interrater and intrarater reliability of the Knosp scale for pituitary adenoma grading. *Journal of neurosurgery*. 126 (5), 1714–1719. doi:10.3171/2016.3.jns153044.

Murphy, G. & Nagase, H. (2008) Progress in matrix metalloproteinase research. *Molecular Aspects of Medicine*. 29 (5), 290–308. doi:10.1016/j.mam.2008.05.002.

Nichol, J.N., Dupéré-Richer, D., Ezponda, T., Licht, J.D. & Jr., W.H.M. (2016) H3K27 Methylation: A Focal Point of Epigenetic Deregulation in Cancer. *Advances in Cancer Research*. 131, 59–95. doi:10.1016/bs.acr.2016.05.001.

Nishioka, H., Inoshita, N., Mete, O., Asa, S.L., Hayashi, K., Takeshita, A., Fukuhara, N., Yamaguchi-Okada, M., Takeuchi, Y. & Yamada, S. (2015) The Complementary Role of Transcription Factors in the Accurate Diagnosis of Clinically Nonfunctioning Pituitary Adenomas. *Endocrine Pathology*. 26 (4), 349–355. doi:10.1007/s12022-015-9398-z.

Noh, T.-W., Jeong, H.J., Lee, M.-K., Kim, T.S., Kim, S.H. & Lee, E.J. (2009) Predicting recurrence of nonfunctioning pituitary adenomas. *The Journal of Clinical Endocrinology and metabolism*. 94 (11), 4406–4413. doi:10.1210/jc.2009-0471.

Ntali, G., Capatina, C., Grossman, A. & Karavitaki, N. (2014) Functioning Gonadotroph Adenomas. *The Journal of Clinical Endocrinology and metabolism*. 99 (12), 4423–4433. doi:10.1210/jc.2014-2362.

Nunes, V. dos S., Dib, R.E., Boguszewski, C.L. & Nogueira, C.R. (2011) Cabergoline versus bromocriptine in the treatment of hyperprolactinemia: a systematic review of randomized controlled trials and meta-analysis. *Pituitary*. 14 (3), 259–265. doi:10.1007/s11102-010-0290-z.

Obari, A., Sano, T., Ohyama, K., Kudo, E., Qian, Z.R., Yoneda, A., Rayhan, N., Rahman, M.M. & Yamada, S. (2008) Clinicopathological features of growth hormone-producing pituitary adenomas: difference among various types defined by cytokeratin distribution pattern including a transitional form. *Endocrine Pathology*. 19 (2), 82–91. doi:10.1007/s12022-008-9029-z.

Onoz, M., Basaran, R., Gucluer, B., Isik, N., Kaner, T., Sav, A. & Elmaci, I. (2015) Correlation between SPARC (Osteonectin) expression with immunophenotypical and

invasion characteristics of pituitary adenomas. *APMIS : acta pathologica, microbiologica, et immunologica Scandinavica*. 123 (3), 199–204. doi:10.1111/apm.12342.

Osamura, R.Y., Kajiya, H., Takei, M., Egashira, N., Tobita, M., Takekoshi, S. & Teramoto, A. (2008) Pathology of the human pituitary adenomas. *Histochemistry and Cell Biology*. 130 (3), 495–507. doi:10.1007/s00418-008-0472-1.

Ostrom, Q.T., Patil, N., Cioffi, G., Waite, K., Kruchko, C. & Barnholtz-Sloan, J.S. (2020) CBTRUS Statistical Report: Primary Brain and Other Central Nervous System Tumors Diagnosed in the United States in 2013-2017. *Neuro-Oncology*. 22 (12 Suppl 2), iv1–iv96. doi:10.1093/neuonc/noaa200.

Paek, K.-I., Kim, S.-H., Song, S.-H., Choi, S.-W., Koh, H.-S., Youm, J.-Y. & Kim, Y. (2005) Clinical significance of Ki-67 labeling index in pituitary macroadenoma. *Journal of Korean medical science*. 20 (3), 489–494. doi:10.3346/jkms.2005.20.3.489.

Panwalkar, P., Clark, J., Ramaswamy, V., Hawes, D., Yang, F., et al. (2017) Immunohistochemical analysis of H3K27me3 demonstrates global reduction in group-A childhood posterior fossa ependymoma and is a powerful predictor of outcome. *Acta Neuropathologica Communications*. 134 (5), 705–714. doi:10.1007/s00401-017-1752-4.

Pappy, A.L., Savinkina, A., Bicknese, C., Neill, S., Oyesiku, N.M. & Ioachimescu, A.G. (2019) Predictive modeling for pituitary adenomas: single center experience in 501 consecutive patients. *Pituitary*. 22 (5), 520–531. doi:10.1007/s11102-019-00982-8.

Park, S.H., Ku, C.R., Moon, J.H., of, E.K.T.J. & 2018 (2018) Age-and sex-specific differences as predictors of surgical remission among patients with acromegaly. *The Journal of Clinical Endocrinology & Metabolism*. 103 (3), 909–916. doi:10.1210/jc.2017-01844.

Parsons, M. & Grabsch, H. (2009) How to make tissue microarrays. *Diagnostic Histopathology*. 15 (3), 142–150. doi:10.1016/j.mpdhp.2009.01.010.

Patel, J., Eloy, J.A. & Liu, J.K. (2015) Nelson's syndrome: a review of the clinical manifestations, pathophysiology, and treatment strategies. *Neurosurgical Focus*. 38 (2), E14. doi:10.3171/2014.10.focus14681.

Pei, L. (2001) Identification of c-myc as a Down-stream Target for Pituitary Tumor-transforming Gene*. *Journal of Biological Chemistry*. 276 (11), 8484–8491. doi:10.1074/jbc.m009654200.

Pei, L. & Melmed, S. (1997) Isolation and characterization of a pituitary tumor-transforming gene (PTTG). *Molecular endocrinology (Baltimore, Md.)*. 11 (4), 433–441. doi:10.1210/mend.11.4.9911.

Pizarro, C.B., Oliveira, M.C., Coutinho, L.B. & Ferreira, N.P. (2004) Measurement of Ki-67 antigen in 159 pituitary adenomas using the MIB-1 monoclonal antibody. *Brazilian journal of medical and biological research = Revista brasileira de pesquisas medicas e biologicas*. 37 (2), 235–243. doi:10.1590/s0100-879x2004000200011.

Plowman, P.N. (1999) Pituitary adenoma radiotherapy–when, who and how? *Clinical Endocrinology*. 51 (3), 265–271. doi:10.1046/j.1365-2265.1999.00854.x.

Potorac, I., Petrossians, P., Daly, A.F., Schillo, F., Slama, C.B., et al. (2015) Pituitary MRI characteristics in 297 acromegaly patients based on T2-weighted sequences. *Endocrine-Related Cancer*. 22 (2), 169–177. doi:10.1530/erc-14-0305.

Raappana, A., Koivikangas, J., Ebeling, T. & Pirilä, T. (2010) Incidence of pituitary adenomas in Northern Finland in 1992–2007. *The Journal of Clinical Endocrinology & Metabolism*. 95 (9), 4268–4275. doi:10.1210/jc.2010-0537","keywords":["magnetic.

Raverot, G., Burman, P., McCormack, A., Heaney, A., Petersenn, S., Popovic, V., Trouillas, J., Dekkers, O.M. & Endocrinology, E.S. of (2018) *European Society of Endocrinology Clinical Practice Guidelines for the management of aggressive pituitary tumours and carcinomas.* http://www.eje-online.org/lookup/doi/10.1530/EJE-17-0796.

Reincke, M., Sbiera, S., Hayakawa, A., Theodoropoulou, M., Osswald, A., et al. (2015) Mutations in the deubiquitinase gene USP8 cause Cushing's disease. *Nature Genetics*. 47 (1), 31–38. doi:10.1038/ng.3166.

Remmele, W., Hildebrand, U., Hienz, H.A., Klein, P.-J., Vierbuchen, M., Behnken, L.J., Heicke, B. & Scheidt, E. (1986) Comparative histological, histochemical, immunohistochemical and biochemical studies on oestrogen receptors, lectin receptors, and Barr bodies in human breast cancer. *Virchows Archiv A*. 409 (2), 127–147. doi:10.1007/bf00708323.

Rempel, S.A., Ge, S. & Gutiérrez, J.A. (1999) SPARC: A Potential Diagnostic Marker of Invasive Meningiomas. *Clinical Cancer Research*. 5 (2), 237–241. doi:10.1073/pnas.94.26.14719.

Rich, J.N., Shi, Q., Hjelmeland, M., Cummings, T.J., Kuan, C.-T., Bigner, D.D., Counter, C.M. & Wang, X.-F. (2003) Bone-related genes expressed in advanced malignancies induce invasion and metastasis in a genetically defined human cancer model. *Journal of Biological Chemistry*. 278 (18), 15951–15957. doi:10.1074/jbc.m211498200.

Righi, A., Agati, P., Sisto, A., Frank, G., Faustini-Fustini, M., Agati, R., Mazzatenta, D., Farnedi, A., Menetti, F., Marucci, G. & Foschini, M.P. (2012) A classification tree approach for pituitary adenomas. *Human pathology*. 43 (10), 1627–1637. doi:10.1016/j.humpath.2011.12.003.

Rim, C.H., Yang, D.S., Park, Y.J., Yoon, W.S., Lee, J.A. & Kim, C.Y. (2011) Radiotherapy for pituitary adenomas: long-term outcome and complications. *Radiation Oncology Journal*. 29 (3), 156–163. doi:10.3857/roj.2011.29.3.156.

Rinderknecht, E. & Humbel, R.E. (1976) Polypeptides with nonsuppressible insulin-like and cell-growth promoting activities in human serum: isolation, chemical characterization, and some biological properties of forms I and II. *Proceedings of the National Academy of Sciences*. 73 (7), 2365–2369. doi:10.1073/pnas.73.7.2365.

Rivenbark, A.G., Coleman, W.B. & Stahl, B.D. (2009) Histone methylation patterns in human breast cancer. *The FASEB Journal*. 23, 38.1-38.1. doi:10.1096/fasebj.23.1_supplement.38.1.

Roelfsema, F., Biermasz, N.R. & Pereira, A.M. (2012) Clinical factors involved in the recurrence of pituitary adenomas after surgical remission: a structured review and meta-analysis. *Pituitary*. 15 (1), 71–83. doi:10.1007/s11102-011-0347-7.

Romero, F., Multon, M.C., Ramos-Morales, F., Domínguez, A., Bernal, J.A., Pintor-Toro, J.A. & Tortolero, M. (2001) Human securin, hPTTG, is associated with Ku heterodimer, the regulatory subunit of the DNA-dependent protein kinase. *Nucleic Acids Research*. 29 (6), 1300–1307. doi:10.1093/nar/29.6.1300.

Rooprai, H.K., Martin, A.J., King, A., Appadu, U.D., Gullan, R.W., Thomas, N.W.M. & Pilkington, G.J. (2020) Lack of Correlation Between Immunohistochemical Expression of SPARC and Invasion in Different Grades of Meningiomas. *Anticancer research*. 40 (6), 3081–3089. doi:10.21873/anticanres.14289.

Rossi, M.K., Gnanamony, M. & Gondi, C.S. (2016) The “SPARC” of life: Analysis of the role of osteonectin/SPARC in pancreatic cancer (Review). *International journal of oncology*. 48 (5), 1765–1771. doi:10.3892/ijo.2016.3417.

Rotenberg, B., Tam, S., Ryu, W.H.A. & Duggal, N. (2010) Microscopic versus endoscopic pituitary surgery: A systematic review. *The Laryngoscope*. 120 (7), 1292–1297. doi:10.1002/lary.20949.

Rothbart, S.B., Dickson, B.M., Raab, J.R., Grzybowski, A.T., Krajewski, K., Guo, A.H., Shanle, E.K., Josefowicz, S.Z., Fuchs, S.M., Allis, C.D., Magnuson, T.R., Ruthenburg, A.J. & Strahl, B.D. (2015) An Interactive Database for the Assessment of Histone Antibody Specificity. *Molecular cell*. 59 (3), 502–511. doi:10.1016/j.molcel.2015.06.022.

Rotondo, F., Cusimano, M., Scheithauer, B.W., Coire, C., Horvath, E. & Kovacs, K. (2012) Atypical, invasive, recurring Crooke cell adenoma of the pituitary. *HORMONES*. 11 (1), 94–100.

Rutkowski, M.J., Alward, R.M., Chen, R., Wagner, J., Jahangiri, A., Southwell, D.G., Kunwar, S., Blevins, L., Lee, H. & Aghi, M.K. (2018) Atypical pituitary adenoma: a

clinicopathologic case series. *Journal of neurosurgery*. 128 (4), 1058–1065. doi:10.3171/2016.12.jns162126.

Sadeghipour, A., Mahouzi, L., Salem, M.M., Ebrahim-Nejad, S., Asadi-Lari, M., Radfar, A., Filip, I. & Babaheidarian, P. (2017) Ki67 Labeling Correlated With Invasion But Not With Recurrence. *Applied immunohistochemistry & molecular morphology : AIMM*. 25 (5), 341–345. doi:10.1097/pai.0000000000000303.

Saeger, W. (2021) [The 2017 WHO classification of pituitary tumors]. *Der Pathologe*. 42 (3), 333–351. doi:10.1007/s00292-021-00932-x.

Saeger, W., Honegger, J., Theodoropoulou, M., Knappe, U.J., Schöfl, C., Petersenn, S. & Buslei, R. (2016) Clinical Impact of the Current WHO Classification of Pituitary Adenomas. *Endocrine Pathology*. 27 (2), 104–114. doi:10.1007/s12022-016-9418-7.

Sakamoto, Y., Takahashi, M., Korogi, Y., Bussaka, H. & Ushio, Y. (1991) Normal and abnormal pituitary glands: gadopentetate dimeglumine-enhanced MR imaging. *Radiology*. 178 (2), 441–445. doi:10.1148/radiology.178.2.1987606.

Samuels, M.H. & Ridgway, E.C. (1995) Glycoprotein-secreting pituitary adenomas. *Bailliere's clinical endocrinology and metabolism*. 9 (2), 337–358. doi:10.1016/s0950-351x(95)80370-x.

Sanmillán, J.L., Torres-Diaz, A., Sanchez-Fernandez, J.J. & Lau, R. (2017) Radiologic Predictors for Extent of Resection in Pituitary Adenoma Surgery. A Single-Center Study. *World Neurosurgery*. 108, 436–446. doi:10.1016/j.wneu.2017.09.017.

Sarno, A.D., Landi, M.L., Marzullo, P., Somma, C.D., Pivonello, R., Cerbone, G., Lombardi, G. & Colao, A. (2000) The effect of quinagolide and cabergoline, two selective dopamine receptor type 2 agonists, in the treatment of prolactinomas. *Clinical Endocrinology*. 53 (1), 53–60. doi:10.1046/j.1365-2265.2000.01016.x.

Sasaki, R., Murakami, M., Okamoto, Y., Kono, K., Yoden, E., Nakajima, T., Nabeshima, S. & Kuroda, Y. (2000) The efficacy of conventional radiation therapy in the management of pituitary adenoma. *International Journal of Radiation Oncology*Biology*Physics*. 47 (5), 1337–1345. doi:10.1016/s0360-3016(00)00503-4.

Sauter, G. & Mirlacher, M. (2002) Tissue microarrays for predictive molecular pathology. *Journal of clinical pathology*. 55 (8), 575–576. doi:10.1136/jcp.55.8.575.

Scheick, S., Amdur, R.J., Kirwan, J.M., Morris, C.G., Mendenhall, W.M., Roper, S. & Friedman, W. (2016) Long-term Outcome After Fractionated Radiotherapy for Pituitary Adenoma. *American Journal of Clinical Oncology*. 39 (1), 49–54. doi:10.1097/coc.0000000000000014.

Scheithauer, B.W., Gaffey, T.A., Lloyd, R.V., Sebo, T.J., Kovacs, K.T., Horvath, E., Yapicier, O., Young, W.F., Meyer, F.B., Kuroki, T., Riehle, D.L. & Laws, E.R. (2006)

Pathobiology of pituitary adenomas and carcinomas. *Neurosurgery*. 59 (2), 341-53-discussion 341-53. doi:10.1227/01.neu.0000223437.51435.6e.

Scheithauer, B.W., Kovacs, K.T., Laws, E.R. & Randall, R.V. (1986) Pathology of invasive pituitary tumors with special reference to functional classification. *Journal of neurosurgery*. 65 (6), 733–744. doi:10.3171/jns.1986.65.6.0733.

Schittenhelm, J., Mittelbronn, M., Roser, F., Tatagiba, M., Mawrin, C. & Bornemann, A. (2006) Patterns of SPARC expression and basement membrane intactness at the tumour?brain border of invasive meningiomas. *Neuropathology and Applied Neurobiology*. 32 (5), 525–531. doi:10.1111/j.1365-2990.2006.00761.x.

Schreckinger, M., Walker, B., Knepper, J., Hornyak, M., Hong, D., Kim, J.-M., Folbe, A., Guthikonda, M., Mittal, S. & Szerlip, N.J. (2013) Post-operative diabetes insipidus after endoscopic transsphenoidal surgery. *Pituitary*. 16 (4), 445–451. doi:10.1007/s11102-012-0453-1.

Schuettengruber, B., Martinez, A.-M., Iovino, N. & Cavalli, G. (2011) Trithorax group proteins: switching genes on and keeping them active. *Nature Reviews Molecular Cell Biology*. 12 (12), 799–814. doi:10.1038/nrm3230.

Schult, D., Hölsken, A., Siegel, S., Buchfelder, M., Fahlbusch, R., Kreitschmann-Andermahr, I. & Buslei, R. (2015) EZH2 is highly expressed in pituitary adenomas and associated with proliferation. *Scientific Reports*. 5 (1), 1–10. doi:10.1038/srep16965.

Schultz, C., Lemke, N., Ge, S., Golembieski, W.A. & Rempel, S.A. (2002) Secreted Protein Acidic and Rich in Cysteine Promotes Glioma Invasion and Delays Tumor Growth in Vivo. *Cancer Research*. 62 (21), 6270–6277. doi:10.1097/00005072-199812000-00002.

Sebastian, P., Balakrishnan, R., Yadav, B. & John, S. (2016) Outcome of radiotherapy for pituitary adenomas. *Reports of Practical Oncology and Radiotherapy*. 21 (5), 466–472. doi:10.1016/j.rpor.2016.06.002.

Shariq, O.A. & Lines, K.E. (2019) Epigenetic dysregulation in pituitary tumors. *International Journal of Endocrine Oncology*. 6 (3). doi:10.2217/ije-2019-0006.

Sheehan, J.M., Douds, G.L., Hill, K. & Farace, E. (2008) Transsphenoidal surgery for pituitary adenoma in elderly patients. *Acta neurochirurgica*. 150 (6), 571–574. doi:10.1007/s00701-008-1581-2.

Shi, Q., Bao, S., Song, L., Wu, Q., Bigner, D.D., Hjelmeland, A.B. & Rich, J.N. (2007) Targeting SPARC expression decreases glioma cellular survival and invasion associated with reduced activities of FAK and ILK kinases. *Oncogene*. 26 (28), 4084–4094. doi:10.1038/sj.onc.1210181.

Sturm, D., Witt, H., Hovestadt, V., Khuong-Quang, D.-A., Jones, D.T.W., et al. (2012) Hotspot Mutations in H3F3A and IDH1 Define Distinct Epigenetic and Biological

Subgroups of Glioblastoma. *Cancer Cell*. 22 (4), 425–437. doi:10.1016/j.ccr.2012.08.024.

Sun, Z., Zhang, Y., Jia, J., Fang, Y., Tang, Y., Wu, H. & Fang, D. (2020) H3K36me3, message from chromatin to DNA damage repair. *Cell & bioscience*. 10 (1), 9–9. doi:10.1186/s13578-020-0374-z.

Sweiss, F.B., Lee, M. & Sherman, J.H. (2015) Extraventricular Neurocytomas. *Neurosurgery Clinics*. 26 (1), 99–104. doi:10.1016/j.nec.2014.09.004.

Tabarin, A., Laurent, F., Catargi, B., Puel, F.O., Lescene, R., Berge, J., Galli, F.S., Drouillard, J., Roger, P. & Guerin, J. (1998) Comparative evaluation of conventional and dynamic magnetic resonance imaging of the pituitary gland for the diagnosis of Cushing's disease. *Clinical Endocrinology*. 49 (3), 293–300. doi:10.1046/j.1365-2265.1998.00541.x.

Taghvaei, M., Sadrehosseini, S.M., Ardakani, J.B., Nakhjavani, M. & Zeinalizadeh, M. (2018) Endoscopic Endonasal Approach to the Growth Hormone-Secreting Pituitary Adenomas: Endocrinologic Outcome in 68 Patients. *World Neurosurgery*. 117, e259–e268. doi:10.1016/j.wneu.2018.06.009.

Taniguchi, M., Hosoda, K., Akutsu, N., Takahashi, Y. & Kohmura, E. (2015) Endoscopic endonasal transsellar approach for laterally extended pituitary adenomas: volumetric analysis of cavernous sinus invasion. *Pituitary*. 18 (4), 518–524. doi:10.1007/s11102-014-0604-7.

Thapar, K., Kovacs, K., Scheithauer, B.W., Stefaneanu, L., Horvath, E., Peter, P., Murray, D. & Laws, E.J. (1996a) Proliferative activity and invasiveness among pituitary adenomas and carcinomas: an analysis using the MIB-1 antibody. *Neurosurgery*. 38 (1), 99–107. doi:10.1097/00006123-199601000-00024","keywords":["immunohistochemistry","carcinoma","pituitary.

Thapar, K., Scheithauer, B.W., Kovacs, K., Pernicone, P.J. & Laws, E.R. (1996b) p53 expression in pituitary adenomas and carcinomas: correlation with invasiveness and tumor growth fractions. *Neurosurgery*. 38 (4), 765–771. doi:10.1227/00006123-199604000-00027","keywords":["immunohistochemistry","carcinoma","pituitary.

Tomlinson, J.W., Holden, N., Hills, R.K., Wheatley, K., Clayton, R.N., Bates, A.S., Sheppard, M.C. & Stewart, P.M. (2001) Association between premature mortality and hypopituitarism. *The Lancet*. 357 (9254), 425–431. doi:10.1016/s0140-6736(00)04006-x.

Toogood, A.A. (2004) Endocrine consequences of brain irradiation. *Growth Hormone & IGF Research*. 14, 118–124. doi:10.1016/j.ghir.2004.03.038.

Torhorst, J., Bucher, C., Kononen, J., Haas, P., Zuber, M. & Köchli, O.R. (2001) Tissue Microarrays for Rapid Linking of Molecular Changes to Clinical Endpoints. *The*

American Journal of Pathology. 159 (6), 2249–2256. doi:10.1016/s0002-9440(10)63075-1.

Tortosa, F. & Webb, S.M. (2016) Atypical pituitary adenomas: 10 years of experience in a reference centre in Portugal. *Neurologia (Barcelona, Spain)*. 31 (2), 97–105. doi:10.1016/j.nrl.2015.06.010.

Toth, M., Chvyrkova, I., Bernardo, M.M., Hernandez-Barrantes, S. & Fridman, R. (2003) Pro-MMP-9 activation by the MT1-MMP/MMP-2 axis and MMP-3: role of TIMP-2 and plasma membranes. *Biochemical and Biophysical Research Communications*. 308 (2), 386–395. doi:10.1016/s0006-291x(03)01405-0.

Toyota, E., Wang, J., Pirouzmand, N., Ijad, N., Ali, M., Nassiri, F. & Zadeh, G. (2019) P.091 Surgical outcomes for patients undergoing repeat endoscopic endonasal trans-sphenoidal surgery for recurrent pituitary adenomas. *Canadian Journal of Neurological Sciences / Journal Canadien des Sciences Neurologiques*. 46 (s1), S38–S38. doi:10.1017/cjn.2019.186.

Trivellin, G., Daly, A.F., Faucz, F.R., Yuan, B., Rostomyan, L., et al. (2014) Gigantism and Acromegaly Due to Xq26 Microduplications and GPR101 Mutation. *The New England Journal of Medicine*. 371 (25), 2363–2374. doi:10.1056/nejmoa1408028.

Trouillas, J., Roy, P., Sturm, N., Dantony, E., Cortet-Rudelli, C., et al. (2013) A new prognostic clinicopathological classification of pituitary adenomas: a multicentric case–control study of 410 patients with 8 years post-operative follow-up. *Acta Neuropathologica Communications*. 126 (1), 123–135. doi:10.1007/s00401-013-1084-y.

Turner, H.E., Nagy, Z., Esiri, M.M., Harris, A.L. & Wass, J.A.H. (2000) Role of Matrix Metalloproteinase 9 in Pituitary Tumor Behavior. *The Journal of Clinical Endocrinology and metabolism*. 85 (8), 2931–2935. doi:10.1210/jcem.85.8.6754.

Tzankov, A., Went, P., Zimpfer, A. & Dirnhofer, S. (2005) Tissue microarray technology: principles, pitfalls and perspectives—lessons learned from hematological malignancies. *Experimental Gerontology*. 40 (8–9), 737–744. doi:10.1016/j.exger.2005.06.011.

Tzao, C., Tung, H.-J., Jin, J.-S., Sun, G.-H., Hsu, H.-S., Chen, B.-H., Yu, C.-P. & Lee, S.-C. (2009) Prognostic significance of global histone modifications in resected squamous cell carcinoma of the esophagus. *Modern Pathology*. 22 (2), 252–260. doi:10.1038/modpathol.2008.172.

Vandeva, S., Jaffrain-Rea, M.-L., Daly, A.F., Tichomirowa, M., Zacharieva, S. & Beckers, A. (2010) The genetics of pituitary adenomas. *Best Practice & Research Clinical Endocrinology & Metabolism*. 24 (3), 461–476. doi:10.1016/j.beem.2010.03.001.

Varier, R.A. & Timmers, H.T.M. (2011) Histone lysine methylation and demethylation pathways in cancer. *Biochimica et Biophysica Acta (BBA) - Reviews on Cancer*. 1815 (1), 75–89. doi:10.1016/j.bbcan.2010.10.002.

Venneti, S., Santi, M., Felicella, M.M., Yarilin, D., Phillips, J.J., Sullivan, L.M., Martinez, D., Perry, A., Lewis, P.W., Thompson, C.B. & Judkins, A.R. (2014) A sensitive and specific histopathologic prognostic marker for H3F3A K27M mutant pediatric glioblastomas. *Acta Neuropathologica Communications*. 128 (5), 743–753. doi:10.1007/s00401-014-1338-3.

Voduc, D., Kenney, C. & Nielsen, T.O. (2008) Tissue Microarrays in Clinical Oncology. *Seminars in Radiation Oncology*. 18 (2), 89–97. message:%3C1292832253.23543454.1520877554257@mail.yahoo.com%3E.

Wang, J. & Liu, Y.-S. (2004) Expression of MMPPs and TIMP and invasiveness in pituitary adenomas. *Journal of Central South University*. 29 (6), 647–650. https://europepmc.org/article/med/16114548.

Wanichi, I.Q., Mariani, B.M. de P., Frassetto, F.P., Siqueira, S.A.C., Musolino, N.R. de C., Cunha-Neto, M.B.C., Ochman, G., Cescato, V.A.S., Machado, M.C., Trarbach, E.B., Bronstein, M.D. & Fragoso, M.C.B.V. (2019) Cushing's disease due to somatic USP8 mutations: a systematic review and meta-analysis. *Pituitary*. 22 (4), 435–442. doi:10.1007/s11102-019-00973-9.

Watts, A.K., Easwaran, A., McNeill, P., Wang, Y.Y., Inder, W.J. & Caputo, C. (2017) Younger age is a risk factor for regrowth and recurrence of nonfunctioning pituitary macroadenomas: Results from a single Australian centre. *Clinical Endocrinology*. 87 (3), 264–271. doi:10.1111/cen.13365.

Webster, J., Peters, J.R., John, R., Smith, J., Chan, V., Hall, R. & Scanlon, M.F. (1994) Pituitary stone: two cases of densely calcified thyrotrophin-secreting pituitary adenomas. *Clinical Endocrinology*. 40 (1), 137–143. doi:10.1111/j.1365-2265.1994.tb02456.x.

Wei, Y., Xia, W., Zhang, Z., Liu, J., Wang, H., Adsay, N.V., Albarracin, C., Yu, D., Abbruzzese, J.L., Mills, G.B., Bast, R.C., Hortobagyi, G.N. & Hung, M.-C. (2008) Loss of trimethylation at lysine 27 of histone H3 is a predictor of poor outcome in breast, ovarian, and pancreatic cancers. *Molecular Carcinogenesis*. 47 (9), 701–706. doi:10.1002/mc.20413.

Wierinckx, A., Auger, C., Devauchelle, P., Reynaud, A., Chevallier, P., Jan, M., Perrin, G., Fèvre-Montange, M., Rey, C., Figarella-Branger, D., Raverot, G., Belin, M.-F., Lachuer, J. & Trouillas, J. (2007) A diagnostic marker set for invasion, proliferation, and aggressiveness of prolactin pituitary tumors. *Endocrine-Related Cancer*. 14 (3), 887–900. doi:10.1677/erc-07-0062.

Wilson, C.B. (1984) A decade of pituitary microsurgery: The Herbert Olivecrona Lecture. *Journal of neurosurgery*. 61 (5), 814–833. doi:10.3171/jns.1984.61.5.0814.

Wirthschaft, P., Bode, J., Soni, H., Dietrich, F., Krüwel, T., et al. (2019) RhoA regulates translation of the Nogo-A decoy SPARC in white matter-invading glioblastomas. *Acta Neuropathologica Communications*. 138 (2), 275–293. doi:10.1007/s00401-019-02021-z.

Woodworth, G.F., Patel, K.S., Shin, B., Burkhardt, J.-K., Tsiouris, A.J., McCoul, E.D., Anand, V.K. & Schwartz, T.H. (2014) Surgical outcomes using a medial-to-lateral endonasal endoscopic approach to pituitary adenomas invading the cavernous sinus: Clinical article. *Journal of neurosurgery*. 120 (5), 1086–1094. doi:10.3171/2014.1.jns131228.

Xue, Y., Chen, R., Du, W., Yang, F. & Wei, X. (2017) RIZ1 and histone methylation status in pituitary adenomas. *Tumor Biology*. 1–7. doi:10.1177/1010428317711794.

Yamada, S., Ohyama, K., Taguchi, M., Takeshita, A., Morita, K., Takano, K. & Sano, T. (2007) A study of the correlation between morphological findings and biological activities in clinically nonfunctioning pituitary adenomas. *The Journal of Clinical Endocrinology & Metabolism*. 61 (3), 580–585. doi:10.1227/01.neu.0000290906.53685.79.

Yan, H., Wang, W., Dou, C., Tian, F. & Qi, S. (2015) Securin promotes migration and invasion via matrix metalloproteinases in glioma cells. *Oncology Letters*. 9 (6), 2895–2901. doi:10.3892/ol.2015.3074.

Yan, Q., Weaver, M., Perdue, N. & Sage, E.H. (2005) Matricellular protein SPARC is translocated to the nuclei of immortalized murine lens epithelial cells. *Journal of Cellular Physiology*. 203 (1), 286–294. doi:10.1002/jcp.20226.

Yang, Y. & Li, G. (2020) Icariin inhibits proliferation, migration, and invasion of medulloblastoma DAOY cells by regulation of SPARC. *Phytotherapy research : PTR*. 34 (3), 591–600. doi:10.1002/ptr.6545.

Yao, X., Gao, H., Li, C., Wu, L., Bai, J., Wang, J., Li, Y. & Zhang, Y. (2017) Analysis of Ki67, HMGA1, MDM2, and RB expression in nonfunctioning pituitary adenomas. *Journal of neuro-oncology*. 132 (2), 199–206. doi:10.1007/s11060-016-2365-9.

Yin, J., Chen, G., Liu, Y., Liu, S., Wang, P., Wan, Y., Wang, X., Zhu, J. & Gao, H. (2010) Downregulation of SPARC expression decreases gastric cancer cellular invasion and survival. *Journal of Experimental & Clinical Cancer Research*. 29 (1), 1–9. doi:10.1186/1756-9966-29-59.

Youssef, A.S., Operative, S.A. & 2005 (2005) Transcranial surgery for pituitary adenomas. *The Journal of Clinical Endocrinology & Metabolism*. doi:10.1227/01.neu.0000163602.05663.86.

Yuhan, L., Zhiqun, W., Jihui, T. & Renlong, P. (2021) Ki-67 labeling index and Knosp classification of pituitary adenomas. *British journal of neurosurgery*. 1–5. doi:10.1080/02688697.2021.1884186.

Zada, G., Woodmansee, W.W., Ramkissoon, S., Amadio, J., Nosé, V. & Laws, E.R. (2011) Atypical pituitary adenomas: incidence, clinical characteristics, and implications. *Journal of neurosurgery*. 114 (2), 336–344. doi:10.3171/2010.8.jns10290.

Zhang, C., Ding, X., Lu, Y., Hu, L. & Hu, G. (2017) Cerebrospinal fluid rhinorrhoea following transsphenoidal surgery for pituitary adenoma: experience in a Chinese centre. *Acta otorhinolaryngologica Italica : organo ufficiale della Societa italiana di otorinolaringologia e chirurgia cervico-facciale*. 37 (4), 303–307. doi:10.14639/0392-100x-1086.

Zhang, F., Zhang, Y., Da, J., Jia, Z., Wu, H. & Gu, K. (2020) Downregulation of SPARC Expression Decreases Cell Migration and Invasion Involving Epithelial-Mesenchymal Transition through the p-FAK/p-ERK Pathway in Esophageal Squamous Cell Carcinoma. *Journal of Cancer*. 11 (2), 414–420. doi:10.7150/jca.31427.

Zhang, X., Horwitz, G.A., Heaney, A.P., Nakashima, M., Prezant, T.R., Bronstein, M.D. & Melmed, S. (1999) Pituitary Tumor Transforming Gene (PTTG) Expression in Pituitary Adenomas. *The Journal of Clinical Endocrinology & Metabolism*. 84 (2), 761–767. doi:10.1210/jcem.84.2.5432.

Zhao, D., Tomono, Y. & Nose, T. (1999) Expression of P27 kip 1 and Ki-67 in Pituitary Adenomas: An Investigation of Marker of Adenoma Invasiveness. *Acta neurochirurgica*. 141 (2), 187–192. doi:10.1007/s007010050285.

Zoli, M., Milanese, L., Bonfatti, R., Sturiale, C., Pasquini, E., Frank, G., G, F. & Mazzatenta, D. (2016) Cavernous sinus invasion by pituitary adenomas: role of endoscopic endonasal surgery. *Journal of Neurosurgical Sciences*. 60 (4), 485–494. https://europepmc.org/article/med/27280543.

Zou, H., McGarry, T.J., Bernal, T. & Kirschner, M.W. (1999) Identification of a Vertebrate Sister-Chromatid Separation Inhibitor Involved in Transformation and Tumorigenesis. *Science*. 285 (5426), 418–422. doi:10.1126/science.285.5426.418.

Internet sources

Beck-Peccoz P, Persani L, Lania A. (2019) Thyrotropin-Secreting Pituitary Adenomas. *Endotext*. https://www.ncbi.nlm.nih.gov/books/NBK278978/ [last visited: March 13, 2022]

Jane J, Laws E. (2016) Surgical Treatment of Pituitary Adenomas. *Endotext*. https://www.ncbi.nlm.nih.gov/books/NBK278983/ [last visited: March 18, 2021]

Snyder PJ, Cooper DS, Martin KA. (2018) Treatment of gonadotroph and other clinically nonfunctioning adenomas. *UpToDate*. https://www.uptodate.com/contents/treatment-of-gonadotroph-and-other-clinically-nonfunctioning-adenomas [last visited: March 13, 2022]

Swaeringen B, Snyder P, Martin K. (2018) Transsphenoidal surgery for pituitary adenomas and other sellar masses. *UpToDate*. https://www.uptodate.com/contents/transsphenoidal-surgery-for-pituitary-adenomas-and-other-sellar-masses [last visited: March 18, 2022]

Yatavelli R, Bhusal K. (2021) Prolactinoma. In: StatPearls. *StatPearls Publishing.* Treasure Island (FL). https://www.ncbi.nlm.nih.gov/books/NBK459347/ [last visited: March 13, 2022]

AWMF. (2019) S2k-Leitlinie Diagnostik und Therapie von hormoninaktiven Hypophysenadenomen. *Arbeitsgemeinschaft der Wissenschaftlichen Medizinischen Fachgesellschaften (AWMF).* https://www.awmf.org/uploads/tx_szleitlinien/089-002l_S2k_Diagnostik-Therapie-hormonaktiver-Hypophsenaddenome_2020-04.pdf [last visited: May 12, 2022]

Figures and Tables

Tabl. 1.1.: Arafah, B.M., Nasrallah, M.P. (2001) Pituitary tumors: pathophysiology, clinical manifestations and management. *Endocrine-related cancer*. 8, p. 287-305

Fig. 1.1.: Micko, A.S.G., Wöhrer, A., Wolfsberger, S. & Knosp, E. (2015) Invasion of the cavernous sinus space in pituitary adenomas: endoscopic verification and its correlation with an MRI-based classification. *Journal of neurosurgery*. 122 (4), p. 806, doi:10.3171/2014.12.jns141083.

Tabl. 1.2.: Lloyd, R.V., Osamura, R.Y., Grossman, A., Korbonits, M., Kovacs, K., lopes, M.B.S., Matsuno, A. & Trouillas, J. (2017) *WHO Classification of Tumours of Endocrine Organs* R.V. Lloyd, R.Y. Osamura, G. Klöppel, & J. Rosai (eds.). p.16

Fig. 2.3.: Kim, S.W., Roh, J. & Park, C.S. (2016) Immunohistochemistry for Pathologists: Protocols, Pitfalls, and Tips. *Journal of Pathology and Translational Medicine*. 50, p. 411, doi:10.4132/jptm.2016.08.08&domain=pdf&date_stamp=2016-11-15.

Erklärung zum Eigenanteil der Dissertationsschrift

Die Arbeit wurde in der Universitätsklinik Tübingen in der Klinik für Neurochirurgie unter Betreuung von Prof. Dr. med. Jürgen Honegger durchgeführt.

Die Konzeption der Studie erfolgte durch Prof. Dr. med Jürgen Honegger, Stellvertretender Chefarzt der Klinik für Neurochirurgie und Dr. med. Felix Behling, Facharzt für Neurochirurgie.

Die Erhebung von Daten aus OP-Berichten, neuropathologischen Befundberichten und Entlassbriefen erfolgte durch mich. Die Begutachtung und Befundung nach Knosp von MRT-Bildern aller inkludierten Fälle, sowie die Erhebung von Rezidivdaten erfolgte durch Dr. Isabella Nasi-Khordisti, Assistenzärztin für Neurochirurgie.

Sämtliche experimentelle Arbeiten wurden von mir in Zusammenarbeit mit und in den Räumlichkeiten der Abteilung für Neuropathologie des Departments für Pathologie und Neuropathologie, Universitätsklinikum Tübingen durchgeführt. Einarbeitung und Anleitung erhielt ich durch Prof. Dr. med. Jens Schittenhelm, Oberarzt für Neuropathologie, Dr. med. Felix Behling, Facharzt für Neurochirurgie sowie Manuel Gödan, medizinisch-technischer Laborassistent. Die Methode der Mikrotomie von Paraffinblöcken, Anfärbung mit Hämatoxylin und Eosin (HE) und die immunhistochemische Anfärbung wurde durch Manuel Gödan durchgeführt. Die Auswertung des Antikörpers CAM5.2 für die Reklassifikation der eingeschlossenen Adenomfälle wurde von Kosmas Kandilaris, Assistenzarzt für Neuropathologie, durchgeführt. Die Aufsuche der Paraffinpräparate und HE-Schnitte im Archiv, Anfertigung der verwendeten TMA-Blöcke und mikroskopische Analyse aller übrigen verwendeten Antikörperfärbungen erfolgte eigenständig durch mich.

Die statistische Auswertung der erhobenen Daten erfolgte mithilfe der Software JMP 15.0.0. eigenständig durch mich.

Ich versichere, die Dissertationsschrift nach bestem Wissen und Gewissen selbstständig verfasst zu haben und keine weiteren als die von mir angegebenen Quellen verwendet zu haben.

Ludwigsburg, den 08. Juni 2022

Acknowledgements

First and foremost, I would like to express my deepest gratitude to Professor Jürgen Honegger and Doctor Felix Behling of the Department of Neurosurgery of the University Medical Center of Tübingen. Without their continuous effort this study would not have been possible. Thanks to the mentoring and qualified advice of Doctor Felix Behling I was able to learn the accurate execution of tissue microarray analysis and reasonable statistical evaluation. The numerous phone calls, emails and meetings in the laboratory helped me tremendously at keeping track of the huge amount of data and at completing working tasks as well as solving problems in an efficient manner. I also owe a debt of gratitude to Professor Jens Schittenhelm of the Department of Neuropathology of the University Medical Center of Tübingen for performing the initial histopathological evaluation of all samples and marking of suitable areas for further tissue analysis, for providing helpful information on adequate antibody scoring methods and for his invaluable intellectual approaches. The mentioned members of my research group all helped promote my scientific thinking. I am very grateful for all that I was taught.

I am also indebted to Doctor Isabella Nasi-Khordisti of the Department of Neurosurgery for her willingness to participate in this study to a great extent by determining the Knosp scores and by acquiring follow-up data of all included cases. I would also like to thank Doctor Kosmas Kandilaris of the Department of Neuropathology for the immunohistochemical evaluation of the transcriptional marker CAM5.2, this effort made an exact classification of the pituitary adenomas into specific subtypes possible. My understanding of the laboratory methods involved in this study was increased by Manuel Goedan of the Department of Neuropathology, whom I am very thankful for his uncomplaining explanations and willing answers to the most detailed technical questions. In general, I am extremely grateful that every member of the team within the Department of Neuropathology, where I conducted most of the research, was at all times welcoming and helpful when questions arose.

Lastly, I would like to thank the many anonymous creators of the jmp statistical software for their intuitive and versatile software and of youtube tutorials for their easily accessible information , I am truly impressed by the voluntarism and selflessness of the bright minds behind those digital solutions. It made me realize the immense value of shared knowledge around the world which is also a key aspect in medical research.